Characterizing the Molecular Genetic, Phenotypic and Virulence Properties of the Invasive Nontyphoidal *Salmonella* Strain D23580: An Integrated Approach

by

Jiseon Yang

A Dissertation Presented in Partial Fulfillment
of the Requirements for the Degree
Doctor of Philosophy

Approved April 2015 by the
Graduate Supervisory Committee:

Cheryl A. Nickerson, Chair
Yung Chang
Valerie Stout
C Mark Ott
Kenneth Roland
Jennifer Barrila

ARIZONA STATE UNIVERSITY

May 2015

ABSTRACT

Invasive salmonellosis caused by *Salmonella enterica* serovar Typhimurium ST313 is a major health crisis in sub-Saharan Africa, with multidrug resistance and atypical clinical presentation challenging current treatment regimens and resulting in high mortality. Moreover, the increased risk of spreading ST313 pathovars worldwide is of major concern, given global public transportation networks and increased populations of immunocompromised individuals (as a result of HIV infection, drug use, cancer therapy, aging, etc). While it is unclear as to how *Salmonella* ST313 strains cause invasive disease in humans, it is intriguing that the genomic profile of some of these pathovars indicates key differences between classic Typhimurium (broad host range), but similarities to human-specific typhoidal *Salmonella* Typhi and Paratyphi. In an effort to advance fundamental understanding of the pathogenesis mechanisms of ST313 in humans, I report characterization of the molecular genetic, phenotypic and virulence profiles of D23580 (a representative ST313 strain). Preliminary studies to characterize D23580 virulence, baseline stress responses, and biochemical profiles, and *in vitro* infection profiles in human surrogate 3-D tissue culture models were done using conventional bacterial culture conditions; while subsequent studies integrated a range of incrementally increasing fluid shear levels relevant to those naturally encountered by D23580 in the infected host to understand the impact of biomechanical forces in altering these characteristics. In response to culture of D23580 under these conditions, distinct differences in transcriptional biosignatures, pathogenesis-related stress responses, *in vitro* infection profiles and *in vivo* virulence in mice were observed as compared to those of classic *Salmonella* pathovars tested.

Collectively, this work represents the first characterization of *in vivo* virulence and *in vitro* pathogenesis properties of D23580, the latter using advanced human surrogate models that mimic key aspects of the parental tissue. Results from these studies highlight the importance of studying infectious diseases using an integrated approach that combines actions of biological and physical networks that mimic the host-pathogen microenvironment and regulate pathogen responses.

DEDICATION

For my biological family in South Korea, ***Jung-Gon Yang****, father****,***

Yeon-Hee Jung*, mother,* ***Dea Hoon Yang****, brother,*

and ***Yun-Joo Lee****, sister-in-law,*

who gave constant support, encouragement, and love while I was away from home.

For my second family in the U.S, ***Dr. Nickerson****,* ***Dr. Jennifer Barrila***

and other lab members, who cheered me up, sweat together (we do lots of push ups!),

laugh together, and dream together.

It was one of the best luck for my life to join Dr. Nickerson's lab.

ACKNOWLEDGMENTS

I am most grateful to my mentor **Dr. Cheryl Nickerson**. She has been the greatest mentor for me, providing her countless hours of reflecting, reading, and supporting throughout the entire process of my Ph.D. study. She constantly encouraged and helped me to overcome my weakness with her incredible patience by saying that there is no one perfect. Also she is a great scientist. Learning from her about multidisciplinary thinking and using multiple approaches, and as a result, this dissertation work was accomplished with efforts using various multidisciplinary approaches. She continuously challenges me to apply multiple approaches to solve a science problem on a bigger scale. She is my role model as a professor and a scientist, especially as a woman scientist.

I sincerely appreciate **Dr. Jennifer Barrila**. She spent her tremendous time to help me throughout the entire project, from being at the lab bench for experiments to the desk for writing. Despite my poor English, she patiently repeated explanations and trained me providing her excellent scientific expertise. I really appreciate her countless hours of helping to train me and revising my writing. The quality of this work greatly improved with her help. It is lucky for me to have her for my work senior!

A special thanks for **Dr. C. Mark Ott** who provided his deep engineering and microbiology insight during scientific discussions and also whom I enjoyed talking with for advice on many aspects of this project; and to **Dr. Kenneth Roland** who provided his expertise in the study of *Salmonella* and for helpful discussions.

I also thank **Jacquelyn Kilbourne** who provided her insight for animal studies, **Dr. Aurelie Crabbé** who generated the confocal microscopic images and for helpful

discussions; **Dr. Seth Nydam** who helped with an infection study and assisted with editing and helpful discussions with data analysis; **Rebecca Forsyth** who helped with animal experiments, supported lab work, and has been a good friend and a nice and fun roommate at NASA-KSC; **Yulong Liu** who helped with an infection study; **Ami Gutierrez-Jensen** and **Christian Castro** who helped with an oxidative stress assay; **Jason Steel** and **Dr. Jin Park** who performed RNA-sequencing and gene annotation; **Richard R. Davis** who supported work in the lab and for being a nice friend; and **Gary Tahmahkera**, the lab coordinator of the MIC 206 lab class which I taught, who helped me to get support from SoLS for 5 years of my Ph.D. study.

I would like to acknowledge and thank my school division at SoLS and the Biodesign Institute for allowing me to conduct my research and providing any assistance requested. Special thanks for SoLS research funding (2013), training funding (2014), awards (2014-2015), and scholarships and fellowships (2012-2015) that were an important part of helping me to complete my degree and grow as a scientist. I am also thankful for the members of the staff development and human resources department for their continued support.

ST313 strains were kindly provided by **Dr. Robert Kingsley** and **Dr. Robert Heyderman** (Malawi-Liverpool-Wellcome Trust Clinical Research Programme).

TABLE OF CONTENTS

Page

CHAPTER Page

CHAPTER Page

LIST OF TABLES

Table Page

LIST OF FIGURES

Figure Page

Figure Page

1 CHAPTER 1: OVERVIEW

1.1 Emergence of multidrug resistant *Salmonella* Typhimurium causing invasive bacteremia in sub-Saharan Africa

1.1.1 Problem: Invasive salmonellosis caused by nontyphoidal *Salmonella*

The global burden of disease caused by *Salmonella* infections is substantial, with more than 90 million human cases and an excess cost of $6 billion annually in the United States and Europe (1-3). Moreover, the emergence and spread of multiply antibiotic-resistant strains of *Salmonella* are a growing threat to public health and a major economic burden (2-4). In sub-Saharan Africa, the emergence of multidrug resistant nontyphoidal *Salmonella* (NTS) strains causing unusually high incidences of fatal bacteremia in young children and immunocompromised individuals is of major concern (5-10). However, despite the magnitude of this public health threat and its intracontinental spread, the pathogenic mechanisms, host tropism, and relationship of these NTS isolates to other *Salmonella* pathovars is poorly understood.

Interestingly, NTS *Salmonella enterica* serovar Typhimurium (Typhimurium) was identified as the major etiological agent of lethal bacteremia associated with sub-Saharan infections, with these isolates being referred to as “highly invasive”. Ironically, it is typhoidal *Salmonella* pathovars such as *Salmonella* Typhi (Typhi) that normally cause invasive salmonellosis (systemic disease), whereas Typhimurium isolates commonly cause self-limiting gastroenteritis (restricted to the gastrointestinal tract) (11-13). Nevertheless, NTS strains are the most common cause of invasive disease in sub-Saharan

Africa with multi-locus sequence analysis identifying these isolates as novel *Salmonella* sequence type, ST313(7, 8, 14-18), ST313 infections are associated with immunocompromised individuals (adults infected with HIV and children with malaria, anemia and malnutrition) and cause greater incidence of disease in parts of Africa than pneumonia, malaria, and typhoid(10, 14-17, 19-23) The lack of reported animal reservoirs for ST313 strains coupled with genomic sequencing has prompted speculation of adaptation and evolution of these isolates toward person-to-person transmission(7, 8, 15, 17, 24)

1.1.2 *Salmonella* Typhimurium ST313

Distinct pathovar characteristics of ST313

Genomic profiles of ST313 strains D23580, A130 and 5579, revealed distinct phage types and evidence of genome degradation, with D23580 exhibiting the largest extent of genome reduction compared to the other isolates (7). The reduced genome content (due to pseudogene formation) showed similarities to human-restricted *Salmonella* pathovars (Typhi and Paratyphi) rather than those of generalist/broad host range Typhimurium isolates (7) Since many host-specific pathogens contain pseudogenes and gene deletions resulting in loss of function mutations, genomic decay is considered an evolutionary indicator of pathogen specialists having limited host tropism (12, 25-27). While exhibiting reduced genome degradation as compared to D23580, strain A130 exhibits a phage type (DT56var) that is most frequently associated with bird mortality(7,

28-32). It remains unclear as to how ST313 pathovars are able to cause atypical NTS-associated invasive disease in humans or how they may spread to other hosts.

Current knowledge of ST313 pathogenesis.

Studies have reported the importance of antibody production and the complement response for bactericidal activity against ST313 pathovars in human serum(33-38) Particularly, antibodies against outer membrane proteins (Omps) are critical to induce serum killing of *Salmonella*(34). In agreement with this finding, Omp-specific antibodies induced complement-mediated killing of *Salmonella* by healthy serum(34). In contrast, high levels of antibodies directed against *Salmonella* lipopolysaccharide (LPS) prevented killing *Salmonella* by HIV-infected serum(34). The study demonstrated that the abnormal humoral immunity to NTS in HIV-patients caused a lack of bactericidal activity(34). A recent study by Parsons et al showed that ST313 strains can cause invasive infection in chickens, but virulence assays were not performed(39). In this same study, the authors showed the rapid infection of ST313 pathovars (including D23580) in the spleen and liver and colonization of the lower gastrointestinal with reduced chemokine expression in the ileum as compared to classic *S*. Typhimurium ST19 strains(39). Another study found that the *st313-td* gene in ST313 is mainly present in invasive *Salmonella* strains and is strongly associated with *Salmonella* invasiveness(40). The role of *st313-td* during systemic infection in mice was shown by impaired colonization of deep tissues of an *st313-td* deletion Typhimurium mutant following intraperitoneal (i.p.) co-infection with the parental wild-type strain (40) More recently, a study reported attenuated flagellin as a phenotypic difference between ST313 and ST19 (most common classic *S*. Typhimurium).

This study suggested an association of flagellin with the highly invasive disease phenotype in ST313 strains, as evidenced by enhanced phagocytosis and survival in macrophages with a simultaneous reduction in inflammatory cytokine production in the infected cells, which is similar to pathogenic characteristics of typhoidal *Salmonella*(41). Although current studies have broadened our knowledge about ST313, it is still not well understood as to why ST313 predominantly causes invasive systemic disease in Africa at such dramatically high rates. It is also not clear as to why there are a lack of reports of ST313 animal infections given that these pathovars are the leading cause of bacteremia in many regions in Africa; an observation which has caused speculation of human-to-human transmission. Hence, studies to advance our understanding of the relationship between ST313 isolates and classic *S*. Typhimurium and *S*. Typhi pathovars will unveil novel pathogenesis mechanisms and host tropism profiles that may lead to effective strategies for treatment and prevention.

1.2 Overview of Salmonella infection – dynamics of the host-pathogen interaction

Salmonella adherence, invasion and intracellular survival.

Salmonella has an impressive arsenal to successfully establish infection in the host, which largely center around adherence, invasion, intracellular survival and replication mechanisms. While a detailed review of *Salmonella* pathogenesis mechanisms is outside the scope of this text, there are several excellent reviews to which the reader is referred for additional information (11, 13, 42) As much of our understanding of

Salmonella pathogenesis mechanisms and host interactions is based on the use of NTS Typhimurium strains *in vitro* (cell culture) and *in vivo* (animal infections), the information below is presented in the context of these classic pathovars. While considerably less information is available regarding *Salmonella* Typhi, key differences between this human restricted pathogen and the broad host range Typhimurium are also presented.

Salmonella can masterfully alter and adapt host signal transduction networks and vesicle trafficking pathways into favorable environments that are critical for its intracellular lifestyle and resistance to host stresses (42-60). Following oral ingestion, *Salmonella* encounter extreme acidity in the stomach, which activates the acid tolerance response (ATR) thereby allowing survival (13, 61-63). Subsequently, *Salmonella* reach the small intestine, where they encounter a different set of stressors (*ex.,* bile salts, osmotic stress and reduced oxygen levels) which act in concert with other environmental signals to reprogram and prepare the bacterium for invasion and an intracellular lifestyle, which is essential for pathogenesis (60, 62-86). Indeed, *Salmonella* can invade and survive within a variety of host cell types, including epithelial cells and macrophages (80, 87-92). Moreover, *Salmonella* can invade or penetrate the intestinal mucosal barrier by different routes: including uptake by macrophages and CD-18 positive dendritic cells, invasion of intestinal epithelial cells (including enterocytes and M cells of Peyer's patches) (11, 13, 54, 87, 88, 93-95).

The *Salmonella* invasion process results in modification of host cell signal pathways and cytoskeletal rearrangements as the bacterium transforms the intracellular environment from a hostile one into one that it can support productive replication and survival (13, 42). *Salmonella* induced-cytoskeletal rearrangements during the invasion process disrupt the normal epithelial brush border and induce formation of membrane ruffles, resulting in engulfment of bacteria within host intracellular structures called *Salmonella* containing vacuoles (SCVs) (96-100). Invasion is mediated, in part, by a type three secretion system (TTSS) associated with *Salmonella* pathogenicity island (SPI)-1(13, 43, 48, 100-106). The SPI-1 TTSS can be induced by a variety of environmental signals found in the intestinal environment, including osmolarity and oxygen levels, as well as bacterial growth state (85, 86) SPI-1 acts to facilitate *Salmonella* invasion and transmission by engaging in complex cross-talk with host signal transduction pathways that results in induction of intestinal inflammation and release of reactive oxygen (ROS) and nitrogen (NOS) species (107-109). The induction of proinflammatory cytokines facilitates migration of monocytes from the submucosa into the intestinal lumen so that bacteria are internalized by phagocytic macrophages(45, 110).

- *Note* – Unlike Typhimurium, *Salmonella* Typhi does not typically induce intestinal inflammation or diarrhea and often presents without any clinical signs of gastrointestinal distress. Rather, Typhi causes the systemic infection typhoid fever. This difference in disease manifestation is due in large part to expression of a capsular polysaccharide (that is missing in Typhimurium), alterations in LPS, and altered regulation of the SPI-TTSS as compared to Typhimurium (42).

Collectively, these mechanisms allow Typhi to evade detection by components of the innate immune system that mediate host responses against Typhimurium.

Once internalized by host cells, *Salmonella* induce expression of a second TTSS called SPI-2, which secretes proteins that remodel the SCV niche into one that is compatible with bacterial survival and replication – including remodeling of the endosomal membrane which alters vacuolar movement and trafficking in the cell – a process that is essential for bacterial transmission and infection of neighboring cells (13, 42, 43, 55, 59, 60, 92, 111-121). The SPI-2 TTSS is induced in response to conditions encountered in the intraphagosomal environment, including limited nutrients, antimicrobial peptides, acid pH, and low Mg^{2+} concentrations(92, 119-122). Sensing of the SCV intracellular environment and membrane remodeling are also facilitated by the actions of several two component regulatory systems in *Salmonella*, including PhoPQ, PmrA-PmrB, and OmpR-EnvZ, that are expressed under the same conditions that induce SPI-2(42, 123-125).

Salmonella tissue dissemination: The extra-intestinal phase.

Professional phagocytes containing intracellular *Salmonella* travel to mesenteric lymph nodes (MLNs), whereafter the pathogen can be disseminated to systemic organs (13, 126, 127). NTS strains including Typhimurium, are prevented from gaining access to deep tissues by the MLNs, thus infections caused by these strains are self-limiting and restricted to the GI tract (in healthy individuals). However, invasive *Salmonella* pathovars such as Typhi bypass the MLN block and travel systemically through the

circulatory system. These pathovars are carried systemically by macrophages that avoid inflammatory responses in the early stages of infection and ultimately cause secondary infections in other tissues/organs such as the spleen, liver, bone marrow, and gall bladder (13, 127). Hence, Typhi causes systemic infection and establishes chronic carriage in the gall bladder (and possibly other tissues) where they are able to form biofilms on gallstones, thus facilitating their reseeding of the intestine (78, 80, 127, 128). During the course of infection, all *Salmonella* pathovars (regardless of their preferred host niche) are required to survive challenge from a myriad of host stresses, including acid, osmotic, starvation, and various toxic compounds such as bile acids, antimicrobial peptides, and reactive oxygen/nitrogen species (11, 93, 127); thus they alter their cellular responses to those stresses to survive and replicate in the host.

Fluid Shear.

Fluid shear is a biomechanical force that is encountered by pathogens in the infected host and thus an important consideration in experimental design to mimic the infection microenvironment (129-134). The response of microbes to changes in fluid shear has important implications for pathogens, which experience wide fluctuations in fluid shear *in vivo* during infection (129-160). However, the majority of studies have not cultured microbes under physiological fluid shear conditions within a range commonly encountered by microbes during host-pathogen interactions - which can range from high shear levels on blood vessel walls to a low shear environment *in utero* and in the protected environment between the brush border microvilli of epithelial cells (129-134, 136, 138, 141, 142, 147-149, 156, 161-163). The latter environment is particularly

relevant to that encountered by numerous microbial pathogens and commensals during their normal life cycles in the gastrointestinal, respiratory, and urogenital tracts. Understanding the basis of microbial responses to fluid shear forces will provide important insight into their adaptations to physiologically relevant conditions within the host and may lead to the development of novel diagnostics, vaccines and therapeutics. Previous work from our lab has shown that microbial pathogens (including *Salmonella* Typhimurium) respond uniquely to changes in fluid shear and has unveiled novel insight into understanding the infection process at the molecular and phenotypic level (104, 129, 135, 139, 140, 143-146, 150-159, 164, 165). This includes identification of evolutionarily conserved responses that are shared between diverse pathogens to regulate their fluid shear (146, 150, 155, 164). Our lab's studies indicate that there may be entire classes of microbial genes and proteins involved in cellular interactions with the host that have never been identified because they have not been assayed under conditions of physiological fluid shear.

1.3 *Salmonella* Typhimurium responses to fluid shear stress

As mentioned above, during the natural course of infection *Salmonella* experiences dynamic changes in physiological fluid shear stress as it travels throughout the GI tract and in other tissues. At the same time, the pathogen encounters various stressful conditions in the host, including low pH in the stomach and in the acidified phagosome, elevated osmolality in intestine, and bactericidal oxidative stresses.

Understanding how this combination of stressors impacts the pathogenesis of *Salmonella* within the context of physiologically relevant biomechanical forces like fluid shear is a critical area of study to consider. Previous studies by our laboratory have demonstrated that physiological fluid shear alters the virulence, pathogenesis-related stress responses, and gene expression of classic *S.* Typhimurium χ3339, in ways that are not observed during conventional culture (135, 143, 144, 146, 154, 157, 159, 165). In particular, the culture of χ3339 under low fluid shear conditions led to increased virulence, stress-resistance, and alterations in the global gene expression profile. It was subsequently demonstrated that other *Salmonella* serovars including Enteriditis and Choleraesuis are also able to sense and respond to changes in fluid shear in ways that alters their pathogenesis-related stress responses (158). However, the importance of physiological fluid shear in regulating the pathogenesis of strains belonging to the ST313 pathovar has not yet been investigated.

1.4 Specific aims

There are growing numbers of immunocompromised populations worldwide due to HIV infection, drug usage, and cancer therapy (166-171). In addition, there is an increased risk for the spread of the invasive MDR disease caused by ST313 strains outside of sub-Saharan Africa to other regions of the world, as international travel has become easier and more frequent (172-175). These strains are multidrug resistant and as

such, are increasingly more difficult to treat. Thus it is important to find effective ways to control the spread of the invasive disease caused by these invasive *Salmonella* strains.

This study was designed to provide additional understanding of the pathogenesis of ST313 using the strain D23580, a representative ST313 isolate that was recovered at the peak of the 2004 Malawi epidemic of invasive salmonellosis (7, 8, 16).

In this thesis, several key questions are addressed:

I. How does the host tropism of D23580 compare to classic Typhimurium?

a) What is the host tropism of D23580? Does it possess a broad host range similar to Typhimurium, or has the Typhi-like genome degradation found in this strain led to a more host-restricted phenotype?

b) If D23580 is able to cause a lethal infection in mice, how does the lethal dose 50 (LD_{50}) and tissue colonization profile compare to the classic Typhimurium strain SL1344?

c) What other similarities and differences exist between D23580 and classic *Salmonella* pathovars (pathogenesis-related stress responses, biochemical profiles and motility)?

II. Predicting *in vivo* responses using a three-dimensional (3-D) *in vitro* model of human intestinal epithelium containing functional macrophages: how does the colonization profile of D23580 compare to classic Typhimurium and Typhi?

a) How does the presence of functional macrophages alter the infection profile of *Salmonella* pathovars, including D23580?

b) How does the colonization profile of D23580 compare to classic Typhi and Typhimurium?

III. What role does physiological fluid shear play in regulating the pathogenesis of D23580 and how does this compare to what was previously observed for classic Typhimurium strain χ3339?

a) Do changes in fluid shear influence the virulence of D23580 in mice?

b) Do incremental changes in fluid shear progressively alter the pathogenesis-related stress responses of D23580?

c) Do incremental changes in fluid shear progressively alter the adherence, invasion and intracellular survival of D23580 *in vitro*?

d) Do incremental changes in fluid shear progressively alter the global gene expression profile of D23580?

1.5 Chapter Summaries

In **Chapter 2,** it is demonstrated that D23580 shares a broad host tropism with Typhimurium, causing a lethal invasive disease in BALB/C mice. Although it had been shown by another team that D23580 could infect a non-human host, the work presented in this thesis is the first to demonstrate that a ST313 strain can cause a lethal infection in animals and is the first to measure a LD_{50}. These studies also demonstrated that D23580 more rapidly colonizes the spleen and gall bladder with greater bacterial load as compared to classic Typhimurium strain SL1344. These findings were supported by *in*

vitro studies indicating that D23580 is inherently more resistant to acid stress (pH 3.5) and has a greater swimming motility than SL1344, which may contribute to the enhanced dissemination properties of this strain in this host. In addition, it was also determined that D23580 possesses different metabolic characteristics from SL1344.

Chapter 3 builds upon these findings and presents the first *in vitro* study to profile the colonization of D23580 in a 3-D organotypic model of human intestinal epithelium containing functional macrophages. Comparisons between D23580 and the classic Typhimurium and Typhi strains (SL1344 and Ty2, respectively) revealed: **1)** all bacterial strains were recovered at lower levels in the 3-D model containing functional macrophages relative to a monotypic model containing only epithelial cells – thus highlighting the functionality and contribution of the macrophages to the colonization profiles; **2)** despite the similar levels of bacterial adherence observed between SL1344 and D23580, the invasion of D23580 was significantly reduced relative to SL1344; and **3)** D23580 displayed significantly enhanced intracellular survival/replication relative to SL1344 and Ty2. Since ST313 is commonly referred to as 'highly invasive nontyphoidal *Salmonella*', this finding indicates that the ability for the ST313 strain D23580 to spread more efficiently throughout the infected host relative to classic Typhimurium may be due to its inherent survival properties rather than an ability to actively invade at higher levels.

As described above, **Chapters 2 and 3** focused on highlighting key infection properties of D23580 that are distinct from classic Typhimurium and Typhi strains. For these studies, the bacteria were grown under traditional laboratory culture conditions (i.e.

shaking flask culture). In **Chapters 4 and 5**, the importance of physiological fluid shear on the pathogenesis and gene expression of D23580 is reported. This is the first study to investigate the impact of fluid shear on any ST313 strain. Using the Rotating Wall Vessel (RWV) bioreactor, it was found that higher levels of fluid shear led to more rapid time-to-death in mice, increased resistance to select pathogenesis-related stress responses (acid, oxidative and macrophage survival), and altered global gene expression profiles of D23580. The incorporation of beads in the RWV to generate progressively higher levels of fluid shear during culture led to incremental increases in acid, oxidative and macrophage survival. These findings were supported by corresponding gene expression analysis of these cultures using RNA-seq, which determined that several gene groups associated with pathogenesis were up-regulated as a function of higher fluid shear including: fimbrial genes (*fimAIDZ*), *Salmonella* pathogenicity island (SPI) genes (*pipBC*, *spiR*, *sopABE2*, *sipADCB*) and pathogenesis-related regulatory genes (*hilAD* and *invA*). Intriguingly, the responses observed were largely different from what had been previously found for the classic Typhimurium strain χ3339, in which low fluid shear culture in the RWV led to increased virulence and enhanced resistance to select pathogenesis-related stressors (143, 159).

The collective body of work presented demonstrates that D23580 differs from classic *Salmonella* in a number of ways, including physiology, metabolism, cellular responses and infection profiles. Importantly, the biomechanical force of fluid shear was found to distinctly regulate key infection properties of D23580 in a manner that differs

from classic Typhimurium, thus emphasizing the importance of studying this important bacterial pathogen under physiologically relevant culture conditions.

2 CHAPTER 2: CHARACTERIZATION OF THE INVASIVE, MULTIDRUG RESISTANT NONTYPHOIDAL *SALMONELLA* STRAIN D23580 IN A MURINE MODEL OF INFECTION

2.1 Abstract

A distinct pathovar of *Salmonella enterica* serovar Typhimurium, ST313, has emerged in sub-Saharan Africa as a major cause of fatal bacteremia in young children and HIV-infected adults. D23580, a multidrug resistant clinical isolate of ST313, was previously shown to have undergone genome reduction in a manner that resembles that of the more human-restricted pathogen, *Salmonella enterica* serovar Typhi. It has since been shown through tissue distribution studies that D23580 is able to establish an invasive infection in chickens. However, it remains unclear whether ST313 can cause lethal disease in a non-human host following a natural course of infection. Herein we report that D23580 causes lethal and invasive disease in a murine model of infection following peroral challenge. The LD_{50} of D23580 in female BALB/c mice was 4.7×10^5 CFU. Tissue distribution studies performed 3 and 5 days post-infection confirmed that D23580 was able to more rapidly colonize the spleen, mesenteric lymph nodes and gall bladder in mice when compared to the well-characterized *S.* Typhimurium strain SL1344. D23580 exhibited enhanced resistance to acid stress relative to SL1344, which may lend towards increased capability to survive passage through the gastrointestinal tract as well as during its intracellular lifecycle. Further analysis revealed that D23580 displayed higher swimming motility relative to SL1344, S. Typhi strain Ty2, and the ST313 strain A130; a characteristic which may also facilitate rapid systemic spread. Biochemical tests revealed that D23580 shares many similar metabolic features with SL1344, with several notable differences in the Voges-Proskauer and catalase tests, as well alterations in melibiose, citrate, and inositol utilization. These results represent the first full duration infection

study using an ST313 strain following the entire natural course of disease progression, and serve as a benchmark for ongoing and future studies into the pathogenesis of D23580.

2.2 Author Summary

A deadly form of nontyphoidal *Salmonella* has emerged as a major cause of invasive disease in sub-Saharan Africa. Initial genomic profiling of this novel *Salmonella* sequence type, ST313, indicated that although it is technically classified as *S.* Typhimurium (a serovar characterized by a broad host range), it may be evolving towards becoming a more human-specific, 'typhoid-like' pathogen. However, it was recently demonstrated that ST313 strains were indeed able to establish an invasive and damaging infection in chickens. Despite these important findings, it remains unclear whether ST313 is able to cause lethal disease in a non-human host, and as such, there are no data available concerning the median lethal dose (LD_{50}) of any ST313 strain. This is an important metric, as the LD_{50} value will serve as a benchmark for mechanistic studies focused on understanding the relationship between virulence and the phenotypic and molecular genetic attributes associated with ST313 infections. Here we report that D23580 causes lethal disease in BALB/c mice and determined the LD_{50} following peroral challenge. Phenotypic characterization revealed distinct differences in tissue distribution, acid stress resistance, and biochemical utilization between D23580 and the 'classic' Typhimurium strain SL1344.

2.3 Introduction

Infectious diseases caused by multidrug resistant (MDR) pathogens continue to be a major global health crisis and challenge current treatment regimens. Invasive nontyphoidal salmonellae (iNTS) are a leading cause of bloodstream infections in sub-Saharan Africa, and are of serious concern due to high rates of morbidity and mortality coupled with increasing problems of MDR (4, 5, 7, 8, 15-17, 19, 20). iNTS have replaced pneumococcus as the most frequent cause of bacteremia in several countries, with *Salmonella enterica* serovar Typhimurium (*S.* Typhimurium) identified as one of the most common serovars recovered from patients with iNTS infections (5, 7, 8, 15, 16, 19, 20, 24, 176). There is currently no vaccine available for prevention of iNTS disease in humans.

A genetically distinct pathovar of *S.* Typhimurium belonging to a novel multilocus sequence type (MLST) designated as ST313 has emerged as a significant cause of morbidity and mortality among HIV-positive adults and children suffering from malaria, severe anemia and/or malnutrition (7, 8, 10, 15, 16, 18, 177). Case fatality rates are high, ranging from 20 – 25% in children and extend up to ~50% in HIV-infected adults (5, 7, 8, 17, 18, 22, 177). Recurrence of the disease due to recrudescence of the same strain and/or reinfection with a separate iNTS strain occurs frequently, and can lead to high mortality rates over the long term (6, 17). No animal reservoir has been identified thus far for ST313, and it has been suggested that unlike other 'classical' foodborne NTS infections, which are often transmitted via zoonotic routes, ST313 strains

may pass primarily through human-to-human contact (5, 24, 176). Rapid and accurate diagnosis is often hindered by the non-specific clinical symptoms associated with the disease, which most commonly present only as a fever with a subset of patients experiencing splenomegaly (10, 15, 16). There is also a marked lack of gastroenteritis in most cases that is often characteristic of NTS infections (<50% of cases) (7, 16). Moreover, the increasing problem of MDR to commonly used antibiotics including ampicillin, trimethoprim-sulfamethoxazole, and chloramphenicol, presents additional challenges in these impoverished regions, as cost and availability can preclude the use of alternative antimicrobial agents (8, 17). Due to the lack of blood diagnostic facilities in many regions where ST313 infections are the most rampant, treatment using an inadequate antibiotic regimen following a misdiagnosis often fails to combat the infection (16). However, even with the appropriate diagnosis and implementation of a rigorous antibiotic regimen, the average case fatality rates still hover around 25% (8).

There is urgent need to understand the pathogenic strategies used by these deadly iNTS strains to cause disease in order to facilitate the development of novel diagnostic tools and for the design of effective treatments and prevention strategies. In recent years, attention has been given towards understanding the distinctive cellular and humoral immune responses associated with ST313 infections (9, 33-38, 178-181) as well as the unique genotypic and phenotypic characteristics associated with the ST313 pathovar (5-7, 24, 39, 40, 176, 182-186). Kingsley et al. performed MLST profiling of 51 iNTS isolates recovered from Malawi and Kenya during the peak of the Blantyr epidemic and identified ST313 as the dominant genotype responsible for iNTS disease in the region (7).

Whole genome sequencing of D23580, a representative MDR ST313 clinical isolate from a pediatric patient in Malawi, indicated that the strain had undergone genome reduction similar to that of other human-restricted serovars like *Salmonella enterica* serovar Typhi (S. Typhi) (7). D23580 was found to contain a novel prophage repertoire, as well as the presence of a large insertion of MDR genes on the large pSLT-BT plasmid. Importantly, a large number of the pseudogenes and deletions identified are consistent with what has been observed for *S*. Typhi (7). These findings, together with the previous clinical and epidemiological observations, including a routine lack of gastroenteritis and evidence of human-to-human transmission, suggested the possibility that the ST313 pathovar may be evolving towards a more host-restricted phenotype similar to that of *S*. Typhi (7, 39).

Recent studies have confirmed that despite some similarities to *S*. Typhi, D23580 still retains a broad host tropism characteristic of *S*. Typhimurium (39, 40). Tissue distribution studies conducted in chickens by Parsons et al. were the first to demonstrate that D23580 is able to infect chickens and displays an invasive phenotype (39). D23580 colonized the ceca, spleen and liver, and elicited a rapid inflammatory CXC chemokine response in the intestine (39). Comparisons made to ST19 isolates 4/74 and F98 indicated that D23580 invaded deeper into the spleen and liver, and colonized the intestinal tract at lower levels. Subsequent studies conducted by Herrero-Fresno et al. in C57/BL6 mice sought to understand the role of the uncharacterized gene, *st313-td,* in ST313 pathogenesis (40, 182). Competition experiments between the wild type ST313 strain 02-03/002 and the *st313-td* deletion mutant following intraperitoneal (i.p.) challenge indicated that while both the wild type and the mutant were able to colonize the spleen,

deletion of *st313-td* led to a severe decrease in invasiveness. These findings correlated well with human clinical data, wherein the presence of the *st313-td* gene in S. Typhimurium correlated strongly with invasiveness with respect to systemic infection (40). Moreover, it was found that while the presence of the gene did not impact invasion into Int-407 intestinal epithelial monolayer cultures, it did affect survival in J774 macrophages (40). Along these lines, it was recently found that ST313 strains were phagocytosed more efficiently and were highly resistant to killing by macrophages of both human and mouse origin, relative to ST19 isolates (41).

While the previous studies have demonstrated that ST313 strains are capable of causing a systemic infection in both chickens and mice, to our knowledge no study to date has yet assessed the lethality of ST313 in animals. Herein we the report the median lethal dose (LD_{50}) of the ST313 strain D23580 in 8-week-old female BALB/c mice following peroral (p.o.) infection. Comparisons made between the tissue colonization patterns of D23580 and the classic *S.* Typhimurium strain SL1344 revealed distinct differences between the two strains and indicated that D23580 was able to more rapidly colonize the spleen, mesenteric lymph nodes and gall bladder in mice. In addition, several assays including acid stress, motility and biochemical profiling were conducted in order to better understand how these factors could play a role in the pathogenesis of D23580.

2.4 Methods

Bacterial strains and growth conditions.

Bacterial strains used in this study are listed in **Table 2-1** (7, 187, 188). For all animal studies and stress assays, bacterial cultures were initiated in Lennox broth (LB) with aeration (180 rpm) overnight for 15 hours at 37°C. The following day, overnight cultures were inoculated into 50 mL sterile LB at a 1:200 dilution and subsequently grown to late log/early stationary phase at 37°C with aeration. To confirm that all bacterial strains used in animal studies and stress assays were at the same phase of growth for all studies, growth curves were performed for those strains under these conditions by plating on LB agar for viable colony-forming units (CFU) and measuring the corresponding optical density at 600 nm (OD_{600}) **(Figure 1-1).**

Table 2-1. Bacterial Strains

Genus and subspecies	Strain	Characteristics	References
S. Typhimurium	SL1344	Wild-type, (Sm^R)	(188)
S. Typhimurium	D23580	ST313, clinical isolate, ($SmSuCAW^R$, K^S)	(7)
S. Typhimurium	A130	ST313, clinical isolate, ($SuKAW^R$, SmC^S)	(7)
S. Typhi	Ty2	Wild-type, $RpoS^-$,Cys^-,OD_1:H_d:-:Vi, V form	(187)

Sm, streptomycin; Su, sulphonamide; C, chloramphenicol; A, ampicillin; K, kanamycin; W, trimethoprim; ^{R}, resistant; ^{S}, sensitive.

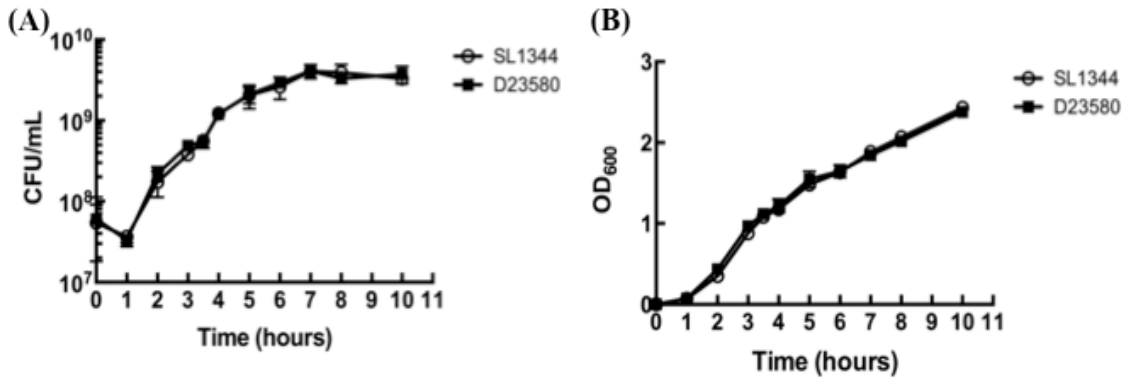

Figure 2-1 Growth curves of D23580 and SL1344.
Bacterial cultures were initiated in LB with aeration (180 rpm) overnight for 15 hours at 37°C. The following day, overnight cultures were inoculated into 5 mL sterile LB at a 1:200 dilution and subsequently grown at 37°C with aeration. Cultures were monitored by plating on LB agar for viable colony-forming units (CFU) and measuring the corresponding optical density at 600 nm (OD600).

Virulence studies.

The virulence of D23580 in 8-week old female BALB/c mice (Charles River Laboratories) was determined by p.o. administration using standard protocols described previously (189). D23580 was cultured to late log/early stationary phase as described above and harvested by centrifugation at 7,000 rpm for 10 minutes. Pellets were resuspended in 1 mL of buffered saline containing 0.01% gelatin (BSG) to a dose of approximately $1x10^9$ CFU per 20 µl. A series of 10-fold dilutions was performed in BSG down to $1x10^2$ CFU per 20 µl dose. Animal inoculations for the determination of the 50% lethal dose (LD_{50}) values were performed as described previously (189). Studies were performed in biological triplicate with five mice per dose. The LD_{50} value was calculated using two of these independent trials, since in the initial trial the dosage was not yet optimized and there was no group with 100% survival, which is a requirement to calculate the median lethal dose using the method of Reed and Muench (190). Time-to-

death (**Figure 1-2**) was plotted to include the results from all three trials. Mice were monitored for up to 30 days for both the LD_{50} and time-to-death studies

Tissue Distribution studies.

Dissemination of D23580 and SL1344 in mice was assessed by separate p.o. inoculations into 8-week old female BALB/c mice. Bacteria were cultured and harvested as described above. Approximately $5x10^8$ CFU per 20 µl was used for inoculating each mouse. Three groups of five mice were infected with D23580, and a matching number of groups with SL1344. Quantitation of viable bacteria in tissues and organs at days 1, 3 and 5 post-infection was performed as described previously [30]. Briefly, mice were euthanized with CO_2, and tissues of interest were promptly dissected and weighed. Bacteria were enumerated from the following tissues/regions: Peyer's patches (7-11 per mouse), intestinal contents, intestinal wall (small and large intestines with Peyer's patches removed), mesenteric lymph nodes (3-5 per mouse), spleen, and gall bladder. Phosphate buffered saline (PBS) was added to a total volume of 1 mL for each isolated tissue, except for intestinal contents and intestinal wall which required resuspension in a total volume of 5 mL PBS. Samples were homogenized with a TissueRuptor (Qiagen) on ice, serially diluted and plated on MacConkey agar plates containing 1% lactose and 20 µg/ml streptomycin in triplicate (both SL1344 and D23580 are resistant to streptomycin). Plates were incubated overnight at 37°C and the number of colonies enumerated the following day. The data represent an average of two independent trials and are presented as mean of either the CFU per gram of tissue or per total organ (for mesenteric lymph

nodes and gall bladder). Statistical comparisons were made using the Mann-Whitney test ($p < 0.05$).

Motility assays.

Bacterial strains were each profiled for swimming motility on plates containing 0.3% top agar and 1.5% bottom agar containing 0.5% NaCl, 1% tryptone and 0.3% glucose. Overnight cultures of each strain were diluted 1:1000 and then spotted onto the agar using a sterile pipette tip. Plates were incubated at 37 °C overnight for 8 hours. Experiments were performed in biological duplicate and technical triplicate.

Acid stress survival assays.

Bacteria were grown as described above to late log/early stationary phase, and immediately subjected to acidic conditions through the addition of a citrate buffer to lower the pH to 3.5. Cells were incubated statically at room temperature during exposure to the stress and the pH was confirmed with an electrode at the end of the assay. Samples were removed at time zero (before the addition of stress) and at various time points thereafter, diluted in phosphate buffered saline (PBS) and then plated on LB agar to determine the numbers of viable CFU. Percent survival was calculated as the number of CFU at each time point divided by the number of CFU at time zero. At least three independent trials were performed. Statistical comparisons were made using the Student's t-test ($p < 0.05$).

Biochemical analysis.

Biochemical analysis of bacterial cultures was performed using the API® 20E kit (bioMérieux, Durham, NC), according to the manufacturer's instructions. The citrate test results were confirmed by using Simmons citrate media. A needle containing pure bacterial culture was tabbed twice into Simmons citrate agar slant media, and then streaked from the base of the tube up along the surface of the slant. For the catalase test, bacterial colonies of each strain were picked from plates grown overnight at 37 °C on sterile polystyrene plastic petri dishes (USA Scientific). One to two drops of hydrogen peroxide was then added simultaneously to each strain and immediately imaged for bubble formation as evidence of catalase activity.

2.5 Results

2.5.1 Virulence of D23580.

To assess the lethality of D23580 in mice, we performed p.o. inoculations of eight-week-old female BALB/c mice with a series of doses ranging from 10^9 to 10^2 CFU per dose, with five mice per dose. Results shown in **Figure 2-2** correspond to representative data from three independent virulence assays. The LD_{50} following p.o. infection was 4.75×10^5 CFU. This is a similar LD_{50} compared to what has been previously reported for SL1344 in BALB/c mice using bacteria cultured to the same phase of growth and a p.o. route of infection ($1.2 \times 10^5 – 1.3 \times 10^5$ CFU) (191, 192).

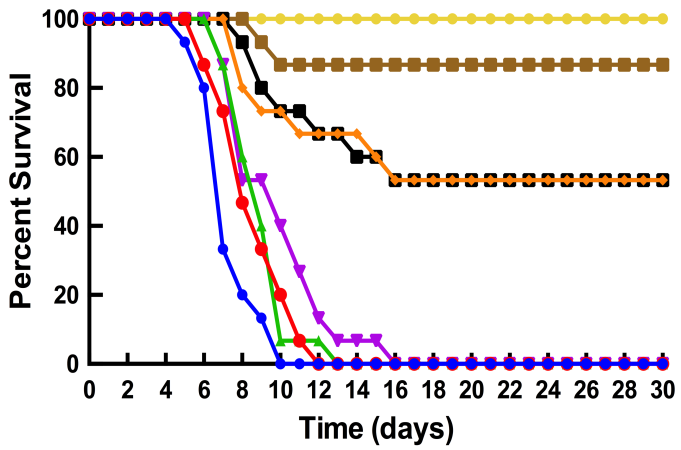

Figure 2-2. Survival of mice following peroral infection with D23580. D23580 was cultured to late log phase and administered p.o. to 8-week-old female BALB/c mice at inoculum titers ranging from 10^2 – 10^9 CFU per dose. The data shown represent the combined results from three independent trials. The median lethal dose was determined by the method of Reed and Muench (190) using two of these independent trials (see Methods section). The percent survival is defined as the percentage of mice surviving at the indicated number of days post-infection.

2.5.2 Tissue distribution of D23580 relative to SL1344.

To assess the pattern of systemic spread of D23580 in mice following p.o. infection relative to the well-characterized *S.* Typhimurium strain SL1344, we infected groups of eight-week-old female BALB/c mice with either D23580 or SL1344 at 5 x 10^8 CFU per dose and determined the CFU of the two strains in several different tissues. Quantitation of viable bacteria in tissues and organs at days 1, 3 and 5 post-infection was performed for the following: intestinal contents, Peyer's patches, intestinal wall (small and large intestine excluding Peyer's patches), mesenteric lymph nodes, spleen, and gall bladder. **Figure 2-3** shows the results from 3 and 5 days post-infection, as no differences were observed one day post-infection (data not shown). At Day 3, no statistical differences were observed in the colonization of the Peyer's patches of D23580 compared to SL1344 (**Figure 2-3 A** $p = 0.2396$), although a slight upward trend could be observed

for D23580. Similarly, in the mesenteric lymph nodes an increased trend could be observed for D23580, but the differences were not statistically significant (**Figure 2-3 B;** 81.3-fold, $p = 0.1056$). However, D23580 exhibited an enhanced ability to colonize the spleen relative to SL1344 (**Figure 2-3 C**; 56.8-fold, $p < 0.05$). No significant differences were observed for the intestinal contents or intestinal wall (excluding Peyer's patches, data not shown), or for the gall bladder on day 3 (**Figure 2-3 D**).

By Day 5, D23580 was still present at significantly higher levels in the spleen (**Figure 2-3 C**; 54.9-fold, $p < 0.01$) and had spread to the gall bladder at higher counts relative to SL1344 (**Figure 2-3 D;** 14.4-fold, $p < 0.05$), which is a hallmark of Typhi infections. The enhanced ability for D23580 to reach the deeper tissues like the spleen and gall bladder as compared to a strain belonging to the ST19 pathovar (SL1344) is consistent with previous findings by Parsons et al. that found the ST19 isolates 4/74 and F98 were slower to invade into the spleen and liver of chickens than D23580 (39).

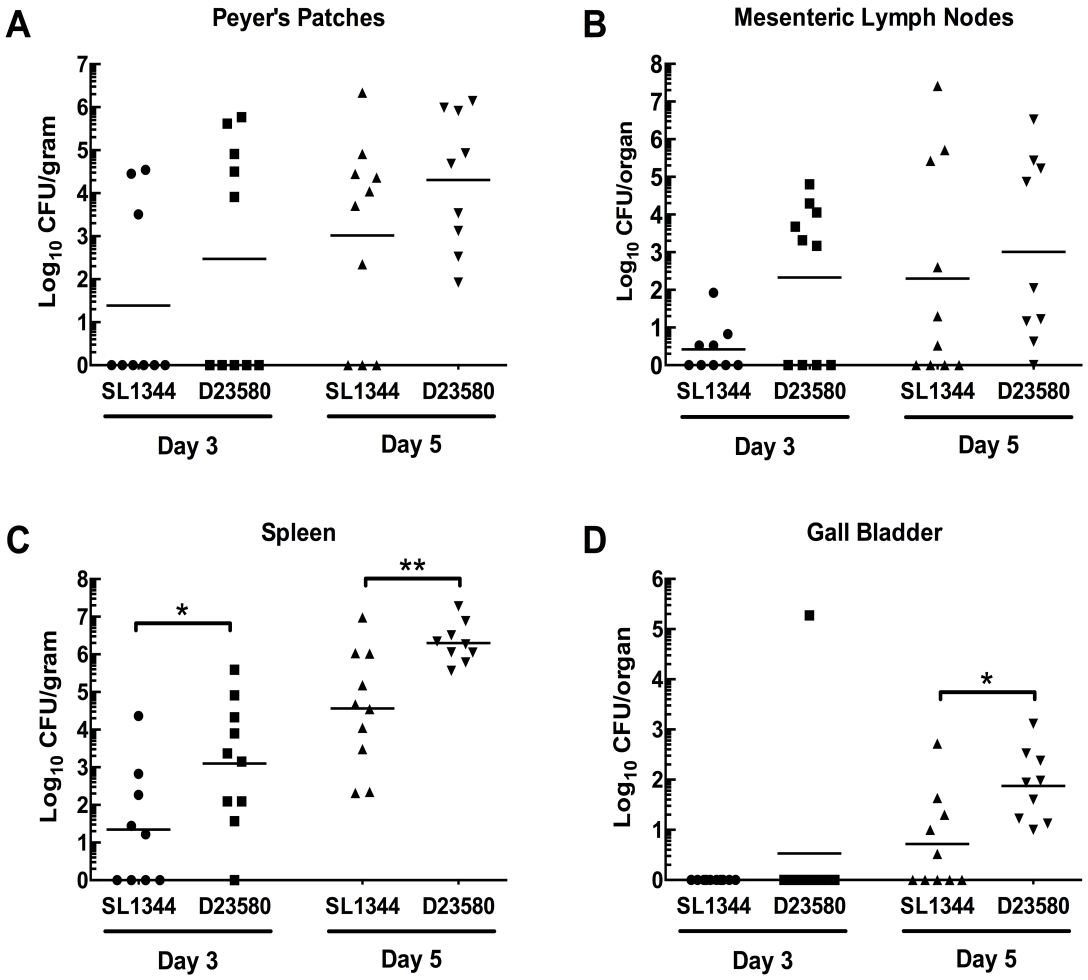

Figure 2-3. Tissue distribution of D23580 in mice following peroral infection.
D23580 cultured to late log phase was administered perorally to 8-week-old female BALB/c mice at 108 CFU per dose. Peyer's patches (A), mesenteric lymph nodes (B), spleen (C) and gall bladder (D) were excised at 3 and 5 days after peroral infection. Five mice were euthanized at each time point per experiment. The data represent an average of two trials and are presented as the mean of either the CFU per gram of tissue or per total organ (for mesenteric lymph nodes and gall bladder). The horizontal bar indicates geometric means and statistical comparisons were made using the Mann-Whitney test (** indicates $p < 0.01$; * indicates $p < 0.05$).

2.5.3 Acid stress resistance.

We considered that D23580 might be recovered in higher numbers from the gallbladder, spleen and MLNs as compared to SL1344 due to increased resistance to environmental stresses normally encountered in these tissues. Thus, to identify potential phenotypic traits of D23580 that may confer a selective advantage for its enhanced dissemination into these tissues as compared to SL1344, we profiled the ability of these two strains to resist low pH, a physiologically relevant stressor normally encountered by *Salmonella* both during transit through the stomach and during intracellular lifestyle within the host (61, 62, 69, 193-195). As shown in **Figure 1-4**, D23580 displayed enhanced resistance to pH 3.5 than SL1344 for all time points tested ($p < 0.05$).

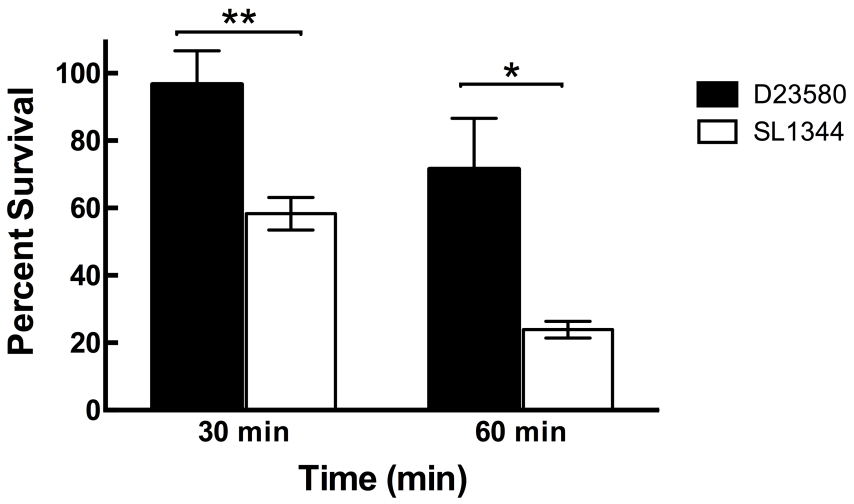

Figure 2-4. Survival of D23580 an SL1344 at pH 3.5.
D23580 (black bars) and SL1344 (white bars) were cultured to late log phase, and immediately subjected to acidic conditions through the addition of a citrate buffer to lower the pH to 3.5. Samples were removed at time zero (before the addition of stress) and at various time points thereafter, diluted in phosphate buffered saline (PBS) and then plated on LB agar to determine the numbers of viable CFU. Percent survival was calculated as the number of CFU at each time point divided by the number of CFU at time zero. At least three independent trials were performed. Statistical comparisons were made using the Student's t-test (** indicates $p < 0.01$; * indicates $p < 0.05$).

2.5.4 Motility.

The swimming motility of D23580 was profiled and compared to SL1344. For a broader comparison, we also included ST313 strain A130 and typhoidal strain Ty2. A130 is a chloramphenicol sensitive ST313 isolate recovered in 1997, prior to the emergence of the full MDR phenotype found in D23580 (7). As shown in **Figure 1-5**, D23580 exhibited the highest swimming motility of all strains profiled. This heightened motility was not conserved across all ST313 isolates, as A130 appeared to be much less motile.

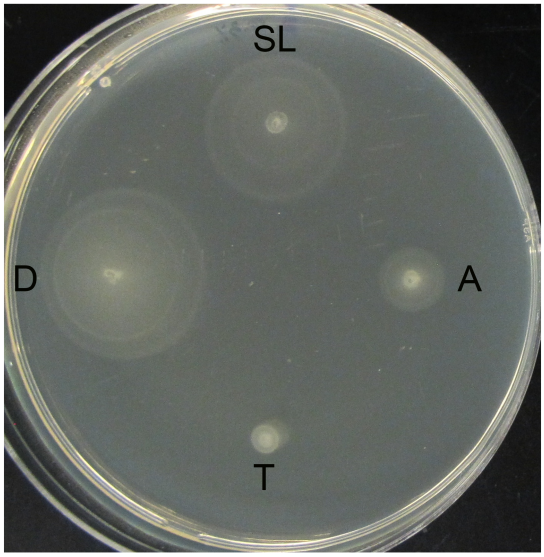

Figure 2-5. Swimming motility of ST313 strains relative to classic NTS and typhoidal strains.
Salmonella strains D23580, A130, SL1344, and Ty2 (identified as D, A, SL, and T respectively in the figure) were each profiled for swimming motility on agar plates containing 0.3% agar, 0.5% NaCl, 1% tryptone. Overnight cultures of each strain were diluted 1:1000 and then spotted onto the agar using a sterile pipette tip. Plates were incubated in RT overnight for 30 hours. Experiments were performed in biological duplicate and technical triplicate.

2.5.5 Biochemical profiling.

The flexible metabolic capabilities that are characteristic of enteric pathogens like *Salmonella* may confer a selective advantage during colonization of host tissues (196). During their natural life cycle, salmonellae adapt to a wide variety of environmental niches both inside and outside of the host that vary in nutrient availability. Understanding the biochemical features that distinguish D23580 from other NTS strains may provide insight into selective pressures influencing its ability to colonize and spread within the infected host. **Table 2-2** shows the results of the biochemical assessment. The data obtained for D23580 and SL1344 showed identical results for the ornithine decarboxylase, hydrogen sulfide production, and rhamnose and arabinose fermentation/ oxidation tests.

Table 2-2. Biochemical characterization

	Test	iNTS		NTS	Typhi
		D23580	A130	SL1344	Ty2
	CAT	$+^{w}$	$+^{w}$	+	–
	ONPG	–	–	–	–
a.a. DC	ADH	+	+	+	+
	LDC	+	+	+	+
	ODC	+	+	+	–
	CIT	+	+	–	–
	H2S	+	+	+	$+^{w}$
	URE	–	–	–	–
	TDA	–	–	–	–
	IND	–	–	–	–
	VP	$+^{w}$	$+^{w}$	–	–
	GEL	–	–	–	–
Carbohydrate fermentation	GLU	+	+	+	+
	MAN	+	+	+	+
	INO	+	+	–	–
	SOR	+	+	+	+
	RHA	+	+	+	–
	SAC	–	–	–	–
	MEL	–	+	+	+
	AMY	–	–	–	–
	ARA	+	+	+	–

Abbreviations: DC: amino acid decarboxylation; CAT: catalase; ONPG: ortho-Nitrophenyl-β-galactoside; ADH: arginine dihydrolase; LDC: lysine decarboxylase; ODC: ornithinine decarboxylase; CIT: citrate utilization; H2S: hydrogen sulfide production; URE: urease - Urea hydrolysis; TDA: tryptophan deaminase; IND: indole production- tryptophanase; VP: Voges Proskauer - acetoin production; GEL: gelatinase; GLU: glucose fermentation / oxidation; MAN: mannitol fermentation / oxidation; INO: inositol fermentation / oxidation; SOR: sorbitol fermentation / oxidation; RHA: rhamnose fermentation / oxidation; SAC: saccharose fermentation / oxidation; MEL: melibiose fermentation / oxidation; AMY: amygdalin fermentation/oxidation; ARA: arabinose fermentation/ oxidation. The w indicates weak positive reaction.

There were striking differences that distinguished D23580 and A130 from other *Salmonella* strains tested. One difference was the ability of both ST313 strains to

ferment inositol, while SL1344 and Ty2 were unable to use this carbohydrate as a sole carbon source. Inositol is produced naturally in the human body, and is found at high levels in the human brain (197), and is also found in certain foods like beans, rice and cereals as well as in soil. While certain *Salmonella* strains have the capability to utilize inositol as a carbon source, it is not ubiquitous (198). Along these same lines, we also found that D23580 was unable to ferment melibiose, a sugar most commonly found in plants, especially legumes. In contrast, all other *Salmonella* strains, including A130, were still melibiose positive. Interestingly, although approximately 95% of *Salmonella* species are melibiose fermenters, it has been previously reported that a loss in the ability to utilize the sugar strongly correlated with clinical isolates that were associated with a *Salmonella* Enteriditis outbreak (199). The Voges-Proskauer (VP) reaction, which is typically negative for *Salmonella* spp., was found to be weakly positive for D23580 and A130. This result indicates that these strains may be capable of fermenting sugars to pyruvate via the butylene glycol pathway, which produces neutral end products, including acetoin and 2,3-butanediol. This is in contrast to other *Salmonella* pathovars, which typically produce acidic end products and as such, SL1344 and Ty2 tested negative in the VP reaction. Both D23580 and A130 presented positive reaction for the citrate test, indicating the ability for these strains to utilize citrate as the sole carbon source, while all other strains tested were negative. These results were confirmed utilizing Simmons' citrate medium. Catalase tests revealed that while SL1344 displayed a strong positive reaction to hydrogen peroxide, both D23580 and A130 showed an extremely weak reaction, which was confirmed by performing a heavier bacterial inoculation as well (**Figure 2-6**). This phenotype was similar to what was observed for Typhi strain

Ty2, which is a naturally occurring *rpoS* mutant and thus impaired in its ability to produce catalase and resist killing by hydrogen peroxide (RW.ERROR - Unable to find reference:354).

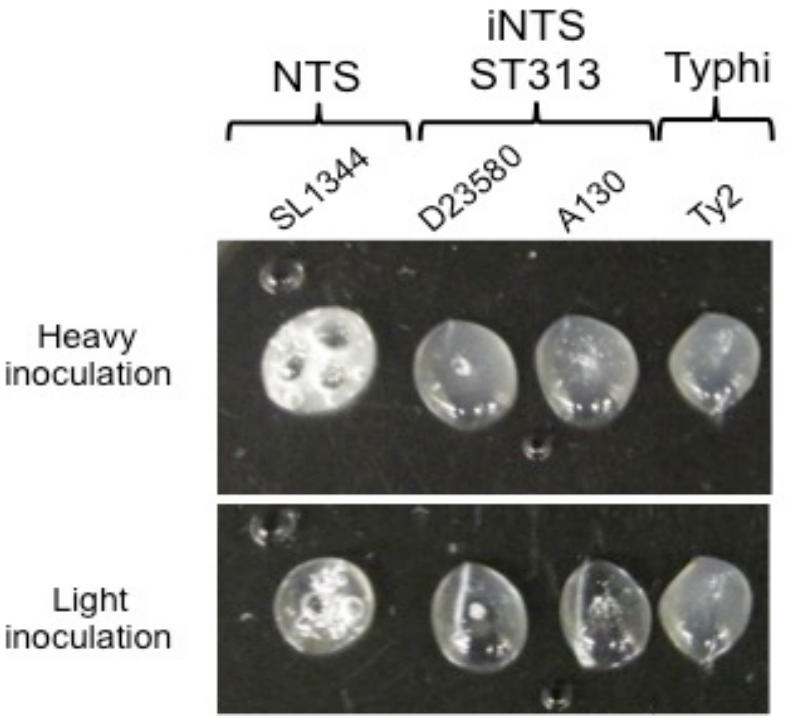

Figure 2-6 ST313 strains display a weakly positive catalase reaction
Bacterial colonies of each strain (D23580, SL1344, A130 and Ty2) were picked onto sterile polystyrene plastic petri dishes from plates grown overnight at 37 °C. One to two drops of hydrogen peroxide was then added simultaneously to each strain and immediately imaged for bubble formation.

2.6 Discussion

Salmonella remains one of the best-characterized microbial pathogens; however we still have limited knowledge regarding the distinct pathogenesis mechanisms

associated with human infections, including the invasive, MDR ST313 pathovar that has been responsible for an outbreak of iNTS infections in sub-Saharan Africa. Although genomic analysis of multiple ST313 strains, including D23580, initially indicated the possibility that this pathovar may be evolving more towards a more host-restricted phenotype like that of *S.* Typhi due to the presence of multiple gene deletions and inactivations (7), a subsequent study confirmed that D23580 and a different ST313 strain, Q456, were not host-restricted and caused an invasive disease in chickens (39). However, no one has yet assessed the potential lethality of any ST313 strain in a non-human model.

In this study, we demonstrate that D23580 indeed causes a lethal disease in eight-week-old female BALB/c mice infected via the peroral route, with a median lethal dose of 4.75×10^5 CFU. This LD_{50} value is close to what was previously reported for the well-characterized *S.* Typhimurium ST19 strain SL1344 (191, 192). This finding is especially intriguing, given that D23580 spread more rapidly than SL1344 into deeper tissues of the mice, including the spleen and gall bladder; a finding which is in line with previous reports demonstrating that D23580 spread faster to the spleen than ST19 strains F98, and 4/74 in chickens (39). In this study, we did not observe any statistical difference between D23580 and SL1344 in the initial colonization of the Peyer's patches or intestinal walls (devoid of Peyer's patches), indicating that the inherent differences between the dissemination of D23580 and SL1344 in the mouse model of infection is most likely not due to differences in the initial adherence/invasion of the pathogens to the intestinal epithelium. It is likely that the differences observed in the systemic

colonization of D23580 within the mouse are multifactorial, including a combination of differences in stress resistance, survival and replication. A recent study by Ramachandran et al (41) found that D23580 survived better than SL1344 in macrophages. This trend was similar across multiple ST313 and ST19 strains profiled. Moreover, it was also found that macrophages infected with either ST313 strain D65 or ST19 strain I77 led to an induction of more proinflammatory cytokines and increased apoptosis in macrophages infected with I77 relative to those infected with D65. These factors may account for the dissemination differences between D23580 and SL1344.

During the course of infection, *Salmonella* encounters a variety of potentially lethal stressors that can alter its pathogenesis, replication and survival. The ability of the pathogen to resist these environmental insults can have a profound impact on the duration and severity of the infection. In this study, we profiled the ability of D23580 to survive exposure to low pH and found that D23580 displayed an enhanced resistance to acid stress relative to SL1344 *in vitro*. *Salmonella* encounters harsh acidic environments in the host, during its transit through the stomach as well as within the macrophage phagolysosome. There is previous evidence suggesting a correlation between the acid tolerance response in *S*. Typhimurium and virulence (65, 193, 194, 201). As mentioned, no reservoir has yet been identified for the ST313 pathovar, and it has been suggested that the mode of transmission may be person-to-person rather than via the food-borne route (5, 24). Certain pathogens like *Shigella*, which are predominantly transmitted person-to-person, tend to possess a high resistance to acid killing in order to survive low gastric pH and other acidic environments *in vivo* (202-204). It is possible that the

increased acid stress resistance of D23580 may be one pathogenesis-related factor that could help to facilitate person-to-person transmission. Future investigations into the role of acid resistance in the pathogenesis of D23580 and other ST313 isolates may provide additional insight in this regard.

D23580 was also found to exhibit a greater swimming motility than all strains profiled in this study. The importance of motility for the virulence of *S. enterica* appears to depend on a variety of factors, including the type of host as well as the local microenvironment during infection (205-209). In mouse models of systemic infection with *S*. Typhimurium, while motility appears to regulate some aspects of pathogenesis, it does not appear to be important for virulence (191, 205, 209). However, in streptomycin-pretreated mice (which serve as a model of colitis) motility was shown to play a role in colonization and in the induction of colitis (210). Similarly, in 1-day old chicks it was demonstrated that motility was important for both the virulence of *S*. Typhimurium as well as its persistence in the liver and spleen (211). In a calf model of enterocolitis, flagella were found to be required for maximum fluid secretion and for the influx of polymorphonuclear leukocytes during infection (209). *In vitro* infection assays have also been used to profile the impact of motility on the ability for *S*. Typhimurium to attach and invade into cells (206, 208, 209, 212-215). While many of these infection studies using flat 2-D monolayer cultures have indicated that the motility is important for the colonization of the intestinal epithelium, a recent study using our 3-D organotypic model of human intestinal epithelium revealed that an *flhDC* flagellar mutant was still able to actively invade at much greater levels than in 2-D monolayers without the need for

centrifugation during the adherence step, although still to a lesser extent than wild type (104) .

Of particular relevance to ST313 strains, it was previously found that the physiological origin of clinical isolates might also impact motility in that *S.* Typhi clinical isolates of blood-borne origin displayed a significantly higher swimming motility than stool-borne strains (216). In addition, a previous study reported that while flagella-mediated motility was not required for invasion, it does lead to enhanced invasion although it was not absolutely required for invasion to occur (208). Thus it is possible that the greater motility observed in this study for D23580 may be associated with the enhanced tissue distribution in systemic mice organs as compared to SL1344. D23580, which is blood-borne in origin, displayed enhanced motility in our present study relative to other strains profiled. However, in our present study we observed a sizeable difference in the motility between the blood-borne ST313 clinical isolates, D23580 and A130, in that A130 was much less motile. A recent comparative study of several ST313 strains (S12, Q55, D65, and S11) with ST19 strains (I77, S52, I41, and I89) found that the ST313 strains were significantly less motile and produced less flagellin than the ST19 strains (41). Additional studies are needed to better understand the potential role of this enhanced response on the infection properties of D23580.

In an effort to identify possible metabolic characteristics of D23580 associated with its enhanced ability to reach deep tissues in mice following p.o. infection, we performed a series of biochemical analyses to identify differences between this ST313

strain and classic *Salmonella* pathovars. Key differences were observed for D23580 for three biochemical tests, including melibiose and inositol utilization and the Voges-Proskauer test. In particular, it is intriguing that both ST313 strains were able to use inositol, since 1) increased inositol levels are found early in the course of HIV-related brain disease (217) and ST313 infections in adults are strongly associated with HIV infected individuals (17, 18, 177), and 2) inositol metabolism is important for the intraerythrocytic development of the malarial parasite *Plasmodium falciparum* (218) and infants with malaria are at high risk for ST313 infections (7, 15, 219). In addition to the differences described above, D23580 was also the only strain unable to use melibiose – a distinct characteristic that has been associated with another clinical outbreak (199), and may be useful for discriminating isolates during biotyping. Collectively, these observations may provide clues for future studies into the metabolic adaptation and pathogenic mechanisms of ST313 strains.

Summary - Chapter 2:

This chapter reports (i) the virulence and tissue distribution profiles of the multidrug resistant, invasive nontyphoidal *Salmonella* (NTS) strain D23580 in a murine infection model, and (ii) the similarities and differences in pathogenesis-related stress responses and metabolic profiles between D23580 and classic *Salmonella* Typhimurium and Typhi pathovars, SL1344 and Ty2, respectively.

- ✓ The LD_{50} of D23580 in female BALB/c mice following peroral infection was 4.7 x 10^5 CFU.
- ✓ D23580 can cause a lethal infection in animals, BALB/C mice, with associated invasive disease, thus sharing a broad host tropism with Typhimurium.
- ✓ D23580 more rapidly colonized the spleen and gall bladder with greater bacterial load as compared to classic Typhimurium strain SL1344.
- ✓ D23580 exhibited enhanced acid stress resistance and motility, relative to SL1344, which may contribute to the enhanced dissemination properties of this strain *in vivo*.
- ✓ D23580 possesses different metabolic characteristics from SL1344, which may be important for survival and dissemination its environmental niche *in vitro* and *in vivo*.

Next, we built upon these findings to understand how D23580 may cause infection in the human host (Chapter 3).

3 CHAPTER 3: THREE-DIMENSIONAL CO-CULTURE MODEL OF INTESTINAL EPITHELIAL CELLS AND MACROPHAGES REVEALS DISTINCT COLONIZATION PROFILES OF *SALMONELLA* TYPHIMURIUM D23580

3.1 Abstract

Macrophages are a key immune cell type targeted by *Salmonella* during infection and intracellular survival in these cells is essential for bacterial virulence. However, intestinal epithelial cell cultures used to model human enteric salmonellosis commonly do not include macrophages. This is an important consideration, as cultures of either epithelial cells or macrophages alone can respond differently to infection with pathogens or treatment with their toxins as compared to co-culture models containing both of these cell types, the latter of which have yielded synergistic phenotypes that are more reflective of the *in vivo* host response. Herein, the contribution of macrophages to the early stages of salmonellosis was analyzed using immunocompetent three dimensional (3-D) co-culture models of human colonic epithelial cells (HT-29) and functional macrophages (U937) capable of phagocytosis. Specifically, these 3-D models were applied to study the colonization of *Salmonella enterica* pathovars with different host adaptations and disease phenotypes, *i.e., S.* Typhimurium strains SL1344 and multidrug resistant D23580, and *S.* Typhi Ty2. All serovars demonstrated significantly decreased adherence, invasion and intracellular survival in the co-culture model (epithelial cells and macrophages) relative to the monotypic model (epithelial cells only), indicating the contribution of macrophages to the infection process. Interestingly, Typhi showed an even greater decrease in adherence to the co-culture model when compared to Typhimurium pathovars. Interestingly, D23580, a ST313 strain reported to be highly invasive with genetic similarity to *S.* Typhi, exhibited lower invasion into both 3-D models than SL1344, but higher intracellular survival as compared to either SL1344 or Ty2. Co-

localization studies indicated that D23580 associated with both epithelial cells and macrophages in the co-culture model in a distribution manner that was different from both classic Typhimurium and Typhi. This distinct phenotype observed using physiologically relevant *in vitro* co-culture models may contribute to the perceived "highly invasive" phenotype of D23580 in infected humans. Collectively, these data show that the immunocompetent 3-D co-culture model could distinguish between challenge with Typhimurium and Typhi pathovars in key ways that differed from the monotypic model comprised solely of epithelial cells, thus reinforcing the importance of using in *vitro* infection models that recapitulate the multicellular complexity normally encountered by *Salmonella* during enteric infection.

3.2 Introduction

3.2.1 *Salmonella* Typhimurium ST313 - infection properties

During the devastating epidemic of invasive Salmonellosis caused by nontyphoidal *Salmonella* in sub-Saharan Africa, many infections were linked to a genetically distinct pathovar of *Salmonella enterica* serovar Typhimurium ST313, which had undergone genome degradation to resemble that of host-adapted *Salmonella* Typhi (Typhi) (5, 7, 176, 177, 184, 186). *Salmonella* Typhimurium, the most common serovar associated with these iNTS infections, is classified as a generalist in terms of its host specificity, causing disease in a wide range of hosts, including humans, associated with self-limiting gastroenteritis in healthy individuals but capable of causing systemic disease in the immunocompromised. Conversely, Typhi is a human-specific pathogen that causes the systemic illness, typhoid fever, and is generally considered to be more invasive than Typhimurium (12, 127) (there is current evidence suggesting that this may not be the case (220)). There is thus concern that ST313 may be evolving toward a human-specific adaptation resembling that of *S.* Typhi (5, 6, 176). However, very limited information is available regarding the host-pathogen interaction characteristics and host specificity of ST313.

In Chapter 2, D23580 was shown to exhibit key differences in its stress-resistance, biochemical characteristics and bacterial load in mouse tissues as compared to classic Typhimurium strain SL1344. In agreement with the observed increased D23580

bacterial load in mouse tissues (chapter 2), a rapid and enhanced invasion of ST313 as compared to classic Typhimurium was also recently reported in the chicken model (39), and that suggested the host tropism of ST313 is more akin to Typhimurium with more aggressive disease phenotype. However, the lack of reports of ST313 in animal infection studies (24) and the prevalent invasive disease dominated by iNTS ST313 in Africa (5, 8, 15-18, 182, 184), mostly associated with immunecompromised people, suggest distinct host-specific interactions between the iNTS ST313 and humans. Thus, understanding the interaction between D23580 and the intestine (initial site of pathogenesis) will provide insight into the early stages of enteric infection and advance our knowledge of disease mechanisms used by this pathogen, which may ultimately contribute to development of effective ways to control infection. The application of *in vitro* 3-D tissue culture models that closely mimic key aspects of the human intestinal mucosa can help us to investigate disease mechanisms in enteric pathogens such as D23580.

3.2.2 *In vivo*-like three-dimensional (3-D) cell culture model of intestinal epithelium in the Rotating Wall Vessel (RWV) bioreactor

The RWV bioreactor is a physiological low fluid shear culture system that is commonly used to establish highly differentiated 3-D cell culture models, including both monotypic (comprised of a single cell lineage) and co-culture models (containing multiple cell lineages) (104, 160, 221-231). The RWV has previously been used to establish 3-D monotypic intestinal models comprised of epithelial cells for the study of *Salmonella* and other enteric infections (160, 222, 225, 228-230). The underlying concept

of the RWV is that cells seeded into these reactors can grow in three-dimensions, aggregate based on natural cellular affinities (thereby facilitating co-culture of multiple cell types), and differentiate into 3-D tissue-like assemblies (232, 233). The cells are grown on porous extracellular matrix (ECM)-coated microcarrier beads which serve as scaffolds upon which they adhere, thereby allowing cells to respond to chemical and molecular gradients in three dimensions (i.e. at their apical, basal, and lateral surfaces) akin to the *in vivo* scenario (160, 224, 229, 234-240). When completely filled with medium, the continuous horizontal rotation of the RWV maintains cells in an optimized low fluid-shear suspension culture environment, which is optimal for cell growth and differentiation (130, 132, 137, 138, 161, 162). Also, the fluid shear levels in the RWV are physiologically relevant to those encountered by enteric pathogens (like *Salmonella*) in the intestinal tract, between the brush border microvilli (132).

We previously used the RWV to establish highly differentiated 3-D intestinal models derived from human epithelial cell lines and demonstrated their ability to predict *in vivo* infection observations and *Salmonella* pathogenic mechanisms (89, 104, 160, 229). While initiated from a single cell type, these monotypic models spontaneously differentiated into multiple epithelial cell types normally found in the intestine, including enterocytes, goblet cells, Paneth cells, and M/M-like cells, while exhibiting extensive tight junction formation, apical and basolateral polarity, and mucin production (89, 104, 160, 221, 229). Following infection with *S*. Typhimurium, these 3-D epithelial-based models exhibited phenotypes that were consistent with *in vivo* infections in animals and humans, including alterations in tissue morphology, adherence, invasion, apoptosis, and

production of cytokines and other inflammatory mediators (104, 160, 221, 229). Moreover, *S*. Typhimurium invaded the 3-D intestinal cells independently of all known *Salmonella* type three secretion systems (TTSSs), i.e. *Salmonella* pathogenesis island (SPI) -1, SPI-2, and the flagellar secretory system, a finding that paralleled *in vivo* infection observations in both animals and humans, and challenged the classical view that SPI-1 is required for invasion of intestinal epithelium (48, 92, 106, 241). Collectively, these findings demonstrate the utility of these models in predicting *in vivo*-like pathogenic mechanisms.

These results led us to postulate that our 3-D monotypic intestinal model could serve as a high fidelity platform for engineering an improved model which is able to further recapitulate the multicellular complexity normally encountered by *Salmonella* during enteric infection.

3.2.3 Immunocompetent 3-D co-culture model of human intestinal epithelial cells in combination with macrophages

Following ingestion, *Salmonella* actively invade and replicate within intestinal epithelial cells and are phagocytosed by macrophages upon crossing the epithelial barrier, at which time they exploit phagocytes as a preferred niche for replication and transport (44). While studies using a single cell type (monotypic) cultures of either intestinal epithelial cells or macrophages have provided important insight into understanding the

interactions between *Salmonella* and the host tissue that occur during enteric infection (43, 45, 57, 92, 242), they lack the multicellular complexity that is important for the differentiated structure and function of the *in vivo* parental tissue which is naturally encountered by the pathogen during infection (221, 243). Importantly, the synergistic interaction between epithelial cells and macrophages has been shown to be important for driving the differentiation of both cell types (244-246). It is thus not surprising that monotypic cultures of either epithelial cells or macrophages have been shown to respond differently to infection with pathogens or treatment with microbial toxins as compared to co-culture models containing both of these cell types, the latter of which is more reflective of the conditions encountered *in vivo* during the natural course of infection (243, 247-251). Moreover, *in vivo* and *in vitro* studies have shown that macrophages may contribute to *Salmonella*-host specificity, and are able to distinguish between the closely related pathovars *S.* Typhimurium and *S.* Typhi, although these studies have shown inconsistent trends, likely due to experimental design differences (12, 252).

Recently, our lab advanced the previously described 3-D intestinal epithelial model (derived from HT-29 colon cells) by incorporation of functional macrophages (activated U937 cells) capable of phagocytosis in order to better replicate the *in vivo* tissue microenvironment naturally encountered by *Salmonella* during enteric infection (manuscript in preparation).

3.2.4 Application of the 3-D co-culture model for infection studies with D23580.

Previous infection studies with ST313 utilized animal infection models (chicken and mice) or monolayers of either epithelial cells or macrophages (39-41). In this study, we applied the 3-D immunocompetent co-culture model to assess the impact of macrophages in the context of colonic epithelium on the colonization profiles of *Salmonella enterica* pathovars with different host adaptations and disease phenotypes. Specifically, we characterized colonization profiles (adherence, invasion, and intracellular survival) of the closely related pathovars, *S.* Typhimurium (SL1344 and D23580) and *S.* Typhi (Ty2). For all studies, comparisons were made between the 3-D co-culture model (HT-29 and U937) and the 3-D monotypic model (HT-29). While D23580 did not exhibit a highly invasive phenotype during infection of our highly differentiated co-culture model, it did show enhanced intracellular survival as compared to the other *Salmonella* strains tested, which may provide insight as to its perceived highly invasive phenotype. Moreover, differential intracellular survival of both Typhimurium strains as compared to Typhi suggests that the co-culture models could distinguish between these pathovars and may represent a useful model for host-specific testing.

This study represents an important application of utilizing a 3-D intestinal epithelial co-culture model that integrates immune cells to mimic the multicellular complexity of the parental tissue to enhance our understanding of the synergistic contribution of different cell types in the context of enteric host-pathogen interactions. In

this chapter, I report contribution of intestinal macrophages in *Salmonella* infection and distinct infection trends of *Salmonella* pathovars in the immunocompetent 3-D co-culture model. Specifically, I highlight that D23580 exhibits adherence similar to Typhimurium, invasion similar to Typhi, and distinct intracellular survival and co-localization profiles within host epithelial cells and macrophages as compared to the other strains

3.3 Materials and methods

Bacterial strains and growth conditions

Salmonella enterica serovar Typhimurium SL1344, *S.* Typhimurium ST313 D23580, *S.* Typhi Ty2 (Ty2), and *Escherichia coli* HB101 (HB101) were used in this study. HB101 served as a non-invasive control that does not survive intracellulary. Bacterial cells were grown in Lennox broth (LB) overnight with aeration at 180 rpm at 37°C. The overnight was diluted 1:100 in fresh LB media, subsequently grown to late log phase of the growth at 37 °C at 180 rpm, and immediately subjected to the infection assays.

Cell lines and culture conditions.

The human colonic adenocarcinoma cell line HT29 (ATCC, HTB-38) and the human monocytic cell line U937 (ATCC, CRL-1593.2) (253) were obtained from the American Type Culture Collection (ATCC, Manassas, VA). For all studies, the cells were cultured in GTSF-2 media (Hyclone) at 37°C in 10% CO_2 as described previously by Höner zu Bentrup et al. (229). GTSF-2 media is formulated using Leibovitz-15 minimum essential medium supplemented with glucose, galactose, fructose, 10% fetal bovine serum (FBS), 2.5 mg/L insulin/transferrin/ sodium selenite supplement. HT-29 cells were initially grown as monolayers in 75cc flasks until reaching confluency. U937 cells were grown initially in 25 cc flasks and then transferred to 75 cc flasks by gently scraping the monolayer. Trypan blue dye exclusion was used to determine cell viability.

Development of 3-D HT29 monotypic and co-culture models.

3-D HT29 monotypic cultures were grown as previously described by Höner zu Bentrup et al. (229).

3-D HT-29-U937 co-culture model. U937 cells grown in suspension in T75 flasks in GTSF-2 media were collected and resuspended in fresh GTSF-2 media at a density of ~2 X 10^6 cells/ml. Approximately 1 X 10^7 U937 cells were added to 5 mg/ml porous Cytodex-3 microcarrier beads (collagen type I-coated, average size 175 um, Sigma) in GTSF-2 medium containing 10^{-8} M phorbol-12-myristate-13-acetate (PMA, inducing differentiation of monocytes into macrophages) to reach a final volume of 50 ml. Exposure of monocytes to PMA induces morphological, physiological and molecular characteristics of terminally differentiated macrophages (254). 5 ml of the mix was transferred to each well of a 6 well plate and incubated for 48 hrs at 37 °C in a 10 % CO_2 atmosphere. PMA-differentiated U937 cells bound to microcarrier beads were gently rinsed with fresh GTSF-2 media and combined with ~2 X 10^6 cells/ml HT-29 cells grown as standard monolayers. HT-29 and U937 cells were then transferred to the RWV bioreactor and co-cultured at 20 rotations per minute (r.p.m). Fresh GTSF-2 medium without antibiotics was replenished after 5 days and then every 24 hours thereafter until the harvest of the cultures at 15-17 days. An overview of the protocol is summarized in **Figure 3-1**.

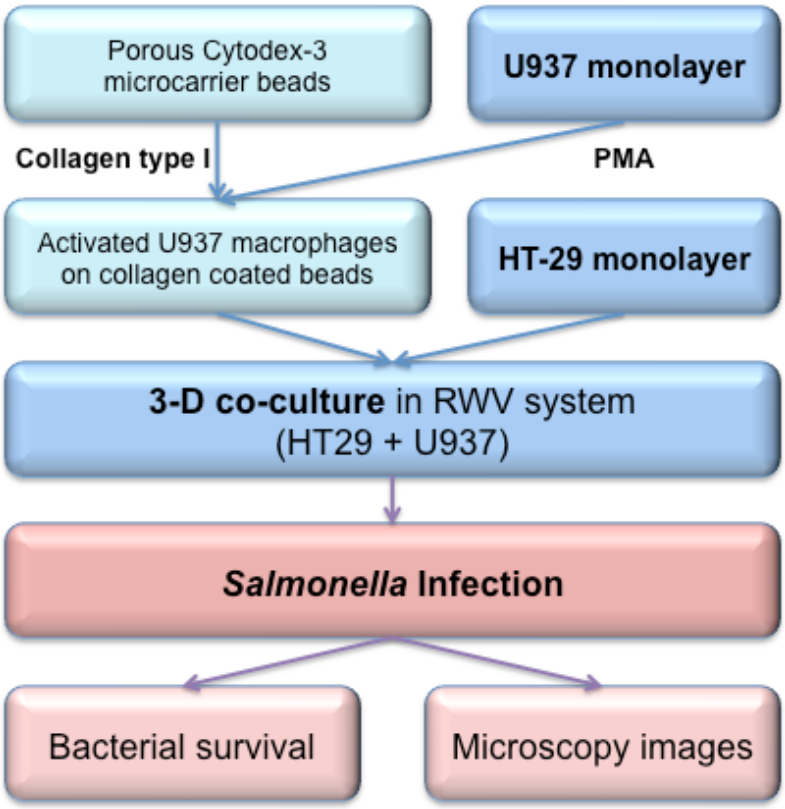

Figure 3-1. Flowchart of key steps in development of the immunocompetent 3-D co-culture model of human intestine and *Salmonella* infection

You should indicate/mention somewhere in this diagram that the infection studies were done in multiwell plates.

Infection study.

All 3-D cell cultures used for infection studies were cultured overnight in antibiotic free media. Upon reaching optimal differentiation, 3-D aggregates of both monotypic cultures (HT-29) and co-cultures (HT-29 - U937) were harvested from the RWV bioreactor and seeded evenly into 24-well plates to a final density of ~1 X 10^6 cells/ml with fresh GTSF-2 media on the day of the infection studies. The number of live cells was enumerated by trypan blue exclusion prior to infection and ~1- 2 x 10^6 cells/mL

were infected by bacteria (SL1344, D23580, Ty2 and HB101) at a multiplicity of infection (m.o.i.) of ~10:1 (bacteria-to-host cells) for 30 min (adhesion), 3 hrs (invasion) and 24 hrs (intracellular survival) as described by our lab previously (189). At the appropriate timepoints, the infected cells were washed 3 times with Hanks' balanced salt solution (HBSS) and lysed with 0.1 % sodium-deoxycholate. Lysates were serially diluted 10-fold with sterile PBS and each dilution plated onto LB agar in triplicate and counted to assess averaged CFU/mL. Percent survival compared to the initial inoculum was calculated as a ratio of the CFU at each time point to the CFU of the infection dose at time zero. Percent survival compared to the previous infection point was calculated as the ratio of the CFU at each time point to the CFU recovered at the previous time point. Three biological replicates were performed independently and each included three technical replicates that were averaged. Data presented represents the average of all three biological replicates. Matched time point controls were included for all studies using the non-invasive *E. coli* strain HB101 and all strains were verified to be gentamycin-sensitive prior to the study.

Statistical evaluation.

All experiments were repeated at least three times. Each experiment included three technical replicates by plating samples onto LB agar in triplicate. Mean values and standard error of means (SEM) were calculated from three or more experiments or biological trials. All comparisons were made using the student t-test (alpha < 0.05). The significances were indicated as *, $p<0.05$; **, $0.001<p<0.01$; and ***, $p<0.001$.

3.4 Results

3.4.1 *Salmonella* exhibits reduced colonization (adherence, invasion, intracellular survival) of the 3-D immunocompetent co-culture model as compared to the 3-D monotypic model

Infection profiles of *Salmonella* pathovars were assessed in the 3-D intestinal co-culture and monotypic models at 0.5 h (adherence), 3 h (invasion), and 24 h (intracellular survival/replication) after infection. All *Salmonella* strains tested were recovered in significantly lower numbers at all colonization time points in the 3-D co-culture (HT29+U937) model as compared to the 3-D monotypic model (HT29) (Fig. 3-2 A-C). The differences in *Salmonella* colonization profiles between the two models were 6.8-fold at 30 mins, 10-fold at 3 hrs, and 13.5-fold at 24 hrs post infection (Table 3-1). These data indicate that the macrophages present in the co-culture model exhibit *in vivo*-like functional properties that are causative for the observed decrease in numbers of colonizing bacteria as compared to epithelial cells alone.

Table 3-1. Fold decrease of bacterial colonization in the 3-D co-culture model (HT-29+U937) as compared to the 3-D monotypic model (HT-29). ($p<0.05$)

	Adherence (30 min)	Invasion (3 hr)	Intracellular survival (24 hr)
SL1344	-2.90	-4.18	-3.22
D23580	-2.50	-5.09	-3.60
Ty2	-6.83	-9.91	-13.36

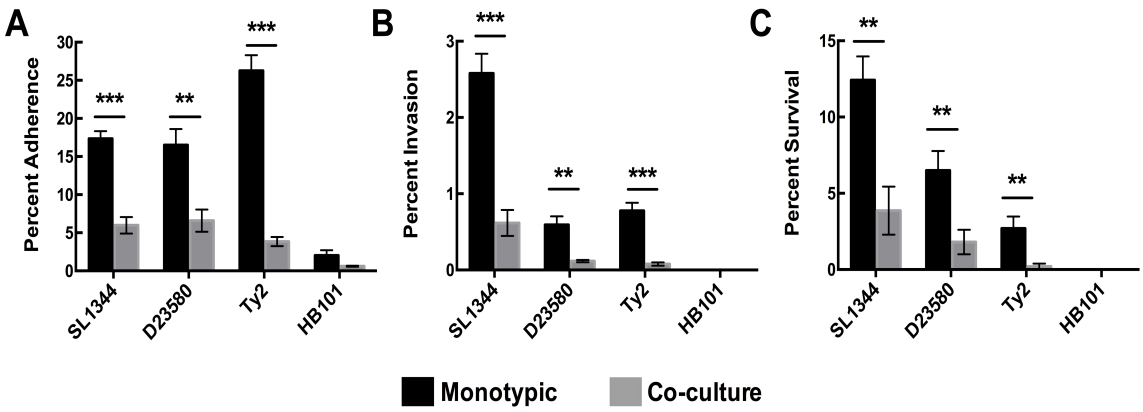

Figure 3-2. Salmonella adheres, invades and survives at lower levels in the 3-D co-culture model containing functional macrophages as compared to the 3-D monotypic model of HT-29 cells alone.

3-D aggregates comprised of either HT-29 cells alone (monotypic model; black bars) or a combination of HT-29 and U937 cells (co-culture model; grey bars) were infected with SL1344, D23580, Ty2, or the non-invasive control HB101 at an m.o.i. of 10:1 (bacteria:host). After addition of the bacteria, cells were incubated for 30 minutes (adherence), 3 hours (invasion), or 24 hours (survival). For bacterial enumeration at each time point, cells were washed, lysed and serial dilutions plated to obtain CFU. After 30 minutes, cells designated for the 3 and 24-hour time points were treated with gentamicin to kill any extracellular bacteria. For all time points, bacterial counts were normalized and plotted as a percent of initial inoculum for each strain. (A) Percent adherence at 30 minutes. (B) Percent invasion after 3 hours. (C) Percent survival after 24 hours. Limit of detection is 100 CFU. Statistical significance was determined using Students t test. * indicates $p < 0.05$; ** indicates $p < 0.01$, and *** indicates $p < 0.001$. Comparisons indicate differences between the 3-D co-culture and monotypic models for each bacterial strain at the time points indicated.

3.4.2 Pathogen-specific bacterial adherence, invasion and intracellular survival

Pathogen specific colonization trends were observed in the 3-D cell culture models. Specifically, D23580 adherence levels were similar to SL1344 for both 3-D cell culture models, with both Typhimurium strains adhering better than Ty2 for the co-culture model, while Ty2 exhibited greater adherence than either Typhimurium strain for the 3-D monotypic model (**Figure 3-3A**). Interestingly, substantially lower invasion was observed for D23580 as compared to SL1344 in both 3-D cell culture models, yet the invasiveness between D23580 and Ty2 were similar. Specifically, only 3.46 % of adhered D23580 was recovered in the 3-D co-culture model at 3 h post infection (2.30 % in 3-D HT-29) while ~15 % of adhered SL1344 was found in the 3-D co-culture model (11.62 % in 3-D HT-29) (**Figure 3-3B**). Evidence of intracellular replication for all *Salmonella* pathovars was indicated as evidenced by over 100% survival at 24 h post infection in both 3-D cell culture models (intracellular survival expressed as a function of those bacteria that invaded). Interestingly, significantly higher numbers of intracellular D23580 were found at 24 h post-infection as compared to SL1344 and Ty2 (**Figure 3-3C**). These data showed a distinct infection trend (adherence, invasion and intracellular survival) of D23580 in 3-D human intestinal models, which was different from both SL1344 and Ty2.

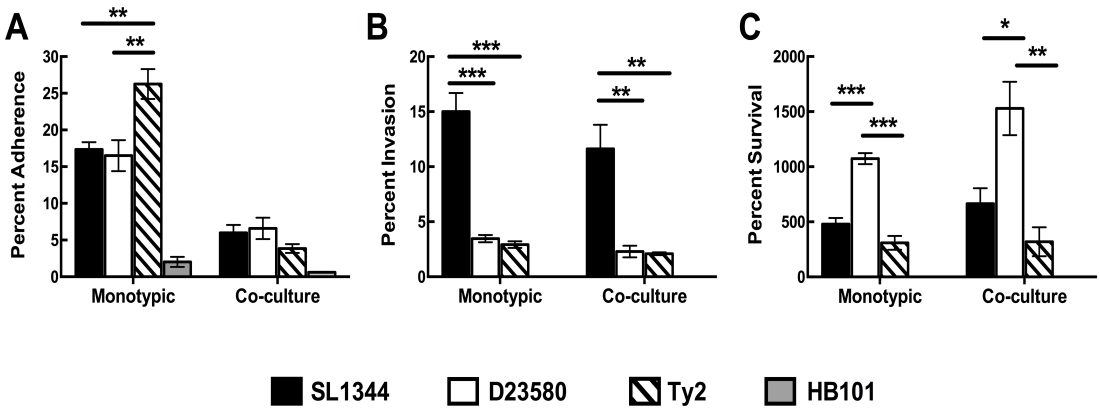

Figure 3-3. D23580 displays low levels of invasiveness but enhanced survival in both the 3-D monotypic and co-culture models relative to SL1344.

Infection studies are identical to those described in Figure 3, except the invasion (B) and survival (C) bacterial counts are plotted as a function of the number of bacteria that adhered or invaded, respectively. (A) Percent adherence at 30 minutes, normalized and plotted as a percent of the initial inoculum for each strain; (B) Percent invasion at 3 hours, normalized and plotted as a percent of the bacteria that adhered for each strain; (C) Percent survival at 24 hours, normalized as a percent of the bacteria that invaded for each strain. Data represent the average of at least two independent experiments from separate batches of cells. Limit of detection is 100 CFU. Statistical significance was determined using Students t test. * indicates $p < 0.05$; ** indicates $p < 0.01$, and *** indicates $p < 0.001$. Comparisons indicate significant differences between bacterial strains at each time point indicated for both the monotypic and co-culture model.

3.4.3 Distribution of intracellular *Salmonella* pathovars

The 3-D co-culture model was infected by *Salmonella* pathovars for 24 hrs and confocal laser scanning microscopy images of bacterial infections were taken by Aurelie Crabbe (Figure 3-4). In SL1344-infected cultures, macrophages were rarely observed and the bacteria were co-localized with epithelial cells (**Figure 3-4B**). In contrast, Ty2, which was recovered in very low numbers from the 3-D co-culture model infection studies, was found co-localized in giant binucleated macrophages that appeared completely filled by this pathovar, but rarely found in epithelial cells (**Figure 3-4D, inset in panel D**). Strain D23580 was associated with both epithelial cells and macrophages in the 3-D co-cultures (**Figure 3-4C**). These data show distinct bacterial colonization patterns of different *Salmonella* pathovars in 3-D monotypic and co-culture models.

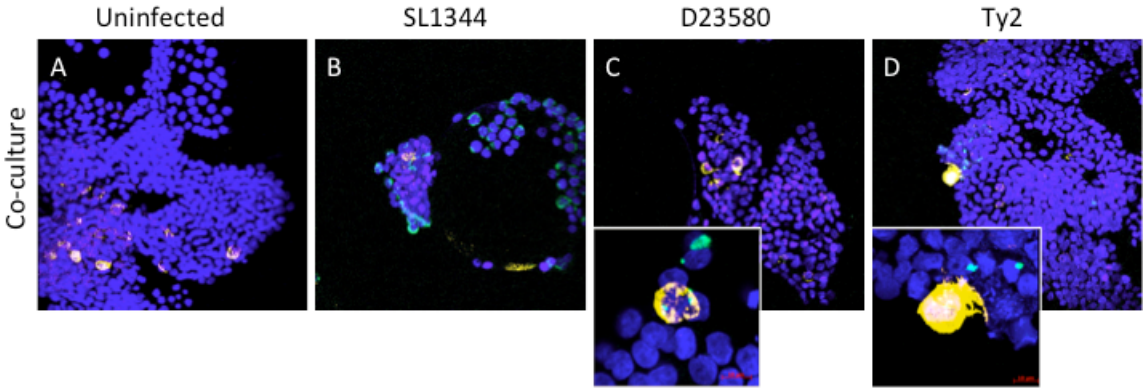

Figure 3-4 Differential association of *Salmonella* pathovars with macrophages in the 3-D co-culture model based on immunofluorescence profiling.
3-D human cell culture models infected with SL1344 (B), D23580 (C) or Ty2 (D) for 24h was co-stained with a CD45 antibody (labeling macrophages yellow) and a *Salmonella* antibody (labeling all pathovars green). Cell nuclei are stained with DAPI (blue). All images are based on 400x magnifications. (A) is uninfected control. *Imaging done by Aurelie Crabbe.

3.5 Discussion

Utilizing organotypic intestinal cell culture models that mimic the 3-D architecture and multicellular complexity normally present in the parental tissue *in vivo* can facilitate an improved understanding of the transition between normal intestinal homeostasis and disease progression caused by ST313. The 3-D monotypic HT-29 models differentiated into multiple epithelial cell types that are normally present in the human colon responded to infection with Typhimurium in key ways that reflect the infection process *in vivo*, including changes in adherence, invasion, tissue pathology, apoptosis, and innate immune responses. The new 3-D co-culture model, utilized in this study, shared key epithelial characteristics with the HT-29 monotypic culture from which it was derived, including well organized tight junctions (indicating apical-basolateral polarity), expression of mucins, and evidence of multiple epithelial cell types normally present in the parental tissue (data are not shown). Also, macrophages in the 3-D co-culture were evaluated to show phagocytic activity and embedded localization underneath epithelial cells (data are not shown), indicating *in vivo*-like architecture and immunocompetence of the model. I report an inhibitory role of intestinal macrophages responding *Salmonella* infection and distinct invasion and intracellular survival/replication trends of ST313 D23580 in common with yet different to classic *Salmonella* serovars by utilizing this advanced 3-D co-culture model.

3.5.1 Contribution of macrophages to *Salmonella* enteric colonization: pathovar-related differences in adherence

The addition of macrophages to the 3-D intestinal co-culture model reduced bacterial colonization for all *Salmonella* pathovars tested as evidenced by decreased adherence, invasion and intracellular survival relative to the 3-D monotypic model. Macrophages are a key immune cell type targeted by *Salmonella* during infection and their intracellular survival in these cells is essential for bacterial virulence. Bacterial infection in either epithelial cells or macrophages alone can be different than bacterial infection in co-culture models containing both of these cell types (243, 247-251), the latter of which is more reflective of the *in vivo* host response yielding synergistic phenotypes. Data from this study are in alignment with the inhibitory role of intestinal macrophages in colonizing *Salmonella* pathovars in host gut tissue (255-258) inferring the importance of initial interactions between multiple host cell types and the pathogen for successful bacterial infection or host immune responses.

Interestingly, distinct *Salmonella* adherence trends were observed by comparing the adherence of pathovars in the 3-D co-culture model to those in the 3-D monotypic model. While all tested strains exhibited decreased colonization in the 3-D co-culture model, the reduction of Ty2 adherence was greater than the D23580 and SL1344 (nontyphoidal *Salmonella* pathovars). The decrease was 6.83-fold for Ty2 as compared to 2.69-fold for NTSs (**Figure 5**). Therefore, these data suggest the importance of

macrophages to influence the adherence of Typhi, implying a potential adherence mechanism(s) that is different between Typhi and Typhimurium.

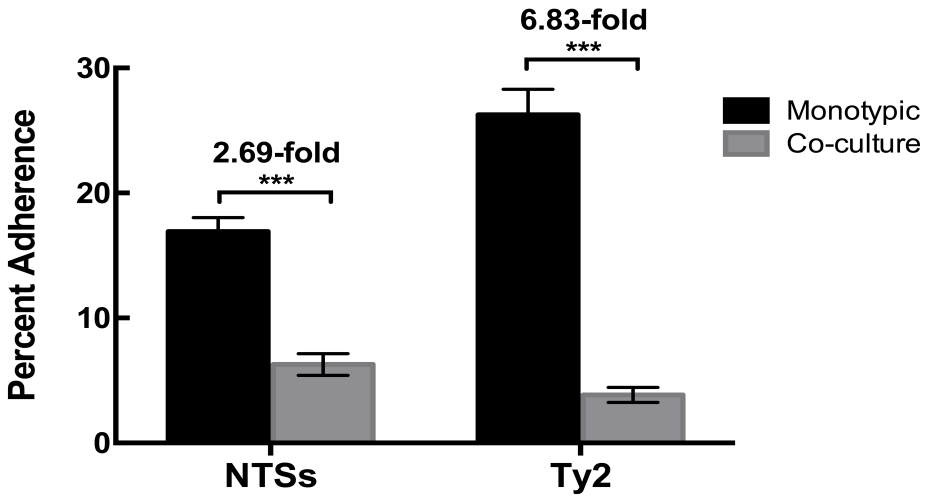

Figure 3-5. Adherence of Typhimurium and Typhi in 3-D monotypic as compared to the co-culture model.
S. Typhi adheres at higher levels to the 3-D monotypic model than the non-typhoidal *Salmonella* strains, but this difference is abrogated in the 3-D co-culture model containing functional macrophages. NTS indicates nontyphoidal *Salmonella* pathovars, including D23580 and SL1344 in this experiment.

Adherence mechanisms in Typhi are still not well understood and the differences in adherence between Typhi and Typhimurium are not well explained. Genomic profiling studies revealed key differences in gene content associated with adhesins in these organisms. Specifically, the Typhi genome contains 5 inactivated fimbrial operons, 3 additional fimbriae, and the Vi capsule biosynthesis operon (a virulence determinant) that are divergent from the Typhimurium genome (25, 259-263). *In vitro* studies with monolayers showed Typhi adherence and invasion were mediated through the type IV

pili and Vi capsule, respectively, however, detailed adherence and invasion mechanisms of Typhi *in vivo* are still not clear (264, 265). Bishop et al in 2008 showed that Typhimurium adhered better than Typhi to both non-polarized Int-407 monolayers and polarized T84 monolayers, while Typhi exhibited increased invasion of the basolateral surface of host cells grown in Transwell inserts (266, 267). The authors also reported that Typhi-only surface structures (*sta, tcf, pil* and Vi capsule) did not influence adherence or invasion of apical or basolateral surfaces in polarized T84 cells (266). Accordingly, it is still not clear how Typhi and Typhimurium interact differently with human cells *in vivo* at the early infection stages through the natural course of infection, which is or particular relevance to ST313 serovar D23580, which shares features of both Typhi and Typhimurium.

Our infection studies utilizing *in vivo*-like 3-D human intestinal co-culture models revealed distinct adherence phenotypes of Typhi as compared to Typhimurium strains. The 3-D co-culture model presents well-differentiated tight junctions indicating apical and basolateral polarity in epithelial cells and also embedded macrophages capable of phagocytosis, with *in vivo*-like localization (data is not shown). While Ty2 exhibited enhanced adherence to 3-D monotypic cultures (HT-29), the adherence of Ty2 in the 3-D co-culture model was inhibited by the addition of macrophages, indicating that Ty2 adherence is differentially influenced by macrophages as compared to Typhimurium in our highly differentiated intestinal model. The iNTS ST313 strain D23580, however, presented a similar adherence pattern to classic Typhimurium SL1344 (neither of which code for the Vi capsule or additional fimbrial genes found in Typhi). Thus, the Typhi-

specific cell surface molecules may be involved in this distinct adherence trend affected by macrophages in the 3-D co-culture model. The detailed mechanisms will be investigated by using the immunocompetent 3-D human intestinal cell culture system co-cultured with human macrophages.

To our knowledge, this is the first report of the contribution of macrophages when co-cultured in the context of highly differentiated intestinal epithelium on adherence phenotypes in NTSs and Typhi.

3.5.2 D23580 displays low levels of invasiveness but enhanced survival in both the 3-D monotypic and co-culture models relative to SL1344

While adherence profiles between D23580 and SL1344 were similar, it was intriguing that D23580 exhibited dramatically lower invasion levels similar to Typhi in both 3-D cell culture models. This finding suggests a that invasion mechanism of D23580 may differ from classic Typhimurium SL1344. Since ST313 is a major causative agent for highly invasive disease with presentation of Typhi-like disease phenotype and genome characteristics, ST313 strains (including D23580) have been considered to be and are often called ‘highly invasive’ iNTS or ‘highly invasive’ ST313 (9, 16, 39, 41, 177, 180, 182, 268). However, our data using highly differentiated 3-D co-culture intestinal models clearly showed that D23580 is substantially less invasive (> 4-fold) than classic Typhimurium, SL1344 (Table 3-2). Interestingly, recent studies provide

hints supporting our data have shown a less invasive phenotype of ST313. A study investigating a potential virulence gene, *st313-td,* showed that insignificant difference for wild type ST313 strain infecting Int-407 monolayers to classic Typhimurium ST19 strains, while the ST313 internalized macrophages better than ST19 strains (40). Another study examining a potential animal reservoir showed lower gastrointestinal colonization of ST313 in chickens while causing more rapid and severe infection in systemic organs relative to ST19 (classic NTS) (39). Therefore, we may need to reconsider referring to all ST313 pathovars as "highly invasive" *Salmonella*, which may be misleading in terms of accurately conveying the true pathogenesis mechanisms of these pathovars, at least in terms of D23580.

Table 3-2. Fold-difference of bacterial survival in 3-D cell culture models relative to internalized bacteria between strains

(A) D23580 vs SL1344

	Mono	Co-culture
Adherence	0.95	1.10
Invasion	**0.23**†	**0.20**†
Sur/repl.	**2.24**†	**2.30**†

(B) D23580 vs Ty2

	Mono	Co-culture
Adherence	**0.63**	1.71
Invasion	1.19	1.09
Sur/repl.	**3.47**†	**4.78**†

Adherence relative to initial inoculum, invasion relative to adhered bacteria, and intracellular survival/replication relative to internalized bacteria. Significant differences ($p<0.05$) are bolded. The '†' indicates differences greater than 2-fold.

Interestingly, D23580 exhibited significantly better intracellular survival/replication in both 3-D models. Although D23580 exhibited substantially lower invasion than classic Typhimurium SL1344, the intracellular survival and replication of D23580 was significantly greater than Ty2, with 3.47-fold and 4.78-fold in mono- and

co-culture, respectively, than SL1344 with more than 2-fold difference (**Table 3-2**). Recently, a study reported that invasive ST313 strains expressing attenuated flagellin demonstrated enhanced intracellular replication and silenced inflammatory responses, which may provide enhanced systemic infection like Typhi and Paratyphi (41). As discussed in **Chapter 2**, D23580 is hyper-motile and causes rapid infection of systemic organs, which is not in agreement with the previous study. Although the detailed mechanisms of how ST313 strains cause systemic disease is not clear, our study and others' show common infection trends of ST313 strains: inefficient invasion in 3-D cell cultures or colonization of gastrointestinal epithelial cells, yet enhanced intracellular survival and replication in various macrophages and in our 3-D cell culture models. The distinct infection kinetics or preferential or selective replication trends of ST313 in infected host cells may infer why NTS ST313 strains are dominant in invasive salmonellosis in Africa more than classic NTS strains and classic invasive Typhoidal strains. It is not clear as to whether the greater intracellular survival/replication of D23580 relative to SL1344 is due to whether D23580 can replicate inside or survive within host cells more effectively than SL1344 or if SL1344 escapes host cells better than D23580.

3.5.3 Pathogen-specific bacterial distribution pattern: host cell type specific distribution of Typhi, Typhimurium SL1344 and D23580

Different *Salmonella* pathovars presented distinct co-localization trends associated with different host cell types in the 3-D co-culture model. Ty2 was noticeably

altered in its localization associated with the infected cell types in 3-D co-culture. In 3-D monotypic culture, Ty2 was found inside epithelial cells; while it was hardly found in 3-D co-culture associated epithelial cells. Instead, although rarely found in 3-D co-culture, Ty2 was found in completely bacterial-filled macrophages that formed giant macrophage syncytia-like structures. The altered distribution-phenotype in 3-D co-culture suggests an importance of including multiple cell types, particularly macrophages, and displaying 3-D architecture as a physiologically relevant *in vitro* infection model for *Salmonella* study.

Previously, Schwan et al showed better intracellular survival of Typhimurium than Typhi in murine macrophages but better survival of Typhi than Typhimurium in human macrophages *in vitro* (91). Tong *et al.* reported the requirement of *in vivo* factors by showing the ability of murine macrophages distinguishing between Typhimurium and Typhi *in vivo*, but were unable to reproduce the phenotype *in vitro* using pure macrophage cultures (252). Recently, Strandberg et al showed increased intramacrophage survival of Typhimurium over time (24 hrs) in primary human monocyte-derived macrophages while numbers of Typhi remained constant (269). Agreeing with Strandberg et al, in part, our infection study using an *in vivo*-like 3-D human cell co-culture model (macrophages + epithelial cells) presented the enhanced intracellular survival and replication of Typhimurium as compared to Typhi at 24 h postinfection. However, the distributions of each of the pathovars tested were different, associating with different host cell types - Typhimurium localized within epithelial cells while Typhi formed a large bolus within macrophages. Recently, the *Salmonella* replication filling in host cells was reported to be associated with SPI-2 (270). The

filling phenotype was also observed *in vivo* in host cells infected with attenuated Typhimurium lacking SPI-2 TTSS, suggesting an important role of SPI-2 TTSS for bacterial spread (270). Interestingly, many SPI-2 effectors present in Typhimurium are missing in Typhi (*sseI, gogB, spvB, spvC, sseK1, sseK2* and *sseK3*) or are pseudogenes (*sopD2* and *sseJ*), which could potentially explain the similar filling phenotype observed in our study for Ty2 infection and the previous reports on SPI-2 T3SS mutants. In 2010, Radtke et al reported that a SPI-2 deletion mutant in Typhimurium was not defective for bacterial intracellular survival in 3-D HT-29 cells, also agreeing with the previous studies (104, 270). Collectively, the data obtained using the immunocompetent 3-D co-culture model might explain the different infection phenotypes of Typhi relative to Typhimurium and may also help explain the seemingly contradictory data resulted from animal infection and single cell type culture *in vitro*. Therefore, this study using 3-D immunocompetent co-culture models provides evidence that the different infection strategies of Typhi and Typhimurium associating host cell type selection and simultaneously provides a study tool to investigate the detailed infection mechanisms that are different between Typhi and Typhimurium, may be related to SPI-2.

Moreover, it is important that microscopy images showed different distribution patterns of D23580, in common with yet distinct from both classic Typhimurium and Typhi. Specifically, D2580 exhibited a Typhimurium-like adherence pattern, Typhi-like invasion phenotype, and a distinctively enhanced intracellular survival and replication pattern. The co-localization pattern of D23580 for the cell types in the 3-D co-culture model was between SL1344 and Ty2, as the bacteria were found in both macrophages

and epithelial cells. D23580 was reported to have undergone a genome reduction, pseudogenes and single nucleotide polymorphisms (SNPs) (7). Interestingly, the pseudogenes include deletion of *sseI* (SPI-2) by an insertion element. SseI was reported to be important for persistent infection in mice and also reported to be associated with bacterial spreading (270-274). Therefore, although it is not clear how the deletion of *sseI* or other pseudogenes could be influenced for the distinct distribution pattern of D23580 in host cells during infection, our study suggests certain infection mechanisms of D23580 may be similar to Typhi. Again, this finding is supported by reports that D23580 showed rapid infection in systemic organs in animals, was better phagocytosed by macrophages following enhanced intracellular survival, yet exhibited reduced colonization in gastrointestinal cells.

While Typhimurium spreads to neighboring intestinal epithelial cells after infection by rapidly replicating inside host cells, ST313, like Typhi, may be more efficient at surviving within and colonizing macrophages, so that circulation in systemic organs causes systemic disease more frequently than classic Typhimurium and Typhi.

3.6 Conclusion

An *in vivo*-like immuncompetent 3-D human intestinal cell culture model developed in our lab was applied to study the early stages of *Salmonella* enteric infection. Results from this study report similar adherence trends between D23580 and classic

Typhimurium but an invasion profile that resembles that of Typhi Ty2. Moreover, D23580 revealed enhanced survival within the 3-D host cells and presented a distinct distribution phenotype relative to the other *Salmonella* pathovars, associated with both epithelial cells and macrophages. Therefore, I conclude that D23580 displays distinct infection properties in common with yet different from both classic Typhimurium and Typhi. In addition, I suggest reconsidering the current trend of referring to D23580 as a "*highly invasive*" nontyphoidal *Salmonella* pathovar, as results from this study using a highly differentiated human intestinal model show it to be less invasive with high intracellular survival.

Summary - Chapter 3:

This chapter reports the colonization profile of D23580 utilizing a highly differentiated *in vivo*-like 3-D human tissue co-culture model consisting of intestinal epithelial cells and macrophages. This is the first *in vitro* study to profile the colonization (adherence, invasion and intracellular survival) of D23580 in a 3-D organotypic model of human intestinal epithelium containing functional macrophages capable of phagocytosis.

- ✓ *Salmonella* exhibited reduced colonization of the 3-D immunocompetent co-culture model as compared to the 3-D monotypic model comprised solely of epithelial cells – thus highlighting the functionality and contribution of the macrophages to the colonization profiles.
- ✓ The adherence ratio between the 3-D monotypic and co-culture models showed similar trends between the NTS strains D23580 and classic Typhimurium

SL1344, but was significantly different from Typhi strain Ty2. This finding highlights the different contribution of macrophages to adherence between these *Salmonella* pathovars.

- ✓ While ST313 is commonly referred to as "highly invasive nontyphoidal *Salmonella"*, D23580 exhibited significantly lower levels of invasion in the 3-D co-culture model as compared to SL1344, but similar to Ty2.
- ✓ D23580 exhibited significantly enhanced intracellular survival/replication relative to SL1344 and Ty2.
- ✓ Findings in this study suggest that the ability for D23580 to spread more efficiently throughout the infected host relative to classic Typhimurium may be due, in part, to its inherent intracellular survival properties rather than an ability to actively invade at higher levels.
- ✓ D23580 displayed distinct patterns of co-localization to both intestinal epithelial cells (IECs) and macrophages in the 3-D co-culture model, while SL1344 was mostly associated with IECs, and Ty2 was mostly associated with macrophages in the co-culture model.

Next, we profiled how the physical force microenvironment naturally encountered by *Salmonella* during the enteric infection process *in vivo* alters D23580 molecular genetic and phenotypic properties.

4 CHAPTER 4: EFFECT OF FLUID SHEAR ON INVASIVE SALMONELLA ST313: PHYSIOLOGICAL FLUID SHEAR ALTERS THE VIRULENCE POTENTIAL OF INVASIVE NON-TYPHOIDAL SALMONELLA TYPHIMURIUM D23580

4.1 Abstract

Salmonella enterica serovar Typhimurium strains belonging to sequence type ST313 are a major cause of fatal bacteremia among HIV-infected adults and children in sub-Saharan Africa. Unlike 'classical' non-typhoidal *Salmonella* (NTS), gastroenteritis is often absent during ST313 infections and isolates are most commonly recovered from the blood, rather than stool. This is consistent with observations in animals, in which ST313 strains displayed lower levels of intestinal colonization and higher recovery from deeper tissues relative to classic NTS isolates. A better understanding of the key environmental factors regulating these systemic infections is urgently needed. Our previous studies using the Rotating Wall Vessel (RWV) bioreactor demonstrated that physiological levels of fluid shear regulate virulence, gene expression, and stress response profiles of classic *S*. Typhimurium. Here we provide the first demonstration that fluid shear alters the virulence potential and stress response profiles of ST313 strain D23580 in a manner that differs from classic NTS.

4.2 Introduction

4.2.1 Invasive nontyphoidal salmonellosis (iNTS)

Recent outbreaks of multidrug resistant invasive NTS in sub-Saharan Africa calls attention to the continual threat of emerging pathogens and emphasizes the urgent need for new insight into the mechanisms by which these novel variants cause disease (4-8, 15-19, 176, 177, 182, 184). Sequence analysis of D23580, a representative isolate belonging to the newly identified ST313 pathovar, revealed genome degradation resembling that of the human-restricted serovar Typhi (7, 12). Combined with the highly invasive clinical presentation in patients, these findings suggested that although it was classified as NTS, D23580 might display a Typhi-like host tropism (7). Subsequent studies confirmed that D23580 still retains a broad host specificity characteristic of serovar Typhimurium, but also revealed key pathogenesis characteristics that distinguish it from classic NTS (39).

4.2.2 *Salmonella* and fluid shear

The pathogenicity of *Salmonella* can be altered in response to a variety of environmental conditions, including pH, temperature, oxygen, and nutrient availability (65, 72, 82, 193, 201). It has also become increasingly clear that physical forces, including fluid shear, play an important role in regulating the virulence, gene expression, and/or pathogenesis-related stress responses for *Salmonella* and other bacteria (135, 139,

140, 143-146, 150-153, 155-157, 159, 164, 165). It was previously demonstrated by our laboratory that culturing *S.* Typhimurium strain χ3339 (an animal passaged-derivative of the classic NTS strain SL1344) in low shear condition in rotating wall vessel (RWV) bioreactor led to increased virulence, global changes in gene expression, and increased resistance to multiple pathogenesis-related stressors (135, 143, 144, 146). It was subsequently shown that several other *Salmonella* serovars are able to sense and respond to alterations in fluid shear (158). A wide range of fluid shear levels can be found both in the environment and *in vivo*, with *in vivo* niches ranging from high fluid shear in the bloodstream to low fluid shear in between the brush border microvilli of epithelial cells (129-134, 137). As a facultative intracellular pathogen that incorporates both a intracellular and cell-free lifestyle, the spread of *Salmonella* throughout the GI tract to the extraintestinal environment of the circulatory system exposes the pathogen to a broad range of fluid shear environments. Understanding how this important environmental signal can regulate the onset of disease and its progression is a critical consideration for the treatment and prevention of invasive salmonellosis by the ST313 pathovar. Therefore, in this study we investigated the influence of physiological fluid shear on the virulence and several pathogenesis-related stress responses of the representative ST313 strain D23580.

4.2.3 Rotating Wall Vessel (RWV) bioreactor

The NASA-engineered Rotating Wall Vessel (RWV) bioreactor is a suspension culture system that allows cells to grow under physiologically relevant low fluid shear

culture conditions when the reactor is oriented in the low shear modeled microgravity (LSMMG) orientation (**Figure 4-1**). The cylindrical bioreactor is completely filled with culture medium and rotated on the horizontal axis (**Fig 4-1B**), which minimizes fluid turbulence and maintains cells in a gentle fluid orbit (135, 143, 144, 154, 275-277). When the RWV is oriented in the high shear control (HSC) orientation (**Fig 4-1A**), cells and particles sediment to the bottom of the reactor, where increased frictional forces disrupt fluid flow due to interactions of the bacteria with the bioreactor membrane as well as with other sedimented bacteria. For both orientations, oxygen is provided through the one side of RWV through a gas-permeable membrane via a peristaltic pump. The RWV has been used to study the effect of fluid shear on microbial pathogenesis, stress responses and/or gene expression for a wide variety of bacteria including: 1) *Salmonella* (135, 143, 146, 153, 157-159, 164, 165, 278), 2) *Pseudomonas aeruginosa* (155, 279), 3) *Staphylococcus aureus* (145, 150, 152), 4) *Escherichia coli* (152, 153, 156, 278, 280-286), and 5) others (285, 287-289). These studies have demonstrated that a broad range of both Gram-negative and Gram-positive bacteria are able to sense and respond to alterations in fluid shear. In this study, the RWV was applied to study impact of fluid shear on virulence and cellular responses of D23580.

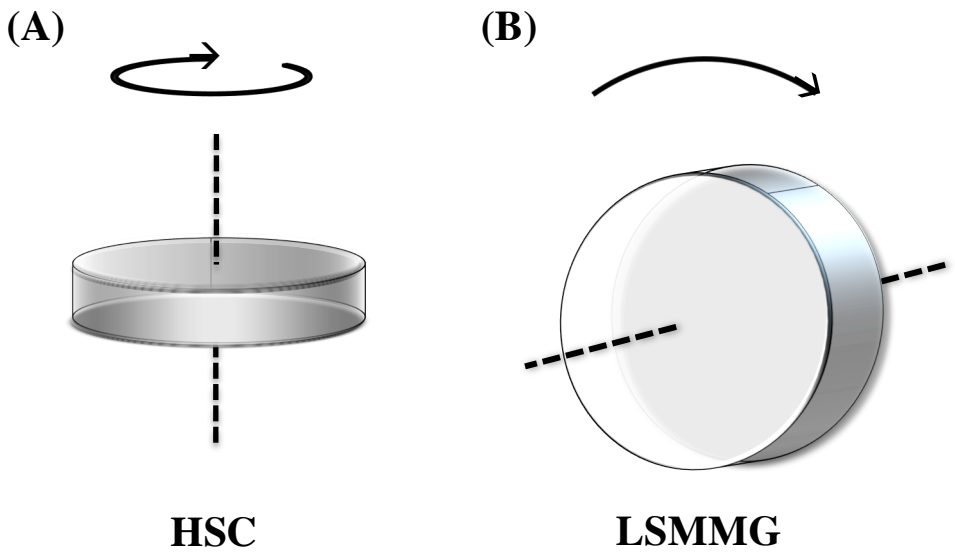

Figure 4-1. Rotating Wall Vessel (RWV) bioreactor cell culture system.
(A) Higher shear control condition (HSC); (B) Low Shear condition (LSMMG).

4.3 Methods

Bacterial growth.

Salmonella enterica serovar Typhimurium ST313 D23580 was used in this study. Bacterial cultures were initiated in Lennox broth (LB) with aeration (180 rpm) overnight for 15 hours at 37°C. The following day, overnight cultures were inoculated into 150 mL sterile LB at a 1:200 dilution and subsequently loaded into two identical RWVs. The bacteria in RWVs were incubated at 37°C, one with LSMMG and the other with HSC positions (**Figure 4-1**) in Lennox Broth (LB) at 25 rotations per minute and 37°C for 4 hours (late log/early stationary phase). Growth curves were performed by plating on LB

agar for viable colony-forming units (CFU) and measuring the corresponding optical density at 600 nm (OD_{600}) to ensure that cultures were profiled at identical phases of growth for all studies (**Figure 4-2**).

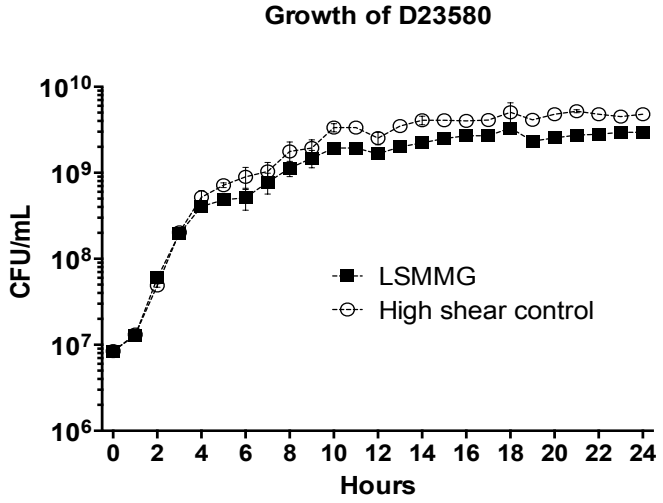

Figure 4-2. Growth curves of D23580 grown in RWVs.
D23580 was grown in RWV one in low shear modeled microgravity (LSMMG) or high shear control (HSC) condition. Cultures were monitored for 24 hrs by plating on LB agar for viable colony-forming units (CFU) and measuring the corresponding optical density at 600 nm (OD_{600}).

Virulence test.

For virulence studies, 8-week old female BALB/c mice (Charles River Laboratories) were fasted for approximately five hours and then perorally infected using standard protocols described previously (189, 190, 290). Bacterial cells grown to late log phase in RWVs were immediately harvested by centrifugation at 7,000 rpm for10 minutes and the pellets were resuspended in buffered saline containing 0.01% gelatin (BSG) to a dose of approximately $1x10^9$ CFU per 20 µl. A series of 10-fold dilutions

was performed in BSG down to $1x10^2$ CFU per 20 µl dose. Mice were acclimated for 7-14 days before the experiments. Total 20 uL volume per dose was given per orally with from 10^2 to 10^9 CFU to BALB/c mice deprived of food and water before infection. Mice were monitored for 30 days. Studies were performed in biological triplicate with five mice per dose. The 50% lethal dose (LD_{50}) value was calculated using two of these independent trials, since in the initial trial the dosage was not yet optimized and there was no group with 100% survival, which is a requirement to calculate the median lethal dose using the method of Reed and Muench (190). Time-to-death (**Figure 4-3**) was plotted to include the results from all three trials.

Stress assays.

Bacteria were grown as described above to late log/early stationary phase, and immediately subjected to the stress. For acid stress, acidic conditions were generated through the addition of a citrate buffer to lower the pH to 3.5. Cells were incubated statically at room temperature during exposure to the stress and the pH was confirmed with an electrode at the end of the assay. For oxidative stress, 6% H_2O_2 was added into cells grown in RWVs for a final concentration of 0.06% H_2O_2. The initial number of bacteria from each sample was determined by taking sample at time zero (before the addition of stress) and plating on LB agar. Culture sample that a testing stress is administrated were taken at various time points thereafter, diluted in phosphate buffered saline (PBS) and then plated on LB agar to determine the numbers of viable CFU. The CFU counts at each select time point were normalized to the initial inoculums to obtain

percent survival. Statistical significance between the LSMMG and control groups was determined using Student's t-test (α=0.05).

4.4 Results and discussion

4.4.1 Virulence of D23580 altered by fluid shear: LD_{50} and Time to death

Mice infected by D23580 grown in LSMMG (LSMMG group) or HSC (HSC group) were monitored for 30 day. The infected mice started to die in about a week after infection (at day 5 – 7) in the both groups. Most mice died in day 6-10 postinfection in the both groups with a trend of the slightly prolonged animal-death in HSC groups (to day 13). The LD_{50} values obtained for the LSMMG and HSC groups were not found to be significantly different, at 7.51x 10^5 CFU and 6.53 x 10^5 colony-forming units (CFU), respectively.

However, an interesting trend was observed that the total number of the dead mice was greater in the HSC group than in the LSMMG group, with 67% of total animal death in HSC and 58% of total death in the LSMMG group. Moreover, the mice infected by D23580 cultured in the control/higher fluid shear condition exhibited more rapid disease progression resulting in earlier time-to-death (**Figure 4-3**). This pattern was observed for dosages ranging from 10^4-10^6 CFU; with the group infected with 10^5 CFU dose (approaching the LD_{50}) displaying the biggest difference. Intriguingly, these results were the opposite of what was previously observed for classic NTS strain χ3339 using the

same media, temperature and phase of growth in which mice infected with χ3339 cultured in the low shear condition led to a more rapid time-to-death and decreased LD_{50}.

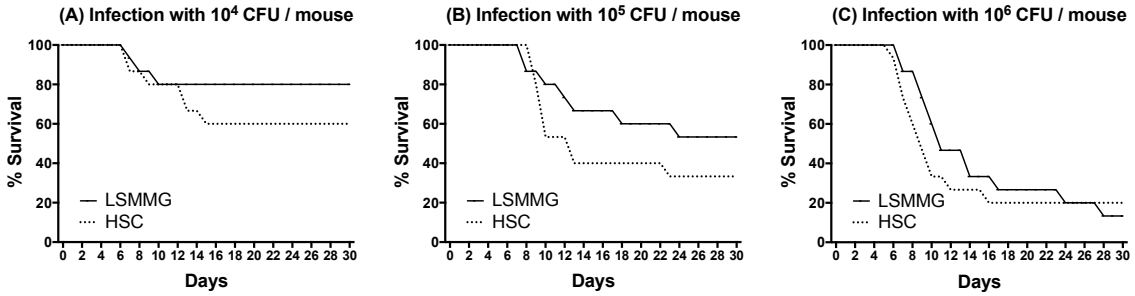

Figure 4-3 Survival of mice following peroral infection with D23580 grown in RWVs.

D23580 was cultured in LSMMG and the higher shear control (HSC) condition, in RWVs, in LB to late log phase. Dose ranging from 102 – 109 CFU per mouse was administered to 8-week-old female BALB/c mice perorally. Mice were monitored 3 times a day for 30 days. An uninfected mice group was included as a (1 x g). Panels (A), (B) and (C) represent the time-to-death of mice infected with the dose of 104,105, and 106, respectively. The percent survival is defined as the percentage of mice surviving at the indicated number of days post-infection. The median lethal dose was determined by the method of Reed and Muench.

4.4.2 Stress assay

Salmonella encounters a number of stressors in the environment and during the course of infection, including acidic pH, oxidative and osmotic stress. To evaluate the influence of fluid shear on the stress resistance of D23580, the strain was cultured in the RWV in the LSMMG or HSC condition and subjected to acid (pH 3.5) and oxidative (0.06 % hydrogen peroxide). D23580 grown in the HSC fluid shear condition exhibited increased resistance to killing by hydrogen peroxide-induced oxidative stress (**Figure 4-4A**) as compared to LSMMG cultures for all time points tested ($p < 0.05$). These

findings are in line with the increased time-to-death finding in mice infected with the higher fluid shear control condition. We also observed the same trend of acid-resistance observed in oxidative stress assay but it was not statistically significant (**Figure 4-4B**).

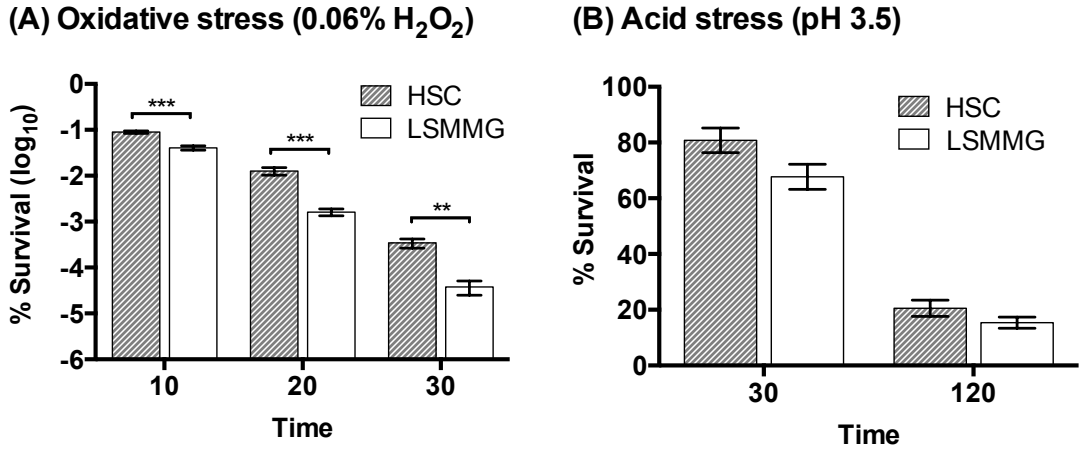

Figure 4-4. Survival of D23580 grown in RWVs responding to pathogenesis-related stresses.

Data were normalized as to the number of initial bacteria subjected to the stress. At least three independent trials were performed. The data are presented with mean values of (1 x g) condition (grey bars) and LSMMG (white bars) and standard error of means (SEM). Statistical comparisons were made using the multiple t-test with 95% confidences (** indicates $p < 0.01$; * indicates $p < 0.05$). (A) Oxidative stress was induced by adding hydrogen peroxide (H2O2) to generate 0.06% of H2O2 in the culture. The log scale fold-decreases are presented. Fold-decrease was found by calculating the number of CFU at each time point divided by the number of CFU at time zero. (B) Acidic conditions were induced by adding a citrate buffer to lower the pH to 3.5. Percent survival was calculated as the number of CFU at each time point divided by the number of CFU at time zero multiplying 100.

4.5 Conclusion

In response to culture under higher fluid shear conditions, D23580 exhibited a more rapid time-to-death in mice and displayed increased resistance to acid and oxidative stress. These findings suggest that D23580 responds to fluid shear in a different manner than previously observed for classic NTS, and that higher fluid shear environments may enhance the resistance of the pathogen to environmental stress responses, which in turn may influence disease progression. To our knowledge, this is the first report to demonstrate that physiological fluid shear regulates disease progression and pathogenesis-related stress responses for any strain belonging to the highly invasive ST313 pathovar.

Summary - Chapter 4:

Pathogens entering the host encounter a wide range of fluid shear stress during the natural course of infection. Previous work from our lab has shown that physiological fluid shear stress plays a critical role in infectious disease progression and virulence. This chapter reports the use of the NASA Rotating Wall Vessel (RWV) bioreactor to characterize the impact of low and high physiological fluid shear stress on the virulence, time-to-death, and pathogenesis-related stress responses of D23580.

- ✓ High fluid shear leads to more rapid time-to-death and increased resistance to select pathogenesis stress responses of D23580, while low fluid shear leads to more rapid time-to-death and increased resistance to select pathogenesis stress responses as compared to classic *S.* Typhimurium χ3339.

Next, we profiled how *incremental increases* in the biomechanical force of fluid shear experienced by pathogens during the natural course of infection *progressively* alter D23580 gene expression and stress response profiles.

5 CHAPTER 5: THE RESPONSE OF D23580 TO INCREMENTAL CHANGES IN FLUID SHEAR STRESS IN THE RWV

5.1 Abstract

Salmonella enterica serovar Typhimurium ST313, a cause of fatal bacteremia in immunocompromised individuals in sub-Saharan Africa, exhibits key features that distinguish it from *Salmonella* serovars Typhimurium and Typhi – including alterations in pathogenesis-related stress resistance, colonization of host tissues, and biochemical profiles (see Chapter 2). However, the detailed pathogenic mechanisms of ST313 are not yet well understood. As described in Chapter 4, D23580, a representative ST313 strain, was found to induce a more rapid time-to-death in BALB/c mice and exhibit increased acid-resistance when cultured under a higher fluid shear environment using the Rotating Wall Vessel (RWV) bioreactor. These findings with NTS D23580 differed from what our laboratory previously observed for the classic *Salmonella* Typhimurium strain χ3339, which exhibited significantly increased virulence and enhanced resistance to several stresses in response to low fluid shear culture conditions in the RWV (when cultured to the same phase of growth). To better understand the effect of fluid shear on altered cellular responses of D23580, beads of different sizes were incorporated during RWV culture of this strain to create a series of cultures with incremental changes in fluid shear. These cultures were then profiled for select stress responses, macrophage survival, and global changes in gene expression using RNA-Seq. In response to incrementally increasing fluid shear conditions, gradual increases in D23580 stress-resistance and macrophage adherence, internalization, and intracellular survival/replication were observed. In agreement with these findings, RNA-seq analysis revealed corresponding

up-regulation in genes encoding fimbriae, SPI-1 (Salmonella Pathogenicity Island 1) regulators, and Type Three Secretion System (TTSS) effectors. This is the first demonstration that incremental changes in fluid shear can alter the stress response profiles and global gene expression profile of any ST313 strain. In addition, this is the first study to perform global gene expression analysis for any ST313 strain.

5.2 Introduction

5.1.1 Review on ST313 D23580 and distinct responses to fluid shear

A novel *Salmonella enterica* serovar Typhimurium (Typhimurium) multilocus sequence type 313 (ST313) prevalent in sub-Saharan Africa causes fatal bacteremia, (invasive disease) in young children and HIV-infected patients (5, 7, 8, 15, 16, 18, 177, 184, 186). Genomic profiling of the ST313 strains revealed a reduced genome resembling *Salmonella enterica* serovar Typhi (Typhi), causing invasive disease, and suggested person-to-person transmission given the lack of reports of animal infection (7, 24, 176). Our previous study showed distinct features of biochemical characteristics, colonization in host tissues and acid stress resistance distinct from both Typhimurium and Typhi (Chapter 2). A previous study determined that ST313 could cause severe infection in animals, indicating the potential for an unidentified animal reservoir (39). Also, previous studies with ST313 serovars found important host-pathogen interactions between host humoral/complement immunity and bacterial O-antigen/outer membrane (33-35), identified a gene important for bacterial virulence during systemic infection (40, 182), found high intracellular survival of ST313 compared to classic Typhi and Typhimurium *in vitro* ((40, 41), and Chapter 3), and relevance of attenuated flagellin to the enhanced bacterial survival in host macrophages (41). However, there are many aspects of ST313 pathogenesis that are not yet well understood.

The ST313 strains are mostly multidrug resistant (MDR) and frequently recurrent after treatment, leading to high mortality (17). There are increasing risks of the strains spreading worldwide due to easy travel and frequent transport globally, and increasing numbers of immunocompromised people worldwide as a result of HIV-infection, drug use, cancer therapy and aging (166-175, 271). It is urgent to have effective ways to control infection by ST313, and understanding the disease-causing mechanisms of these bacteria are important for developing ways to treat and prevent these infections. In this study, evidence is provided for the role of fluid shear in regulating the stress resistance, macrophage infection profiles, and global gene expression profiles of D23580. To our knowledge, this is the first study to report global gene expression in D23580 is altered by fluid shear stress, which is physiologically relevant to levels encountered by the pathogen *in vivo* in the infected host.

The classic *Salmonella* Typhimurium strain χ3339 was previously demonstrated by our lab to display increased virulence, enhanced stress resistance (for select stressors), and global changes in gene expression in response to low fluid shear culture conditions exhibited in spaceflight and in the RWV bioreactor (146, 157-159, 164, 165), a spaceflight analogue cell culture system that can be used for culturing cells under physiological levels of fluid shear (132, 144, 153, 154, 276, 291). Interestingly, despite the increased virulence of χ3339 in response to low fluid shear culture, microarray analysis did not reveal any known virulence genes to be induced, indicating the possibility that a previously uncharacterized mechanism(s) may be involved. These

studies also identified the evolutionarily conserved RNA-binding protein Hfq as a key regulator for the response of *Salmonella* to physiological low fluid shear culture (164).

As mentioned in previous Chapters, the ST313 strain D23580 showed different cellular responses and virulence potential than χ3339 in response to low fluid shear culture in the RWV (Chapter 4). D23580 also exhibited more sensitive responses to oxidative stress and delayed disease progression when grown in the RWV under the low shear condition (Chapter 4). It is not clear why D23580 exhibits different phenotypes than classic Typhimurium χ3339 in response to low fluid shear culture.

5.1.2 Investigating the effect of incremental changes in fluid shear that are physiologically relevant to those encountered by ST313 during infection

Typhimurium causes self-limiting gastroenteritis and does not normally induce systemic infection in healthy humans (12, 292). This is in contrast to Typhi, which causes the invasive disease known as Typhoid fever (292). ST313 is classified as Typhimurium yet causes a fatal bacteremia in immunocompromised people predominantly in sub-Saharan Africa. *Salmonella* entering the host body experience a wide range of fluid shear levels during the course of infection, with low fluid shear conditions found between the brush border microvilli of epithelial cells where *Salmonella* adhere at the first site of infection (132). As a facultative intracellular pathogen that incorporates both an intracellular and cell-free lifestyle, the spread of *Salmonella*

throughout the GI tract to the extra-intestinal environment of the circulatory system exposes the pathogen to a broad range of fluid shear environments. In particular, given the capacity of ST313 to routinely cause systemic disease - understanding the influence of the high fluid shear environment found within the blood stream (as well as in select regions of the GI tract) on the disease-causing properties of this pathovar is an important consideration.

This chapter focuses on understanding the effect of incremental increases of fluid shear on targeted stress responses, global gene expression profiles, and infection properties of ST313 strain D23580. The studies presented here build upon our lab's previous research conducted using the classic Typhimurium strain χ3339, which demonstrated that stress responses and gene expression could be incrementally altered in response to progressive increases in fluid shear in the RWV by incorporating beads of different sizes during culture (154). The central hypothesis is that incremental changes in fluid shear relevant to these encountered in the intestine and bloodstream will uniquely alter the stress responses, global gene expression profile, and infection properties of D23580.

5.3 Methods

Statistical evaluation.

All experiments were repeated at least 3 times. Each experiment included three technical replicates by plating samples onto LB agar in triplicate. Mean values and standard error of the mean (SEM) were calculated from three or more experiments or biological trials. All comparisons were made using the Student's t-test ($\alpha < 0.05$). The significances were indicated as *, $P<0.05$; **, $0.001<P<0.01$; and ***, $P<0.001$.

Generation of a range of incremental levels of fluid shear in RWV.

The RWV bioreactor was used in this study to generate different levels of fluid shear. Beads of different sizes were included in the RWV during culture, as previously described (154) to increase fluid shear during bacterial culture. Beads of differing size and density were used in the current study to generate a range of incrementally increasing fluid shear in bacterial culture in the RWV: 3/32-inch (2.381 mm) diameter polypropylene (**3/32-PP**); 1/8-inch (3.175 mm) diameter polypropylene (**1/8-PP**); and 1/8-inch diameter ceramic (**1/8-C**) (Baltec, Inc., Los Angeles, CA.). The fluid shear levels previously quantified by Nauman et al, in the RWV with and without bead addition are shown in **Figure 5-1**. The RWV without beads generates a low fluid shear environment with less than 1 dynes/cm^2 and a 3/32-PP or a 1/8-PP generates 5.2 dynes/cm^2 or 7.8 dynes/cm^2, respectively, based on the steady-state Navier-Stokes equations (154, 275). The ceramic bead, which is denser than polypropylene, was included to further increase the fluid shear (this has not yet been quantified). To generate

an even higher fluid shear condition, two beads were added simultaneously to the RWV bioreactor (1/8-PP and 1/8-C). Beads were sterilized and subsequently added into RWVs aseptically. For ease of reference, the five different incrementally increasing fluid shear conditions ranging from low-to-high as a result of bead addition(s) in the RWV are designated as follows: Shear 1 (**S1; no bead**); Shear 2 (**S2; 3/32 PP**); Shear 3 (**S3; 1/8 PP**); Shear 4 (**S4; 1/8 C**), and Shear 5(**S5; 1/8 PP and 1/8 C**).

Bacterial strains and growth conditions.

S. Typhimurium D23580 was used as a representative ST313 strain in this study and was cultured in Lennox broth (LB) at 37°C in all experiments. An overnight culture of D23580 grown for 15-16 h with aeration was diluted 1:200 into fresh LB and loaded into the RWV bioreactors. The RWV was completely filled with culture medium and air bubbles were removed to avoid additional fluid shear. The RWVs were incubated at 25 rpm for 24 h with aeration and growth curves were performed by determining live colony forming units per milliliter (CFU/mL) at various time points to define bacterial growth in different fluid shear conditions (**Figure 5-2**). For all studies, bacterial cells were grown for 24 hours to stationary phase.

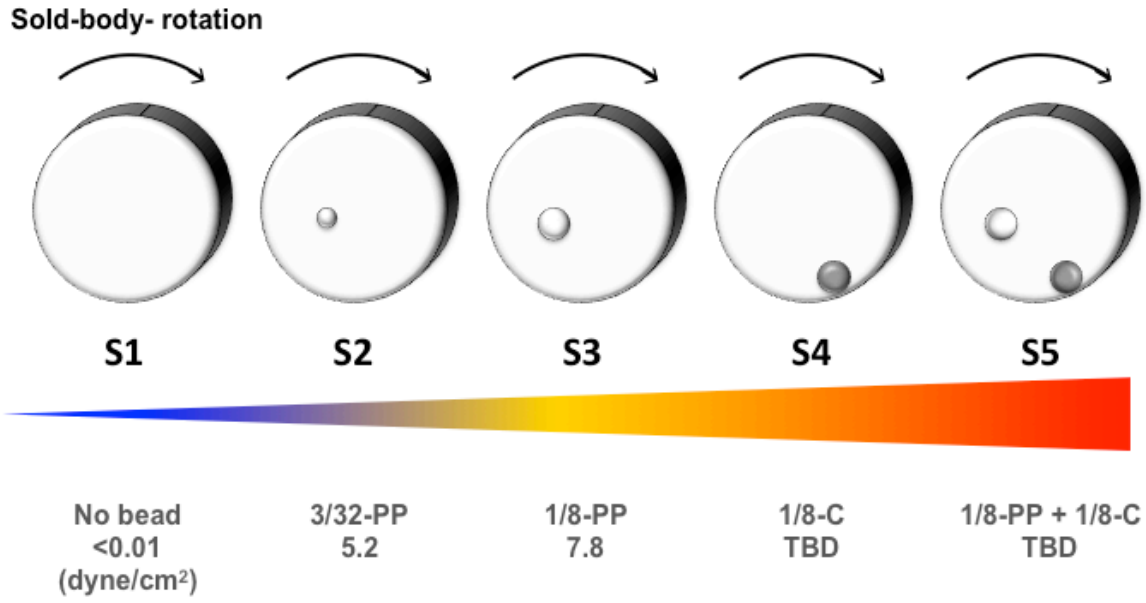

Figure 5-1. Diagram of RVW bioreactor including beads of varying size and densities to induce incremental increases in fluid shear stress.

The RWV bioreactors are completely filled with culture medium and rotated on their horizontal axis at 25 rpm, which creates a solid body rotation of the media. Bacteria are maintained in a suspension culture in a gentle fluid orbit, and in the absence of a bead, bacteria experience a low fluid shear stress of less than 1 dyne/cm2. Maximum mechanical forces of fluid shear stress surrounding the bead in fluid in RWV bioreactors, quantified by Nauman et al, are 5.2 dynes/cm2 in 3/32-PP and 7.8 dynes/cm2 in 1/8-PP. A dyne is defined as the force required to accelerate a mass of one gram at a rate of one centimeter per second squared (1 dyne = 1 g·cm/s2). The maximum shear force generated by the 1/8-Cera bead has not yet been determined. The density of the ceramic bead is greater than the polypropylene bead, so that the ceramic bead falls to the bottom of the RWV at the same rotating speed and rolls on the bottom surface inside the RWV, while the polypropylene bead floats within a steady-state position under the same conditions.

S1 indicates that the RWV contains no beads; S2 indicates that the RWV contains a 3/23-inch polypropylene bead; S3 indicates that the RWV contains a 1/8-inch polypropylene bead; S4 indicates that the RWV contains a 1/8-inch ceramic bead; and S5 indicates that the RWV contains both a 1/8-inch polypropylene bead and a 1/8-inch ceramic bead. The RWV reactors are depicted as a scaled series of incrementally increasing fluid shear biosystems, with shear (S) levels ranked on a scale of low-to-high as a result of bead(s) addition (with S1 being low and S5 being high).

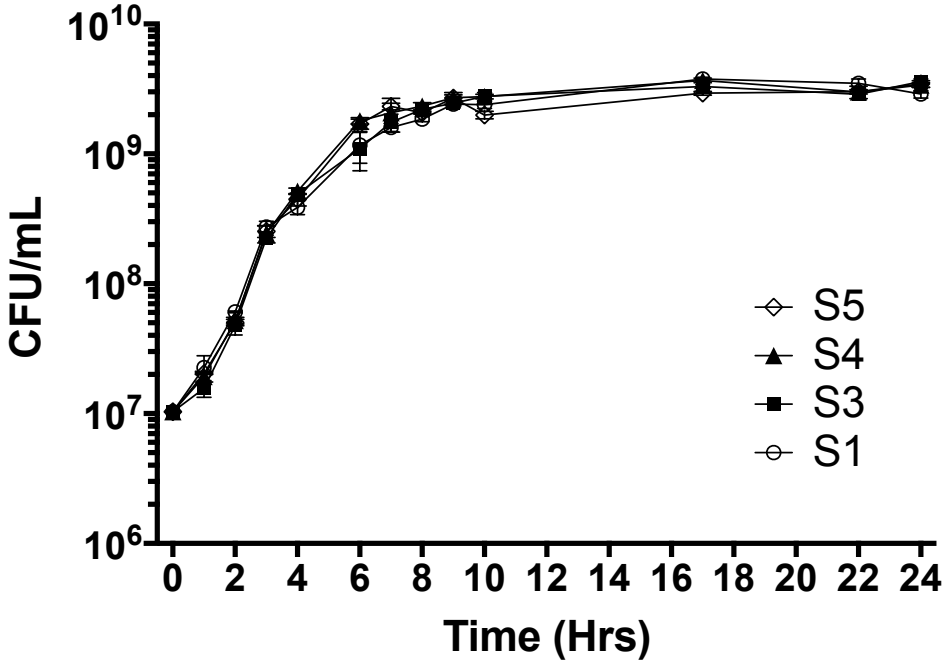

Figure 5-2. Growth curve of D23580 grown in RWV bioreactors with or without beads.

D23580 was inoculated into LB with aeration (180 rpm) for 15 hours at 37°C. These cultures were diluted at 1:200 in fresh LB and loaded into RWVs (~50 mL per bioreactor) with or without beads and subsequently incubated at 37°C and 25 rpm on their horizontal axis. Cultures were monitored by plating on LB agar for viable colony-forming units (CFU).

Stress survival assays.

Bacteria were grown as described above to stationary phase, and 10 mL of each culture was immediately subjected to the tested stresses. For acid stress assays, sterile 1M citrate buffer was added to lower the pH to 3.5. For oxidative stress assays, 6% hydrogen peroxide was added to the culture samples to a final concentration of 0.12%. Cells were incubated statically at room temperature during exposure to the stress and the pH was confirmed with an electrode at the end of the assay. Samples were removed at time zero

(before the addition of stress) and at various time points thereafter, diluted in phosphate buffered saline (PBS) for the acid stress assay or 0.1M sodium bicarbonate buffer (0.1M-Na_2CO_3 0.1M-$NaHCO_3$, pH 7.5) for the oxidative stress assay and then plated on LB agar to determine the CFU. Percent survival was calculated as the ratio of the CFU at each time point to the CFU at time zero. At least three independent trials were performed.

J774A.1 macrophage infection.

J774A.1 cell line was purchased from the American Type Culture Collection (ATCC, Cat. #TIB-67 ^{TM}) and cultured in high glucose-Dulbecco's Modified Eagle's Medium (DMEM) (GIBCO #11995) containing 4mM Lglutamine, 4500 mg/L glucose, 1 mM sodium pyruvate, and 3700 mg/L sodium bicarbonate with heat-inactivated 10 % fetal bovine serum. The cells were grown as monolayers at 37°C with 5% CO_2 without antibiotics. The number of live cells was enumerated by trypan blue exclusion prior to infection and ~1- 2 x 10^5 cells/mL (~75% confluency) were infected by D23580 cultured as described above at a multiplicity of infection (m.o.i.) of ~10 for 30 min (adhesion). The infected cells were washed 3 times with Hanks' balanced salt solution (HBSS) and lysed with 0.1 % sodium-deoxycholate or incubated further in DMEM with 50 μg/mL gentamycin (50Gen) for 2.5 hrs at 37°C with 5% CO_2 (total 3 hrs infection for intracellular invasion). The infected cells incubated in DMEM-50Gen were then washed 3 times with HBSS and either lysed or further incubated in fresh DMEM with 10 μg/mL gentamycin (10Gen) for 21 hrs (total 24 hrs infection for intracellular survival/replication). The infected cells in DMEM-10Gen were then washed and lysed as previously described. Lysates were serially diluted 10-fold with sterile PBS and each

dilution plated onto LB agar three times and counted to assess averaged CFU/mL. Percent survival compared to the initial inoculum was calculated as a ratio of the CFU at each time point to the CFU of the infection dose at time zero. Percent survival compared to the previous infection point was calculated as the ration of the CFU at each time point to the CFU recovered at the previous time point. Three biological replicates were performed independently and each included three technical replicates that were averaged. Data presented represents the average of all three biological replicates. Matched time point controls were included for all studies using the non-invasive *E. coli* strain HB101. D23580 was verified to be gentamycin-sensitive prior to the study.

RNA sequencing.

RNA sequencing (RNA-Seq) was performed on an Illumina HiSeq-2000 sequencer to profile the entire transcriptome of D23580. Three RNA sample types were processed- no bead (S1), 1/8-PP (S3), and 1/8-C (S4) For all three RWV conditions (S1, S3 and S4), the RNA samples were prepared from two sets of biological replicates of bacterial cultures (D23580) grown in LB medium to stationary phase for 24 hours at 37 °C. Total RNA was purified using the miRNeasy kit (Qiagen) and quantified using a Nanodrop spectrophotometer, and the integrity verified by formaldehyde-agarose gel electrophoresis (**Figure 5-3**). The sample cDNA libraries were generated utilizing the encore complete prokaryotic RNA-Seq library systems, enriching non-rRNA during cDNA synthesis and providing barcoded adaptors to enable multiplex sequencing. The barcode indexes for samples were 'CGATGT' for N1 sample, 'TGACCA' for N2, 'ACAGTG' for PP1, 'GCCAAT' for PP2, 'CAGATC' for C1, and 'CTTGTA' for C2.

The synthesized cDNAs (generated with Nugen's Ovation SPIA chemistry) were fragmented, ligated with adaptors using Kapa Biosystems NGS library preparation kit, and PCR-amplified using Kapa Biosystems HiFi polymerase to generate sequencing libraries. Six-plexed 2x100 bp paired-end DNA sequencing yielded a total of 202 million pairs of reads, and the reads per sample ranged from 28 to 48 millions (**Table 5-1**). The reads were then aligned to the *S.* Typhimurium D23580 chromosome FN424405 and plasmid pST-BT FN432031, counted per gene, and quantified as FPKM (Fragments Per Kilobase Per Million Reads) by *TopHat* and *Cufflinks* software (PMID: 22383036). When data from duplicated samples for each group were merged, we detected an average of ~2,500 genes (out of ~4,500 protein coding genes in the genome) with FPKM > 1 with average coverage of ~50x (**Table 5-2**). Pair-wise comparisons among no-bead (S1), 1/8-inch polypropylene bead (S3), and 1/8-inch ceramic bead (S4) samples were performed by using t-test, and differentially expressed genes were selected with thresholds of >2 fold changes (either up- or down-regulated) and $P < 0.05$.

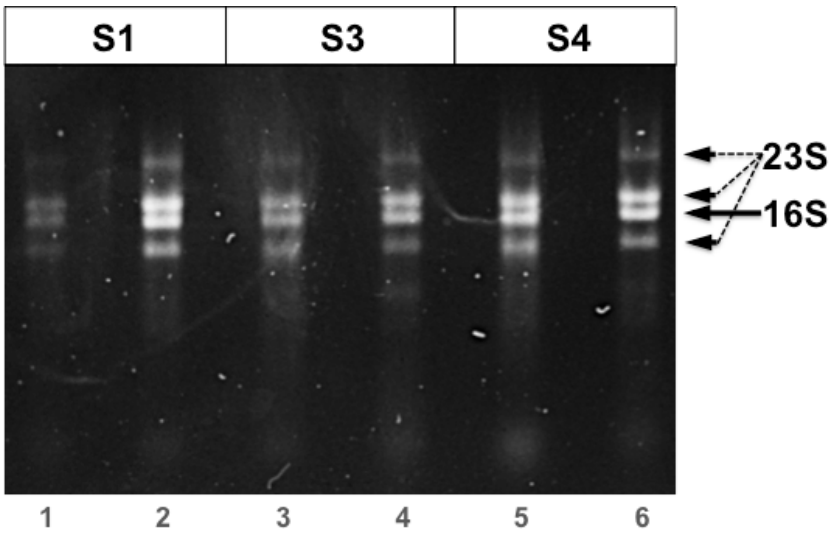

Figure 5-3. Purified RNAs in D23580.

RNA was purified from D23580 grown in the RWV for 24 hrs in the S1, S3, or S4 conditions . The purified total RNA samples were verified by formaldehyde-agarose gel electrophoresis in 1.5 % agarose gel. 16S rRNA and fragmented 23S rRNA are shown (arrows). The fragmentation of 23S rRNA is a characteristic of *S.* Typhimurium (293). *Imaging done by Jennifer Barrila

Table 5-1. RNA sequencing results.

(A) RNA-Seq read counts

		1 (S1)	2 (S1)	3 (S3)	4 (S3)	5 (S4)	6 (S4)
Total paired Reads		28,733,271	29,829,775	48,462,255	27,930,881	35,214,995	32,034,443
Mapped Reads	**Count**	24,859,509	26,183,706	41,624,296	23,979,855	30,927,263	27,654,979
	%	**86.50%**	**87.80%**	**85.90%**	**85.90%**	**87.80%**	**86.30%**
Unmapped Reads	**Count**	3,873,763	3,646,070	6,837,960	3,951,027	4,287,733	4,379,465
	%	**13.50%**	**12.20%**	**14.10%**	**14.10%**	**12.20%**	**13.70%**

(B) Gene counts and coverage

		S1 (no bead)	S3 (1/8-PP)	S4 (1/8-C)
Detected Genes	FPKM > 0	3005	2756	2620
	FPKM > 1	2731	2504	2300
Ave. Coverage		**51.2**	**67.6**	**38**

5.4 Results

5.1.3 Acid resistance of D23580 is influenced by changes in physiological fluid shear in a reciprocal manner.

To investigate the effect of incremental changes of fluid shear on the acid stress response of D23580, bacteria were cultured as described above (**Figure 5-1**) in S1, S2, S3 and S4 conditions. As shown in **Figure 5-4**, as D23580 was exposed to incrementally increasing levels of fluid shear, a progressive increase was observed in the acid stress resistance. In particular, the highest fluid shear condition (S4) significantly increased the resistance of D23580 to the acid stress at all time points tested. Moreover, the effect of increased acid resistance between fluid shear conditions became greater over time. Specifically, differences between the highest (S4) and the lowest (S1) fluid shear conditions were 4.27-fold at 30 mins, 8.00-fold at 60 mins, 11.54-fold at 90 mins, and 44.25-fold at 180 mins. It should be noted that the S2 condition did not show significantly different acid resistance when compared to the lowest fluid shear condition (S1), suggesting a potential threshold of the fluid shear force on the surface of D23580 to initiate changes in bacterial responses to acid stress.

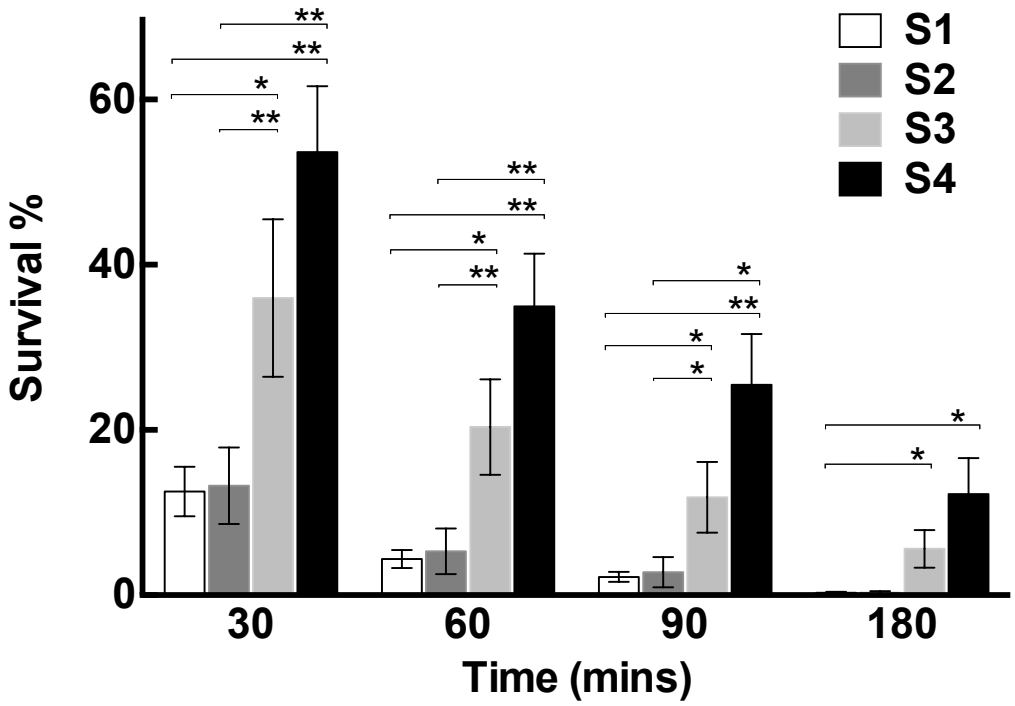

Figure 5-4. Survival at pH 3.5 of D23580 grown under incremental fluid shear in the RWV.

D23580 was cultured in the RWVs with either no bead (S1, white bars), 3/32-PP bead (S2, dark grey bars), 1/8-PP bead (S3, light grey bars), or 1/8-C bead (S4, black bars). Surviving bacteria were examined in every 30 min after cells were subjected to acid stress of pH 3.5. Percent survival of each sample were determined by the ratio of CFU/mL at the tested times to the CFU/mL at time zero. Five independent trials were performed. Mean values, standard error of means, and p-values are indicated. Statistical significance was evaluated as described above.

5.1.4 J774A.1 macrophage infection of D23580 grown under incremental fluid shear in the RWV

Classic *S.* Typhimurium χ3339 grown to log phase in low fluid shear in the RWV (no bead) was reported to survive better in J774 macrophages than when bacteria were

grown in the higher fluid shear control condition (143, 159). Infection of J774 cells with strain D23580 cultured under incrementally increasing levels of fluid shear had not previously been assessed. Bacterial adherence (30 min post-infection), invasion/phagocytosis (3 h post-infection), and intracellular survival/replication (24 h post-infection) was measured after D23580 was grown in a range of fluid shear conditions (S1, S3, and S4) in the RWVs. The condition of S2 was excluded in this study because the condition did not lead to a significant alteration in acid-resistance of D23580 (see above). The results showed that incremental increases in fluid shear progressively increased the adherence, internalization (invasion/phagocytosis**)** and intracellular survival of D23580 in J774 monolayers, which included a ≥ 2-fold difference between the N and C conditions at each time point (**Figure 5-5**). In particular, a representative biological trial displayed significant increases in adherence (4.71-fold), invasion (5.20-fold) and intracellular survival (3.96-fold) when D23580 was grown in incrementally increasing fluid shear (**Figure 5-5B**). These results demonstrate that D23580 infection of J774 macrophages is enhanced by changes in fluid shear stress.

In chapter 3, low levels of D23580 internalization (invasion/phagocytosis) into 3-D immunocompetent intestinal cell culture models containing phagocytic macrophages was reported when the bacteria were grown in shake flasks. In this study, progressive increases in internalization into pure cultures of J774 monolayers was observed when D23580 was grown under incrementally increasing fluid shear in the RWV bioreactor. The apparent paradox in invasion between these studies may be related to differences in experimental design, including a) the use of flask grown bacteria in the 3-D infection

studies as compared to RWV grown bacteria in the monolayer studies, which would result in different fluid shear and oxygen levels, and b) the use of different host cell types alone or in combination. Another important consideration is bacterial access to phagocytic cells in the two studies. While monolayers were composed solely of J774 phagocytes (with 100% bacterial access), the majority of cells in the 3-D co-culture model were epithelial, with macrophages being present in much lower numbers and often localized beneath the epithelial cells in the lamina propria region (which would not have direct access to bacteria). The elevated numbers of D23580 at 24 h post infection in J774 macrophages demonstrates enhanced bacterial survival and intracellular replication. These data are in agreement with the intracellular survival/replication trends for D23580 in 3-D co-cultures in chapter 3.

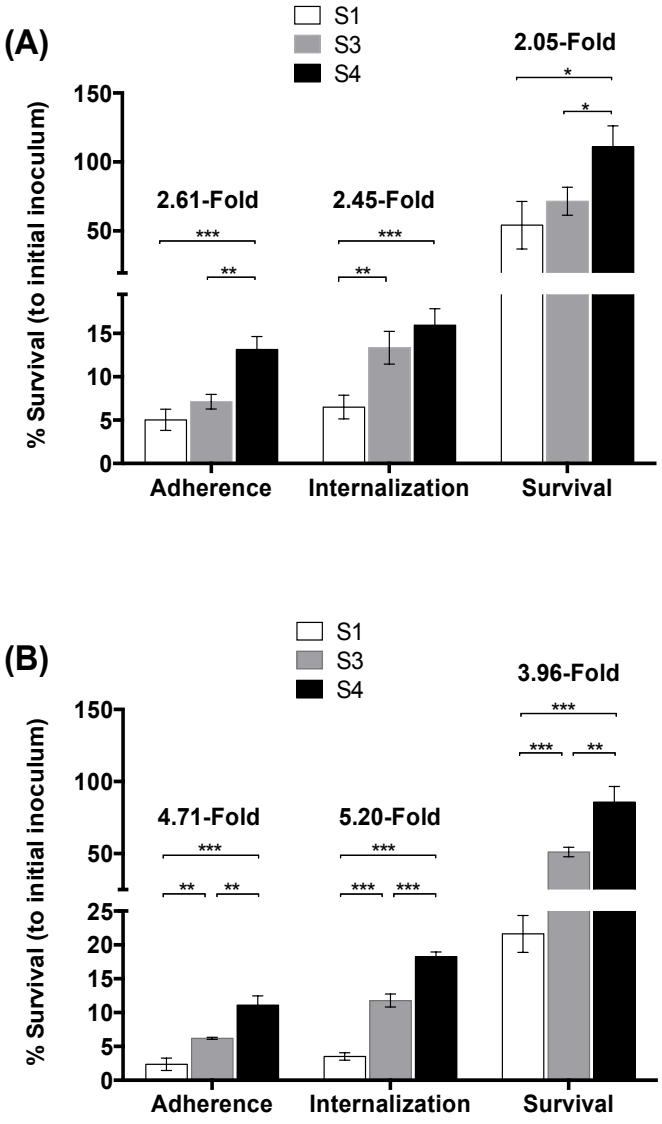

Figure 5-5 J774 infection profile of D23580 cultured in the RWV with and without addition of beads.

J774A.1 monolayers were infected with D23580 grown in RWVs without a bead (S1, white bars), 1/8-PP (S3, grey bars), and 1/8-C (S4, black bars). Live bacteria were recovered at 0.5 h, 3h, and 24 h post-infection and the percent survival (normalized to the initial inoculum) were calculated as described above. (A) Three independent trials including three technical replicates per trial were plotted. Mean values, standard error of means are indicated. (B) A representative graph from one biological trial is shown. Mean values, standard error of means, and p-values are indicated. Statistical significance was evaluated as described above.

5.1.5 Fluid shear-induced alterations in the global gene expression profile of D23580.

To explore the impact of a range of physiological fluid shear levels on gene expression in D23580, we profiled changes in global expression of transcripts using RNA-sequencing. Total RNA from D23580 grown in the RWV with no bead **(S1)**, 1/8-PP **(S3)**, and 1/8-C **(S4)** was sequenced and screened for genes showing differential expression. A total of 4643 ORFs were found to be expressed and of those 109 genes showed statistically significant differences in expression ($P< 0.05$). Of these, 12 genes were expressed only in the highest fluid shear condition (S4, FPKM>1), while 20 genes were expressed only in the low fluid shear condition (S1, FPKM>1) (**Table 5-2**).

Table 5-2. Genes expressed above baseline in only one fluid shear condition
(A) Genes expressed only in the highest fluid shear condition (S4),; or (B) the lowest fluid shear condition (S1) (P<0.05, FPKM>1). Averaged FPKMs are listed. ORFs differentially expressed (p<0.05) influenced by fluid shear were screened. Genes with FPKM>1 were considered to be expressed and are shown in bold text; while genes with FPKM1 <1 were considered to have little-to-no expression and are not bold.

STMMW	Description	S1	S3	S4
(A) Genes expressed only in S4				
11001	hypothetical protein	0.14	0.05	**1.08**
17321	TonB protein	0.02	0.11	**1.22**
15381	uptake hydrogenase small subunit	0.29	0.83	**1.37**
16521	putative membrane transport protein	0.08	0.30	**1.40**
44551	hypothetical protein	0.04	0.20	**1.63**
24391	nucleoside permease	0.02	0.03	**1.67**
20971	secreted protein SopA	0.06	0.32	**1.93**
13351	putative outer membrane protein	0.19	0.69	**3.08**
35051	MalT regulatory protein	0.77	0.87	**3.24**
12881	hypothetical protein	0.55	0.23	**3.26**
30081	hypothetical protein	0.31	0.07	**3.91**
12601	putative cytochrome	0.89	0.17	**10.95**

(B) Genes expressed only in S1

44631	hypothetical protein	**1.07**	0.08	0.12
07191	hypothetical protein	**1.07**	0.01	0.29
14731	hypothetical protein	**1.18**	0.01	0.02
30441	putative oxidoreductase	**1.19**	0.36	0.02
08941	putative formate acetyltransferase 3	**1.21**	0.02	0.03
00881	putative sulfatase	**1.25**	0.16	0.01
15531	putative glycogen debranching protein	**1.27**	0.19	0.09
30941	hexuronate transporter	**1.33**	0.08	0.30
12321	spermidine/putrescine transport system permease protein PotC	**1.74**	0.05	0.09
27571	putative GAB DTP gene cluster repressor	**1.80**	0.04	0.89
40711	5,10 methylenetetrahydrofolate reductase	**1.99**	0.04	0.86
37821	putative carbohydrate kinase	**2.19**	0.05	0.50
09511	hypothetical protein	**2.28**	0.01	0.07
23761	histidine-binding periplasmic protein	**2.44**	0.19	0.40
06341	hypothetical protein	**2.49**	0.22	0.16
21681	phage protein	**2.73**	0.09	0.33
15811	ATP-binding protein	**3.01**	0.04	0.17
09801	transport protein	**3.59**	0.00	0.04
22031	putative oxidoreductase	**4.67**	0.09	0.16
37081	lipopolysaccharide 1,6-galactosyltransferase	**7.55**	0.65	0.38

S1 indicates no bead condition; S4, 1/8-PP bead; S4, 1/8-C bead. FPKM>1 are bolded

We proceeded to analyze these data for significant upregulation and downregulation of genes related to fluid shear through comparative analysis of each condition using inclusion criteria of ≥ 2-fold change, $p < 0.05$ (upregulation) and ≤ -2-fold change, $p < 0.05$ (downregulation). Using these criteria, 77 genes showed significant upregulation in response to increasing fluid shear conditions and 48 genes were significantly downregulated (**Table 5-3 and 5-4**). Of the upregulated genes, 53.25% (41/77) were found in the S3 to S1 comparison, while 40.26% (31/77), and 18.18% (14/77) were present in S4 compared to S1, and S4 compared to S3 conditions, respectively (**Table 5-3**). Of the downregulated genes, 50% (24/48) were present in S3 to

S1 comparison **(**19.17% (14/48) were present in the S4 to S1 comparison, and 37.5% (18/48) were present in the S4 to S3 comparison (**Table 5-4**). Of note, more than 50% of the genes upregulated or downregulated in the higher fluid shear condition were present in the S3 to S1 comparison, indicating that the fluid shear between 0.01 and 7.8 dyne/cm^2 may be responsible for approximately half of the observed changes in gene expression.

Table 5-3. Genes showing increased expression in response to higher fluid shear (2-fold cutoff, *P*<0.05, n = 77 genes)

ORFs upregulated in higher fluid shear conditions with ≥2-fold change are listed. (A) Upregulation in S3 is more than 2-fold greater than in S1; (B) Upregulation in S4 is more than 2-fold greater than in S1; Upregulation in S4 is more than 2-fold greater than in S3.

STMMW	Gene	Description	Fold Change
(A) S1 < S3 (41 genes)			S1 to S3
06281	*ykgD*	araC family transcriptional regulator	59.72
44881	*yjjA*	hypothetical protein	55.12
30541	*endA*	endonuclease I	51.02
40021	*fdhD*	FdhD protein	46.10
15271	-	hypothetical protein	36.37
43411	*fklB*	FkbP-type peptidyl-prolyl cis-trans isomerase	31.93
06171	*fimZ*†	transcriptional regulator (FimXZ protein)	29.68
28381	*hilA*†	invasion protein transcriptional regulator	29.33
18031	*ycgN*	hypothetical protein	27.35
02551	*yafC*	transcriptional regulator	26.09
27791	-	putative transmembrane transport protein	25.37
13751	*sufA*	hypothetical Fe-S cluster assembly protein SufA	25.25
31411	*parE*	topoisomerase IV subunit B	18.96
44041	*pyrI*	aspartate carbamoyltransferase regulatory subunit	18.59
10881	*helD*	helicase IV (75 kD helicase)	17.49
28461	*sipC*†* (*sspC*)	SPI1 TTSS effector: translocation machinery (cell invasion protein)	15.28
24301	-	putative ion-channel protein	14.57
44161	*yjgD*	hypothetical protein	13.49
39291	*recQ*	ATP-dependent DNA helicase	13.34
14681	*manA*	mannose-6-phosphate isomerase	13.01
12491	-	putative bacteriophage protein	11.55
18311	*kdgR*	transcriptional regulator KdgR	11.32
26631	*srmB*	ATP-dependent RNA helicase SrmB	10.81
28471	*sipB*†* (*sspB*)	SPI1 TTSS effector: translocation machinery component	10.71
34881	*hslO*	heat shock protein	10.29
36021	*yhjJ*	putative zinc-protease precursor	10.00
35931	-	hypothetical protein	9.78
14521	*tyrS*	tyrosyl-tRNA synthetase	9.72

06141	*fimD*†	outer membrane usher protein FimD	9.61	
39281	*pldA*	detergent-resistant phospholipase A	9.48	
28981	*cysD*	ATP sulfurylase (ATP:sulfate adenyltransferase)	9.20	
SLT-BT0141	-	conserved hypothetical protein	8.00	
30001	*lysS*	LysRS	7.72	
24251	*yfdZ*	putative aminotransferase	6.94	
33411	*sspA*	stringent starvation protein A	6.63	
28451	*sipD*†* (*sspD*)	SPI1 TTSS secretory apparatus, translocon (cell invasion protein)	6.38	
44361	-	putative ATP-dependent Lon protease	6.11	
11031	*sopB*†*	SPI1 TTSS effector, cell invasion protein	5.33	
00061	*talB*	transaldolase B	5.30	
21121	*gnd*	6-phosphogluconate dehydrogenase	4.70	
11731	*grxB*	glutaredoxin	3.44	

(B) S1 to S4 (31 genes)

			S1 to S4
24391	*xapB*	nucleoside permease	73.09
29071	*ygcB*	hypothetical protein	61.98
17321	*tonB**	TonB protein	54.19
44551	-	hypothetical protein	44.41
20971	*sopA*†	SPI1 TTSS effector (invasion-associated)	34.96
18441	*sopE2*†	SPI1 TTSS effector (invasion-associated)	32.66
17731	*ychM*	putative sulfate transporter	21.75
28381	*hilA*†	invasion transcriptional regulator HilA	18.98
28441	*sipA*†* (*sspA*)	SPI1 TTSS effector (invasion-associated)	18.17
16521	*zntB*	putative membrane transport protein	18.01
13351	-*	putative outer membrane protein	16.24
29401	*fucK*	L-fuculose kinase	13.32
30081	*ygfZ*	hypothetical protein	12.72
12601	-	putative cytochrome	12.36
11031	*sopB*†*	SPI1 TTSS effector (invasion-associated)	10.87
06111	*fimA*†*	type-1 fimbrial protein	10.42
28581	*invA*†	TTSS secretory apparatus (associated with virulence)	9.09
11021	*pipC*†*	cell invasion protein (SPI3 chaperone, similar to TTSS SigE)	8.86
28451	*sipD*†* (*sspD*)	SPI1 TTSS secretory apparatus, translocon (cell invasion protein)	8.14
16021	-	Putative lipoprotein YdcL	5.06
23401	*nuoM*	NADH dehydrogenase I subunit M	4.77
15381	*hyaA2*	uptake hydrogenase small subunit	4.72
35051	*malT**	MalT regulatory protein	4.20

06121	*fimI*†	Fimbrial protein FimI (major pilin protein)	4.09	
07981	*cydB**	cytochrome D ubiquinol oxidase subunit II	3.85	
42121	*siiE*	hypothetical protein	3.15	
30781	-	putative hydrolase	3.13	
34901	*pckA*	phosphoenolpyruvate carboxykinase	2.88	
09761	*dmsA**	anaerobic dimethyl sulfoxide reductase subunit A	2.82	
13971	*spiR*†*	putative two-component sensor kinase SsrA; TTSS regulation	2.60	
28371	*hilD*†*	Transcriptional regulator (activator for invasion genes)	2.51	
(C) S3 < S4 (14 genes)				S3 to S4
14981	*dmsA2*	putative dimethyl sulfoxide reductase subunit		129.34
12601		putative cytochrome		63.99
24391	*xapB*	nucleoside permease		62.02
30081	*ygfZ*	Putative global regulator		59.94
29071	*ygcB*	hypothetical CRISPR-associated endonuclease/Helicase Cas3		34.98
27571	*ygaF*	putative GAB DTP gene cluster repressor		25.31
11001	*pipB*†	SPI2 TTSS effector		21.15
31241	*yqhD*	probable alcohol dehydrogenase		14.14
12881	*yeaK*	hypothetical protein		14.05
16021	-	putative lipoprotein		9.19
04391	*prpC*	methylcitrate synthase		8.68
35401	*ggt*	gamma-glutamyltranspeptidase		6.60
31141	-	hypothetical protein		5.63
30781	-	putative hydrolase		4.28

*, genes with incremental increases in expression in in concert with increasing fluid shear; †, pathogenesis/virulence associated genes; -, not available;

Table 5-4. Genes showing decreased expression in response to higher fluid shear (2-fold cutoff, *P*<0.05, n = 48 genes).

ORFs downregulated in the higher fluid shear condition with ≤ -2-fold change are listed. Negative values indicate decreased gene expression between the tested conditions (A) Genes downregulated in S3 as compared to S1 (fold cut-off ≤2); (B) Genes downregulated in S4 as compared to S3 (fold cut-off ≤2); and (C) Genes downregulated in S4 as compared to S3 (fold cut-off ≤2).

STMMW	Gene	Description	Fold Change
(A) S1 > S3 (24 genes)			S1 to S3
09511	*ybjE*	hypothetical protein	-187.32
14731	-	hypothetical protein: Metallo-dependent hydrolase	-125.67
07191	*ybeQ*	hypothetical protein	-119.29
15811	-	hypothetical protein: ATP-binding protein	-72.66
32801	*deaD*	ATP-dependent RNA helicase (dead-box protein)	-63.06
08941	*pflF*	putative formate acetyltransferase 3	-58.62
40711	*metF*	5,10 methylenetetrahydrofolate reductase	-53.73
27571	*ygaF*	putative GAB DTP gene cluster repressor	-51.02
22031	*yohF*	putative oxidoreductase: Acetoin dehydrogenase	-50.66
37821	-	putative carbohydrate kinas: Ribokinase	-48.15
26011	-	putative prophage protein: Putative transposase	-39.13
12321	*potC*	spermidine/putrescine permease	-36.85
21681	*sseK2*†	TTSS2 (minor role in virulence)	-30.39
30941	*exuT*	hexuronate transporter	-17.50
22511	*yejG*	hypothetical protein	-17.40
04131	-	hypothetical rtn protein	-17.12
44631	*yjiN*	hypothetical protein	-13.91
30191	*ygfB*	hypothetical protein	-13.59
11851	*flgE*	flagellar hook	-12.82
23761	*hisJ*	histidine-binding periplasmic protein	-12.80
37081	*rfaB*†	lipopolysaccharide 1,6-galactosyltransferase	-11.61
06341	*ybdG*	hypothetical Miniconductance mechanosensitive channel	-11.18
20351	*yeeI*	hypothetical protein: DgsA anti-repressor MtfA	-11.01
38601	*asnCb*	DNA-binding transcriptional repressor of asnA	-8.16

(B) S1 > S4 (14 genes)			S1 to S4
00881	-	putative sulfatase	-195.04
22511	*yejG*	hypothetical protein	-129.13
09801	*ycaM*	probable transport protein: Inner membrane transporter	-87.37
30441	-	Putative mannitol dehydrogenase	-47.96
08941	*pflF*	putative formate acetyltransferase 3	-37.09
40301	-	putative Na+/galactoside symporter	-27.97
30191	*ygfB*	hypothetical protein	-23.06
38601	*asnCb*	DNA-binding transcriptional repressor of asnA	-20.28
37081	*rfaB*†	lipopolysaccharide 1,6-galactosyltransferase	-19.98
06341	*ybdG*	hypothetical protein: Miniconductance mechanosensitive channel	-15.58
15531	-	putative glycogen debranching protein	-14.50
20351	*yeeI*	hypothetical protein: DgsA anti-repressor MtfA	-14.27
15941	*pdgL*	D-alanyl-D-alanine dipeptidase	-12.29
27801	*emrR*	putative transcriptional regulator	-11.80

(C) S3 > S4 (18 genes)			S3 to S4
15271	-	hypothetical inner membrane protein	-231.09
30541	*endA*	endonuclease I	-160.63
18031	*ycgN*	hypothetical protein	-136.97
34881	*hslO*	heat shock protein: Hsp33-like chaperonin	-92.03
27791	-	putative transmembrane transport protein	-62.15
44161	*yjgD*	hypothetical protein: RNase E inhibitor protein	-61.53
44041	*pyrI*	aspartate carbamoyltransferase regulatory subunit	-58.93
14681	*manA*	mannose-6-phosphate isomerase	-57.84
09281	*potF*	putrescine-binding periplasmic protein	-51.89
36791	*sadA*	putative inner membrane protein	-37.84
36021	*yhjJ*	putative zinc-protease precursor	-36.35
39291	*recQ*	ATP-dependent DNA helicase	-36.09
39281	*pldA*	detergent-resistant phospholipase A	-31.65
40301	-	putative sugar transport protein	-26.20
33411	*sspA*	stringent starvation protein A	-22.16
14521	*tyrS*	tyrosyl-tRNA synthetase	-16.20
24251	*yfdZ*	putative aminotransferase	-14.85
18311	*kdgR*	transcriptional regulator KdgR	-11.05

*, genes with incremental decrease expression in concert with increasing fluid shear; †, pathogenesis/virulence associated genes; -, not available.

Of the differentially expressed genes, 21.19% were found to respond to incremental changes in physiological fluid shear; 14 genes showed incremental increases with increasing fluid shear, while 9 genes showed incremental decreases with increasing fluid shear (**Table 5-5**). Interestingly, of the genes upregulated in higher fluid shear with greater than 2-fold change, 17 genes were found to be related to bacterial infection, including fimbrial genes (*fimAIDZ*) and TTSS1 and TTSS2 related genes (*pipBC*, *spiR*, *sopABE2*, *hilAD*, *invA*, *sipADCB*) (**Table 5-5**). Among those, expression of 9 genes (*fimA, pipC, spiR, sopB, hilD, sipA, sipD, sipC, sipB*) exhibited incremental increases in expression (S1<S3<S4) in increasing fluid shear conditions (S1-S3-S4). The *rfaB* gene, associated with LPS synthesis, and *emrR*, a multidrug efflux repressor, were detected to be downregulated incrementally (S1>S3>S4) in increasing fluid shear conditions (S1-S3-S4).

Table 5-5 Selected genes altered in expression as a function of fluid shear (24 genes).

Fold-changes between two conditions are presented and the significant differences with greater than 2-fold are bolded (≥2-fold, $P<0.05$). Incrementally up- or down-regulated genes in incrementally increasing fluid shear are listed. Only genes, up- or down-regulated, with greater than 2-fold changes in at least one incremental change are listed and the significant fold-changes are bolded. * - genes of incremental increase in gene expression in incremental fluid shear; †, pathogenesis/virulence associated genes; -, not available. Statistical significance was evaluated as described above. Fold-differences greater than 2 are bold (≥2-fold change, $P<0.05$). (A) Incrementally upregulated genes in higher fluid shear, and (B) incrementally downregulated genes in higher fluid shear.

STMMW	Gene	Description	Fold Change		
(A) Genes with incremental increase (15 genes)			S1 to S3	S3 to S4	S1 to S4
06111	*fimA*†*	Type-1 fimbrial protein	4.46	2.34	**10.42**
06121	*fimI*†	Fimbrial protein FimI (major pilin protein)	~1	4.68	**4.09**
06141	*fimD*†	Outer membrane usher protein FimD	**9.61**	~1	2.60
06171	*fimZ*†	Transcriptional regulator (FimXZ protein)	**29.68**	-4.97	5.97
11001	*pipB*†	SPI-2 TTSS effector	~1	**21.15**	7.50
11021	*pipC*†*	Cell invasion protein (SPI-3 chaperone, similar to TTSS SigE)	4.00	2.21	**8.86**
13971	*spiR*†*	Putative two-component sensor kinase SsrA; TTSS regulation	2.00	1.30	**2.60**
18441	*sopE2*†*	SPI-1 TTSS effector (invasion-associated)	11.63	2.81	**32.66**
11031	*sopB*†*	SPI-1 TTSS effector (cell invasion protein)	**5.33**	2.04	**10.87**
20971	*sopA*†	SPI-1 TTSS effector (invasion-associated)	~1	~1	**34.96**
28371	*hilD*†*	Transcriptional regulator (activator for invasion genes)	2.14	1.17	**2.51**
28381	*hilA*†	Invasion transcriptional regulator HilA	**29.33**	-1.55	**18.98**
28581	*invA*†*	TTSS secretory apparatus (associated with virulence)	3.58	2.54	**9.09**
28441	*sipA*†* *(sspA)*	SPI-1 TTSS effector (invasion-associated)	6.22	2.92	**18.17**
28451	*sipD*†* *(sspD)*	SPI-1 TTSS secretory apparatus, translocon (cell invasion protein)	**6.38**	1.27	**8.14**
28461	*sipC*†* *(sspC)*	SPI-1 TTSS effector: translocation machinery (cell invasion protein)	**15.28**	2.61	**39.86**
28471	*sipB*†* *(sspB)*	SPI-1 TTSS effector: translocation machinery component	**10.71**	1.91	**20.50**

07981	*cydB**	Cytochrome D ubiquinol oxidase subunit II	1.47	2.62	**3.85**
09761	*dmsA**	Anaerobic dimethyl sulfoxide reductase subunit A	2.01	1.40	**2.82**
17321	*tonB*	TonB protein	~1	~1	**54.19**
30081	*ygfZ*	Putative global regulator	~1	**59.94**	**12.72**
35051	*malT**	MalT regulatory protein	~1	3.70	**4.20**
13351	−*	Putative outer membrane protein	3.63	4.47	**16.24**
(B) Genes with incremental decrease (9 genes)			S1 to S3	S3 to S4	S1 to S4
22511	*yejG**	hypothetical protein	**-17.40**	-7.42	**-129.13**
30191	*ygfB**	hypothetical protein	**-13.59**	-1.70	**-23.06**
38601	*asnCb**	DNA-binding transcriptional repressor of *asnA*	**-8.16**	-2.48	**-20.28**
37081	*rfaB*†*	lipopolysaccharide 1,6-galactosyltransferase	**-11.61**	~1	**-19.98**
06341	*ybdG**	hypothetical miniconductance mechanosensitive channel	**-11.18**	~1	**-15.58**
20351	*yeeI**	hypothetical protein: DgsA anti-repressor MtfA	**-11.01**	-1.30	**-14.27**
40301	-*	putative Na+/galactoside symporter	~1	**-26.20**	**-27.97**
15941	*pdgL**	D-alanyl-D-alanine dipeptidase	-4.85	-2.54	**-12.29**
27801	*emrR**	repressor of multidrug efflux *emrAB*	-4.95	-2.38	**-11.80**

*, genes of incremental increase in gene expression in incremental fluid shear; †, pathogenesis/virulence associated genes; -, not available. Significant fold-changes are bold (P<0.05, fold-difference>2). ~1, -1.2<Fold-difference<1.2 or one or both of RPKM<1

5.1.6 Alteration of oxidative stress resistance of D23580 as assessed under an extended range of fluid shear levels.

As shown above, D23580 alters its acid stress resistance, infection profiles in macrophages, and global gene expression in response to changes in fluid shear. We expanded our study on the influence of fluid shear by adding yet another high fluid shear

condition S5, by including two beads with the same size (1/8-inch) but differing densities (1/8-PP + 1/8-C) during RWV culture (**Figure 5-1**). D23580 grown in RWV in the fluid shear conditions of **S1** (no bead), **S3** (/8-PP), **S4** (1/8-C), and **S5** (1/8-PP + 1/8-C) was tested for bacterial survival in the presence of H_2O_2-induced oxidative stress. Observed increases in fluid shear correlated with increased survival of oxidative stress at each time point (**Figure 5-6**). D23580 grown in the highest fluid shear conditions possessed the most resistance to oxidative stress, showing more than 5-fold increased survival as compared to the lowest fluid shear condition at each of the observed time points (**Table 5-6**). The results demonstrate the effects of fluid shear on resistance to H_2O_2-induced oxidative stress in D23580.

Table 5-6. Fold-increase of D23580 survival under H_2O_2-induced oxidative stress in high fluid shear conditions.

The ratio of the percent survival of D23580 in higher fluid shear conditions to the percent survival in the lower fluid shear condition was calculated: (% S4)/(%S1), (% S5)]/(%S1), (%S5)/(%S4). Mean values, standard error of means, and p-values are indicated. Statistical significance was evaluated as described above.

(mins)	S1 < S4	S4 < S5	S1 < S5*
30	3.14*	2.17	6.81*
45	1.91	4.05*	7.71*
60	2.18	2.38	5.18*
75	7.35*	1.47	10.78*

*, $p<0.05$; S1, no bead; S3, 1/8-PP bead; S4, 1/8-C bead; and S5, 1/8-PP + 1/8-C.

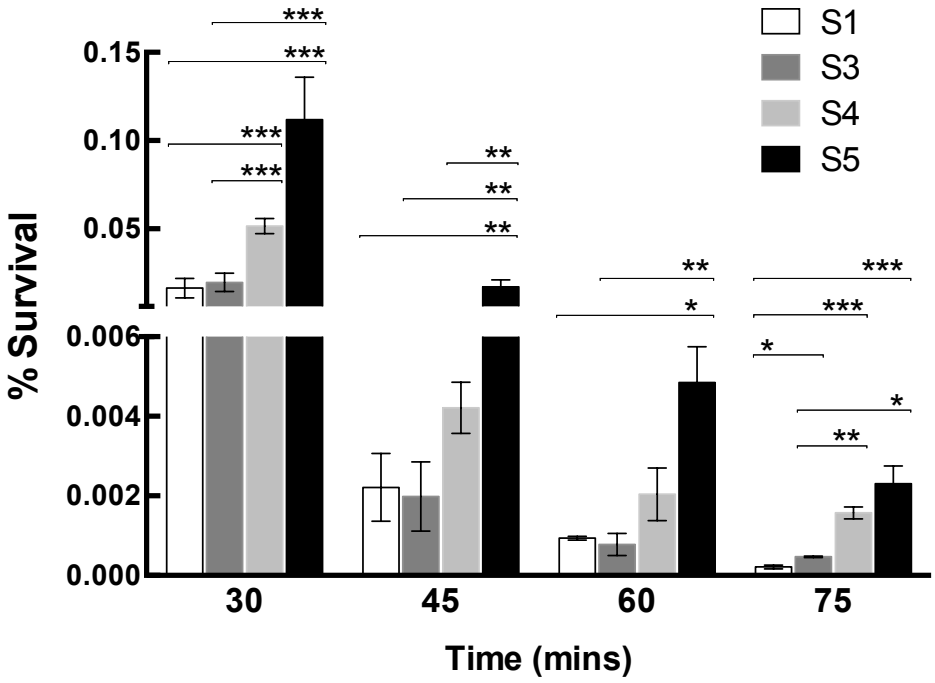

Figure 5-6 Oxidative stress response of D23580 cultured in the RWV with and without addition of beads.

D23580 in RWVs with no bead (S1, white bars), 1/8-PP (S3, dark grey bars), 1/8-C (S4, light grey bars), and 1/8-PP + 1/8-C (S5, black bars) were tested. Surviving bacteria were examined every 15 min after cells were subjected to oxidative stress (0.12% H_2O_2). Percent survival of each sample was determined by the ratio of CFU/mL at each tested times to the CFU/mL at time zero. Six independent trials were performed. Mean values, standard error of means, and p-values are indicated. Statistical significance was evaluated as described above.

5.5 Discussion

During the course of infection, *Salmonella* experiences a wide range of fluid dynamics, from low fluid shear in between the brush border of epithelial cell microvilli to high fluid shear in certain regions of the gastrointestinal tract and circulatory system. While classic *S.* Typhimurium normally causes gastroenteritis in healthy humans, a novel

sequence type of *S*. Typhimurium, ST313, causes a systemic infection with a marked lack of gastroenteritis symptoms (7, 15-17, 24). While previous studies showed that low fluid shear culture of the classic Typhimurium strain χ3339 led to increased virulence and pathogenesis-related stress resistance for a select panel of stress responses (143, 146, 157, 164, 165), the experiments presented in this chapter demonstrate that fluid shear alters the cellular responses of the ST313 strain D23580 in a different manner than classic Typhimurium. In this study, we explored the effect of incrementally increasing fluid shear on infection kinetics, stress resistance, and gene expression in D23580. To our knowledge, this is the first evidence that D23580 can respond to different levels of fluid shear.

5.1.7 Commonalities in the fluid shear-mediated transcriptomic alterations between D23580 and classic Typhimurium χ3339

Our data indicate that fluid shear stress induced global alterations in the transcriptomic profile of D23580. Approximately 2.35% of the total transcripts detected in this study were differentially expressed in response to environmental fluid shear stress. While low fluid shear was previously shown to be an environmental signal that significantly influences bacterial cellular responses and pathogenesis (135, 137, 139, 140, 143-146, 150, 152-158, 164, 165), the precise mechanism by which bacteria can translate this signal and alter their infection mechanisms still remains unknown. Previous studies implicated the RNA-binding protein Hfq as a key regulatory protein involved in

the fluid shear mediated response of classic Typhimurium χ3339 (164). In comparing the gene expression profiles between D23580 and χ3339 to evaluate the potential for commonalities across the two pathovars, similarities could be found between the two studies. The virulence-related genes of *fimA*, *invA, sipD* and the regulatory gene *malT* were upregulated both in χ3339 (microarray) and in D23580 (RNA-seq) in response to high fluid shear conditions. In addition, genes in the SUF system, important for biosynthesis of iron-sulfur clusters (Fe-S), were upregulated in high fluid shear conditions: *sufA* (iron-sulfur cluster assembly scaffold protein) in D23580 and *sufC* and *sufS* (part of SUF system involved in inserting iron-sulfur clusters into proteins) in χ3339. In addition, *rfa* genes involved in LPS core synthesis were downregulated in high fluid shear conditions: *rfaG* in χ3339 and *rfaB* in D23580 (146). Furthermore, as pathogenesis-related genes in D23580 such as *pip, sop, sip, spi*, *inv, hil, and fim* were downregulated in low fluid shear, SPI-1 and -2 genes (*orgA, prgH, pigB, sseBJ, ssaLV*) and regulators (*rseA*, *inv* genes, *himA*) were also suppressed in response to low fluid shear for χ3339 (146) Previous microarray studies demonstrated that expression of the master response regulator *hfq* and its regulons were significantly altered by extreme low fluid shear conditions in spaceflight conditions for χ3339 (164). However, our RNA-seq analysis of D23580 found no statistically significant difference in the expression of *hfq* under the conditions of this study (although a downward trend was observed under low fluid shear conditions). Overall, the data suggests that there are common mechanisms in *S.* Typhimurium χ3339 and ST313 D23580 responsible for regulating gene expression in

response to environmental fluid shear stress which ultimately lead to alteration of cellular responses that include bacterial physiology and virulence.

5.1.8 Fluid shear-mediated incremental changes in the gene expression of D23580

Strikingly, 16.51% (18/109) of the differentially expressed genes were directly associated with bacterial infection (**Table 5-5**, indicated with '†') and 66.67% (12/18) of them presented incremental changes in their expression with changes in fluid shear (**Table 5-5**, indicated with '†*'). Of these, 91.67% (11/12) showed incremental upregulation with increasing fluid shear. Specifically, *fimA* (Type-1 fimbrial protein) was upregulated, as were invasion protein genes *pipC* (cell invasion protein, SPI-3), *spiR* (related to TTSS regulation), *sopB*/*sopE2* (SPI-1 TTSS, invasion proteins), *hilD* (regulator activating invasion genes), *invA* (regulator activating invasion genes), and *sipA/sipD/sipC/sipB* (SPI-1 TTSS effectors). SPI-1 TTSS gene *sopA* (SPI-1 TTSS) also showed upregulation, but only in the S4 condition, the highest fluid shear condition used in this experiment. Upregulation of these fimbrial and invasion genes are consistent with the results obtained in D23580 infection of J774A.1 macrophages.

RNA-seq analysis showed that *ygfZ* (putative global gene regulator) was incrementally upregulated and *rfaB* (LPS synthesis protein (294)), *ybdG* (hypothetical miniconductance mechanosensitive channel), STMMW_40301 (putative Na+/galactoside symporter), and *emrR* (MDR repressor) were incrementally downregulated with

increasing fluid shear. The differential expression of genes encoding hypothetical proteins, cell surface-associated molecules, transporters, and regulators identified in this work may be important in the overall response of D23580 to physiological fluid shear, ranging from sensing biomechanical fluid shear stress on the cellular surface, transferring these signals into molecular changes, and altering cellular responses. More studies examining the specific role of each gene will help to determine answers to these questions.

5.1.9 Fluid shear-mediated incremental changes in D23580 colonization in J774 macrophages

Incremental changes in fluid shear led to progressive increases in the adherence, internalization (invasion/phagocytosis), and survival of D23580 in in J774 monolayers. Relevant to these findings, gene expression analysis revealed the upregulation of *fimAIDZ* in the two high fluid shear conditions (S3 or S4) relative to the low fluid shear condition (S1) (**Table 5-3 and 5-5**). Moreover, the higher internalization of D23580 into J774 macrophages as a function of increasing fluid shear is consistent with the progressive upregulation of *Salmonella* invasion-related genes (SPI-1 and TTSS) with increasing fluid shear. The enhanced survival of D23580 that was observed in response to acid and oxidative stresses following higher fluid shear culture was also consistent with the higher intracellular survival and replication in macrophages. The enhanced adherence

and invasion of D23580 as observed with increasing fluid shear stress may also have been contributed to the enhanced intracellular survival of D23580 in J774 macrophages.

Ramachandran et al previously showed enhanced intracellular survival and replication of flagellin-attenuated ST313 strains followed by higher phagocytosis by macrophages compared to classic Typhimurium ST19 strains (41). These findings are consistent with what we have also observed (**Chapter 3**), wherein infection of our novel immunocompetent, 3-D intestinal cell culture model with D23580 showed decreased invasion relative to classic Typhimurium strain SL1344, yet significantly enhanced intracellular survival/replication. Moreover, we and others have shown that ST313 strains are recovered at higher numbers from deeper tissues of the host than classic Typhimurium ST19 strains ((39); and Chapter 2, manuscript submitted). In this regard, the studies presented in this chapter have demonstrated that high fluid shear conditions alter the pathogenesis-related stress responses, infection profile and global gene expression of D23580 in important ways that may contribute to its rapid systemic dissemination within the host.

Summary - Chapter 5:

This chapter reports the impact of *incremental increases* in the physiological force of fluid shear on global gene expression and pathogenesis-related stress response profiles of D23580 during culture in the RWV bioreactor. The incremental increases in fluid shear

were imparted by incorporation of spherical beads of different sizes and densities into the bioreactor during bacterial culture. The results of this work demonstrated a progressive relationship between the applied fluid shear and D23580 molecular genetic and phenotypic responses.

- ✓ D23580 responds to different levels of fluid shear stress. Specifically, incremental increases in fluid shear increased bacterial resistance to acid and oxidative stresses.
- ✓ Fluid shear alters global gene expression in D23580, including genes encoding fimbriae (*fimAIDZ*), *Salmonella* pathogenicity island/SPI-1) (*pipBC*, *spiR*, *sopABE2*, *sipADCB, invA*), and transcriptional regulators of pathogenesis (*hilAD*).
- ✓ Incremental increases in fluid shear up-regulate expression of pathogenesis-related genes in D23580. This includes families of genes encoding products whose functions are in alignment with observed fluid-shear induced alterations in phenotypic properties (*fimA, pipC, spiR, sopB, hilD, sipA, sipD, sipC, sipB*).
- ✓ Incremental increases in fluid shear increased bacterial survival in macrophages as evidenced by enhanced adherence, internalization and intracellular survival/replication.

FINAL SUMMARY:

The collective body of work presented in this dissertation demonstrates that D23580 differs from classic *Salmonella* pathovars Typhimurium and Typhi in a number of key ways, including physiology, metabolism, pathogenesis-related stress responses, infection and virulence profiles. Importantly, the biomechanical force of fluid shear was found to distinctly regulate key infection properties of D23580 in a manner that differs from classic Typhimurium, thus emphasizing the importance of studying this important bacterial pathogen under physiologically relevant culture conditions.

In **future studies**, we will investigate:

1) How the distinct phenotypic and metabolic characteristics of D23580 contribute to the enhanced ability of this pathovar to cause disease.
2) Why and how D23580 displays the distinct co-localization pattern associating with different host cell types observed using an *in vitro 3-D co-culture model*, and whether it is relevant to the disease phenotype *in vivo*.
3) How the pathogenesis-related genes up-regulated in high fluid shear conditions are associated with bacterial infection and disease properties – adherence, invasion, intracellular survival/replication, and dissemination in host tissues.
4) What are the regulatory mechanisms used by D23580 to both sense environmental fluid shear stress and translate the signal to initiate molecular genetic and cellular responses.

REFERENCES

1. **CDC.** 2011. Vital signs: incidence and trends of infection with pathogens transmitted commonly through food—foodborne diseases active surveillance network, 10 U.S. sites, 1996–2010. MMWR Morb. Mortal. Wkly. Rep. **60:**749-755.

2. **Adhikari, B, Angulo, F, Meltzer, M.** 2004. Abstr. Economic burden of *Salmonella* infections in the United States. Annu. Meet. Am. Agric. Econ. Assoc. Abstr. 20050.

3. **Hoffmann, S, Tobenna, DA.** 2013. Making Sense of Recent Cost-of-Foodborne-Illness Estimates. United States Department of Agriculture. **Economic Information Bulletin No. (EIB-118):**35.

4. **US Department of Health and Human Services.** 2013. Antibiotic resistance threats in the United States, 2013. Atlanta: CDC. .

5. **Okoro, CK, Kingsley, RA, Connor, TR, Harris, SR, Parry, CM, Al-Mashhadani, MN, Kariuki, S, Msefula, CL, Gordon, MA, de Pinna, E, Wain, J, Heyderman, RS, Obaro, S, Alonso, PL, Mandomando, I, MacLennan, CA, Tapia, MD, Levine, MM, Tennant, SM, Parkhill, J, Dougan, G.** 2012. Intracontinental spread of human invasive Salmonella Typhimurium pathovariants in sub-Saharan Africa. Nat. Genet. **44:**1215-1221. doi: 10.1038/ng.2423 [doi].

6. **Okoro, CK, Kingsley, RA, Quail, MA, Kankwatira, AM, Feasey, NA, Parkhill, J, Dougan, G, Gordon, MA.** 2012. High-resolution single nucleotide polymorphism analysis distinguishes recrudescence and reinfection in recurrent invasive nontyphoidal Salmonella typhimurium disease. Clin. Infect. Dis. **54:**955-963. doi: 10.1093/cid/cir1032 [doi].

7. **Kingsley, RA, Msefula, CL, Thomson, NR, Kariuki, S, Holt, KE, Gordon, MA, Harris, D, Clarke, L, Whitehead, S, Sangal, V, Marsh, K, Achtman, M, Molyneux, ME, Cormican, M, Parkhill, J, MacLennan, CA, Heyderman, RS, Dougan, G.** 2009. Epidemic multiple drug resistant Salmonella Typhimurium causing invasive disease in sub-Saharan Africa have a distinct genotype. Genome Res. **19:**2279-2287. doi: 10.1101/gr.091017.109 [doi].

8. **Gordon, MA, Graham, SM, Walsh, AL, Wilson, L, Phiri, A, Molyneux, E, Zijlstra, EE, Heyderman, RS, Hart, CA, Molyneux, ME.** 2008. Epidemics of invasive Salmonella enterica serovar enteritidis and S. enterica Serovar typhimurium infection associated with multidrug resistance among adults and children in Malawi. Clin. Infect. Dis. **46:**963-969. doi: 10.1086/529146 [doi].

9. **Ley, B, Le Hello, S, Lunguya, O, Lejon, V, Muyembe, JJ, Weill, FX, Jacobs, J.** 2014. Invasive Salmonella enterica serotype typhimurium infections, Democratic

Republic of the Congo, 2007-2011. Emerg. Infect. Dis. **20:**701-704. doi: 10.3201/eid2004.131488 [doi].

10. **Morpeth, SC, Ramadhani, HO, Crump, JA.** 2009. Invasive non-Typhi Salmonella disease in Africa. Clin. Infect. Dis. **49:**606-611. doi: 10.1086/603553 [doi].

11. **Andrews-Polymenis, HL, Baumler, AJ, McCormick, BA, Fang, FC.** 2010. Taming the elephant: Salmonella biology, pathogenesis, and prevention. Infect. Immun. **78:**2356-2369. doi: 10.1128/IAI.00096-10 [doi].

12. **Baumler, A, Fang, FC.** 2013. Host specificity of bacterial pathogens. Cold Spring Harb Perspect. Med. **3:**a010041. doi: 10.1101/cshperspect.a010041 [doi].

13. **Fabrega, A, Vila, J.** 2013. Salmonella enterica serovar Typhimurium skills to succeed in the host: virulence and regulation. Clin. Microbiol. Rev. **26:**308-341. doi: 10.1128/CMR.00066-12 [doi].

14. **Mweu, E, English, M.** 2008. Typhoid fever in children in Africa. Trop. Med. Int. Health. **13:**532-540. doi: 10.1111/j.1365-3156.2008.02031.x [doi].

15. **Brent, AJ, Oundo, JO, Mwangi, I, Ochola, L, Lowe, B, Berkley, JA.** 2006. Salmonella bacteremia in Kenyan children. Pediatr. Infect. Dis. J. **25:**230-236. doi: 10.1097/01.inf.0000202066.02212.ff [doi].

16. **Feasey, NA, Dougan, G, Kingsley, RA, Heyderman, RS, Gordon, MA.** 2012. Invasive non-typhoidal salmonella disease: an emerging and neglected tropical disease in Africa. Lancet. **379:**2489-2499. doi: 10.1016/S0140-6736(11)61752-2 [doi].

17. **Gordon, MA, Banda, HT, Gondwe, M, Gordon, SB, Boeree, MJ, Walsh, AL, Corkill, JE, Hart, CA, Gilks, CF, Molyneux, ME.** 2002. Non-typhoidal salmonella bacteraemia among HIV-infected Malawian adults: high mortality and frequent recrudescence. AIDS. **16:**1633-1641.

18. **Gordon, MA.** 2008. Salmonella infections in immunocompromised adults. J. Infect. **56:**413-422. doi: 10.1016/j.jinf.2008.03.012 [doi].

19. **Graham, SM.** 2010. Nontyphoidal salmonellosis in Africa. Curr. Opin. Infect. Dis. **23:**409-414. doi: 10.1097/QCO.0b013e32833dd25d [doi].

20. **Reddy, EA, Shaw, AV, Crump, JA.** 2010. Community-acquired bloodstream infections in Africa: a systematic review and meta-analysis. Lancet Infect. Dis. **10:**417-432. doi: 10.1016/S1473-3099(10)70072-4 [doi].

21. **Milledge, J, Calis, JC, Graham, SM, Phiri, A, Wilson, LK, Soko, D, Mbvwinji, M, Walsh, AL, Rogerson, SR, Molyneux, ME, Molyneux, EM.** 2005. Aetiology of

neonatal sepsis in Blantyre, Malawi: 1996-2001. Ann. Trop. Paediatr. **25:**101-110. doi: 10.1179/146532805X45692 [doi].

22. **Berkley, JA, Lowe, BS, Mwangi, I, Williams, T, Bauni, E, Mwarumba, S, Ngetsa, C, Slack, MP, Njenga, S, Hart, CA, Maitland, K, English, M, Marsh, K, Scott, JA.** 2005. Bacteremia among children admitted to a rural hospital in Kenya. N. Engl. J. Med. **352:**39-47. doi: 352/1/39 [pii].

23. **Crump, JA, Luby, SP, Mintz, ED.** 2004. The global burden of typhoid fever. Bull. World Health Organ. **82:**346-353.

24. **Kariuki, S, Revathi, G, Gakuya, F, Yamo, V, Muyodi, J, Hart, CA.** 2002. Lack of clonal relationship between non-typhi Salmonella strain types from humans and those isolated from animals living in close contact. FEMS Immunol. Med. Microbiol. **33:**165-171. doi: S0928824402003097 [pii].

25. **McClelland, M, Sanderson, KE, Clifton, SW, Latreille, P, Porwollik, S, Sabo, A, Meyer, R, Bieri, T, Ozersky, P, McLellan, M.** 2004. Comparison of genome degradation in Paratyphi A and Typhi, human-restricted serovars of Salmonella enterica that cause typhoid. Nat. Genet. **36:**1268-1274.

26. **Fookes, M, Schroeder, GN, Langridge, GC, Blondel, CJ, Mammina, C, Connor, TR, Seth-Smith, H, Vernikos, GS, Robinson, KS, Sanders, M.** 2011. Salmonella bongori provides insights into the evolution of the Salmonellae. PLoS Pathogens. **7:**e1002191.

27. **Thomson, NR, Clayton, DJ, Windhorst, D, Vernikos, G, Davidson, S, Churcher, C, Quail, MA, Stevens, M, Jones, MA, Watson, M, Barron, A, Layton, A, Pickard, D, Kingsley, RA, Bignell, A, Clark, L, Harris, B, Ormond, D, Abdellah, Z, Brooks, K, Cherevach, I, Chillingworth, T, Woodward, J, Norberczak, H, Lord, A, Arrowsmith, C, Jagels, K, Moule, S, Mungall, K, Sanders, M, Whitehead, S, Chabalgoity, JA, Maskell, D, Humphrey, T, Roberts, M, Barrow, PA, Dougan, G, Parkhill, J.** 2008. Comparative genome analysis of Salmonella Enteritidis PT4 and Salmonella Gallinarum 287/91 provides insights into evolutionary and host adaptation pathways. Genome Res. **18:**1624-1637. doi: 10.1101/gr.077404.108 [doi].

28. **Hughes, LA, Shopland, S, Wigley, P, Bradon, H, Leatherbarrow, AH, Williams, NJ, Bennett, M, de Pinna, E, Lawson, B, Cunningham, AA, Chantrey, J.** 2008. Characterisation of Salmonella enterica serotype Typhimurium isolates from wild birds in northern England from 2005 - 2006. BMC Vet. Res. **4:**4-6148-4-4. doi: 10.1186/1746-6148-4-4 [doi].

29. **Hughes, LA, Wigley, P, Bennett, M, Chantrey, J, Williams, N.** 2010. Multi-locus sequence typing of Salmonella enterica serovar Typhimurium isolates from wild birds in

northern England suggests host-adapted strain. Lett. Appl. Microbiol. **51:**477-479. doi: 10.1111/j.1472-765X.2010.02918.x [doi].

30. **Duff, J.** 2003. Wildlife diseases in the UK 2002. Veterinary Laboratories Agency Report. 18-24.

31. **Pennycott, TW, Cinderey, RN, Park, A, Mather, HA, Foster, G.** 2002. Salmonella enterica subspecies enterica serotype Typhimurium and Escherichia coli O86 in wild birds at two garden sites in south-west Scotland. Vet. Rec. **151:**563-567.

32. **Pennycott, TW, Park, A, Mather, HA.** 2006. Isolation of different serovars of Salmonella enterica from wild birds in Great Britain between 1995 and 2003. Vet. Rec. **158:**817-820. doi: 158/24/817 [pii].

33. **MacLennan, CA, Gondwe, EN, Msefula, CL, Kingsley, RA, Thomson, NR, White, SA, Goodall, M, Pickard, DJ, Graham, SM, Dougan, G, Hart, CA, Molyneux, ME, Drayson, MT.** 2008. The neglected role of antibody in protection against bacteremia caused by nontyphoidal strains of Salmonella in African children. J. Clin. Invest. **118:**1553-1562. doi: 10.1172/JCI33998 [doi].

34. **MacLennan, CA, Gilchrist, JJ, Gordon, MA, Cunningham, AF, Cobbold, M, Goodall, M, Kingsley, RA, van Oosterhout, JJ, Msefula, CL, Mandala, WL, Leyton, DL, Marshall, JL, Gondwe, EN, Bobat, S, Lopez-Macias, C, Doffinger, R, Henderson, IR, Zijlstra, EE, Dougan, G, Drayson, MT, MacLennan, IC, Molyneux, ME.** 2010. Dysregulated humoral immunity to nontyphoidal Salmonella in HIV-infected African adults. Science. **328:**508-512. doi: 10.1126/science.1180346 [doi].

35. **Rondini, S, Lanzilao, L, Necchi, F, O'Shaughnessy, CM, Micoli, F, Saul, A, MacLennan, CA.** 2013. Invasive African Salmonella Typhimurium induces bactericidal antibodies against O-antigens. Microb. Pathog. **63:**19-23. doi: 10.1016/j.micpath.2013.05.014 [doi].

36. **Goh, YS, MacLennan, CA.** 2013. Invasive African nontyphoidal Salmonella requires high levels of complement for cell-free antibody-dependent killing. J. Immunol. Methods. **387:**121-129. doi: 10.1016/j.jim.2012.10.005 [doi].

37. **Siggins, MK, O'Shaughnessy, CM, Pravin, J, Cunningham, AF, Henderson, IR, Drayson, MT, MacLennan, CA.** 2014. Differential timing of antibody□mediated phagocytosis and cell□free killing of invasive African Salmonella allows immune evasion. Eur. J. Immunol. **44:**1093-1098.

38. **Onsare, RS, Micoli, F, Lanzilao, L, Alfini, R, Okoro, CK, Muigai, AW, Revathi, G, Saul, A, Kariuki, S, MacLennan, CA, Rondini, S.** 2015. Relationship between Antibody Susceptibility and Lipopolysaccharide O-Antigen Characteristics of Invasive

and Gastrointestinal Nontyphoidal Salmonellae Isolates from Kenya. PLoS Negl Trop. Dis. **9:**e0003573. doi: 10.1371/journal.pntd.0003573 [doi].

39. **Parsons, BN, Humphrey, S, Salisbury, AM, Mikoleit, J, Hinton, JC, Gordon, MA, Wigley, P.** 2013. Invasive non-typhoidal Salmonella typhimurium ST313 are not host-restricted and have an invasive phenotype in experimentally infected chickens. PLoS Negl Trop. Dis. **7:**e2487. doi: 10.1371/journal.pntd.0002487 [doi].

40. **Herrero-Fresno, A, Wallrodt, I, Leekitcharoenphon, P, Olsen, JE, Aarestrup, FM, Hendriksen, RS.** 2014. The role of the st313-td gene in virulence of Salmonella Typhimurium ST313. PLoS One. **9:**e84566. doi: 10.1371/journal.pone.0084566 [doi].

41. **Ramachandran, G, Perkins, DJ, Schmidlein, PJ, Tulapurkar, ME, Tennant, SM.** 2015. Invasive Salmonella Typhimurium ST313 with Naturally Attenuated Flagellin Elicits Reduced Inflammation and Replicates within Macrophages. PLoS Neglected Tropical Diseases. **9:**e3394.

42. **LaRock, DL, Chaudhary, A, Miller, SI.** 2015. Salmonellae interactions with host processes. Nature Reviews Microbiology. **13:**191-205.

43. **Abrahams, GL, Hensel, M.** 2006. Manipulating cellular transport and immune responses: dynamic interactions between intracellular Salmonella enterica and its host cells. Cell. Microbiol. **8:**728-737. doi: CMI706 [pii].

44. **Haraga, A, Miller, SI.** 2003. A Salmonella enterica serovar typhimurium translocated leucine-rich repeat effector protein inhibits NF-kappa B-dependent gene expression. Infect. Immun. **71:**4052-4058.

45. **Hobbie, S, Chen, LM, Davis, RJ, Galan, JE.** 1997. Involvement of mitogen-activated protein kinase pathways in the nuclear responses and cytokine production induced by Salmonella typhimurium in cultured intestinal epithelial cells. J. Immunol. **159:**5550-5559.

46. **Haraga, A, Miller, SI.** 2006. A Salmonella type III secretion effector interacts with the mammalian serine/threonine protein kinase PKN1. Cell. Microbiol. **8:**837-846. doi: CMI670 [pii].

47. **Miao, EA, Brittnacher, M, Haraga, A, Jeng, RL, Welch, MD, Miller, SI.** 2003. Salmonella effectors translocated across the vacuolar membrane interact with the actin cytoskeleton. Mol. Microbiol. **48:**401-415. doi: 3456 [pii].

48. **Zhou, D.** 2001. Collective efforts to modulate the host actin cytoskeleton by Salmonella type III-secreted effector proteins. Trends Microbiol. **9:**567-9; discussion 569-70. doi: S0966-842X(01)02227-2 [pii].

49. **Bernal-Bayard, J, Ramos-Morales, F.** 2009. Salmonella type III secretion effector SlrP is an E3 ubiquitin ligase for mammalian thioredoxin. J. Biol. Chem. **284:**27587-27595. doi: 10.1074/jbc.M109.010363 [doi].

50. **Hersh, D, Monack, DM, Smith, MR, Ghori, N, Falkow, S, Zychlinsky, A.** 1999. The Salmonella invasin SipB induces macrophage apoptosis by binding to caspase-1. Proc. Natl. Acad. Sci. U. S. A. **96:**2396-2401.

51. **Jones, RM, Wu, H, Wentworth, C, Luo, L, Collier-Hyams, L, Neish, AS.** 2008. Salmonella AvrA Coordinates Suppression of Host Immune and Apoptotic Defenses via JNK Pathway Blockade. Cell. Host Microbe. **3:**233-244. doi: 10.1016/j.chom.2008.02.016 [doi].

52. **Kurita, A, Gotoh, H, Eguchi, M, Okada, N, Matsuura, S, Matsui, H, Danbara, H, Kikuchi, Y.** 2003. Intracellular expression of the Salmonella plasmid virulence protein, SpvB, causes apoptotic cell death in eukaryotic cells. Microb. Pathog. **35:**43-48. doi: S0882401003000664 [pii].

53. **van der Velden, AW, Lindgren, SW, Worley, MJ, Heffron, F.** 2000. Salmonella pathogenicity island 1-independent induction of apoptosis in infected macrophages by Salmonella enterica serotype typhimurium. Infect. Immun. **68:**5702-5709.

54. **Watson, KG, Holden, DW.** 2010. Dynamics of growth and dissemination of Salmonella in vivo. Cell. Microbiol. **12:**1389-1397.

55. **Brumell, JH, Scidmore, MA.** 2007. Manipulation of rab GTPase function by intracellular bacterial pathogens. Microbiol. Mol. Biol. Rev. **71:**636-652. doi: 71/4/636 [pii].

56. **Haraga, A, Ohlson, MB, Miller, SI.** 2008. Salmonellae interplay with host cells. Nature Reviews Microbiology. **6:**53-66.

57. **Hernandez, LD, Hueffer, K, Wenk, MR, Galan, JE.** 2004. Salmonella modulates vesicular traffic by altering phosphoinositide metabolism. Science. **304:**1805-1807. doi: 10.1126/science.1098188 [doi].

58. **McGhie, EJ, Brawn, LC, Hume, PJ, Humphreys, D, Koronakis, V.** 2009. Salmonella takes control: effector-driven manipulation of the host. Curr. Opin. Microbiol. **12:**117-124.

59. **Shotland, Y, Kramer, H, Groisman, EA.** 2003. The Salmonella SpiC protein targets the mammalian Hook3 protein function to alter cellular trafficking. Mol. Microbiol. **49:**1565-1576. doi: 3668 [pii].

60. **Uchiya, K, Barbieri, MA, Funato, K, Shah, AH, Stahl, PD, Groisman, EA.** 1999. A Salmonella virulence protein that inhibits cellular trafficking. EMBO J. **18:**3924-3933. doi: 10.1093/emboj/18.14.3924 [doi].

61. **Foster, JW, Hall, HK.** 1991. Inducible pH homeostasis and the acid tolerance response of Salmonella typhimurium. J. Bacteriol. **173:**5129-5135.

62. **Foster, JW.** 1991. Salmonella acid shock proteins are required for the adaptive acid tolerance response. J. Bacteriol. **173:**6896-6902.

63. **Park, Y, Bearson, B, Bang, SH, Bang, IS, Foster, JW.** 1996. Internal pH crisis, lysine decarboxylase and the acid tolerance response of Salmonella typhimurium. Mol. Microbiol. **20:**605-611.

64. **Foster, JW, Hall, HK.** 1992. Effect of Salmonella typhimurium ferric uptake regulator (fur) mutations on iron- and pH-regulated protein synthesis. J. Bacteriol. **174:**4317-4323.

65. **Lee, I, Lin, J, Hall, HK, Bearson, B, Foster, JW.** 1995. The stationary□phase sigma factor σS (RpoS) is required for a sustained acid tolerance response in virulent Salmonella typhimurium. Mol. Microbiol. **17:**155-167.

66. **Bang, IS, Kim, BH, Foster, JW, Park, YK.** 2000. OmpR regulates the stationary-phase acid tolerance response of Salmonella enterica serovar typhimurium. J. Bacteriol. **182:**2245-2252.

67. **Hall, HK, Foster, JW.** 1996. The role of fur in the acid tolerance response of Salmonella typhimurium is physiologically and genetically separable from its role in iron acquisition. J. Bacteriol. **178:**5683-5691.

68. **Lee, IS, Slonczewski, JL, Foster, JW.** 1994. A low-pH-inducible, stationary-phase acid tolerance response in Salmonella typhimurium. J. Bacteriol. **176:**1422-1426.

69. **Small, PL, Waterman, SR.** 1998. Acid stress, anaerobiosis and gadCB: lessons from Lactococcus lactis and Escherichia coli. Trends Microbiol. **6:**214-216. doi: S0966-842X(98)01285-2 [pii].

70. **De Biase, D, Tramonti, A, Bossa, F, Visca, P.** 1999. The response to stationary-phase stress conditions in Escherichia coli: role and regulation of the glutamic acid decarboxylase system. Mol. Microbiol. **32:**1198-1211. doi: mmi1430 [pii].

71. **Castanie-Cornet, MP, Foster, JW.** 2001. Escherichia coli acid resistance: cAMP receptor protein and a 20 bp cis-acting sequence control pH and stationary phase expression of the gadA and gadBC glutamate decarboxylase genes. Microbiology. **147:**709-715.

72. **Rychlik, I, Barrow, PA.** 2005. Salmonella stress management and its relevance to behaviour during intestinal colonisation and infection. FEMS Microbiol. Rev. **29:**1021-1040. doi: 10.1016/j.femsre.2005.03.005.

73. **Setta, A, Barrow, PA, Kaiser, P, Jones, MA.** 2012. Immune dynamics following infection of avian macrophages and epithelial cells with typhoidal and non-typhoidal Salmonella enterica serovars; bacterial invasion and persistence, nitric oxide and oxygen production, differential host gene expression, NF-kappaB signalling and cell cytotoxicity. Vet. Immunol. Immunopathol. **146:**212-224. doi: 10.1016/j.vetimm.2012.03.008 [doi].

74. **Poole, RK.** 2005. Nitric oxide and nitrosative stress tolerance in bacteria. Biochem. Soc. Trans. **33:**176-180. doi: BST0330176 [pii].

75. **Nathan, C, Cunningham-Bussel, A.** 2013. Beyond oxidative stress: an immunologist's guide to reactive oxygen species. Nature Reviews Immunology. **13:**349-361.

76. **Lahiri, A, Das, P, Chakravortty, D.** 2008. Arginase modulates Salmonella induced nitric oxide production in RAW264.7 macrophages and is required for Salmonella pathogenesis in mice model of infection. Microbes Infect. **10:**1166-1174. doi: 10.1016/j.micinf.2008.06.008 [doi].

77. **He, H, Genovese, KJ, Swaggerty, CL, Nisbet, DJ, Kogut, MH.** 2012. A comparative study on invasion, survival, modulation of oxidative burst, and nitric oxide responses of macrophages (HD11), and systemic infection in chickens by prevalent poultry Salmonella serovars. Foodborne Pathog. Dis. **9:**1104-1110. doi: 10.1089/fpd.2012.1233 [doi].

78. **Crawford, RW, Gibson, DL, Kay, WW, Gunn, JS.** 2008. Identification of a bile-induced exopolysaccharide required for Salmonella biofilm formation on gallstone surfaces. Infect. Immun. **76:**5341-5349. doi: 10.1128/IAI.00786-08 [doi].

79. **Crawford, RW, Reeve, KE, Gunn, JS.** 2010. Flagellated but not hyperfimbriated Salmonella enterica serovar Typhimurium attaches to and forms biofilms on cholesterol-coated surfaces. J. Bacteriol. **192:**2981-2990. doi: 10.1128/JB.01620-09 [doi].

80. **Gonzalez-Escobedo, G, Gunn, JS.** 2013. Gallbladder epithelium as a niche for chronic Salmonella carriage. Infect. Immun. **81:**2920-2930. doi: 10.1128/IAI.00258-13 [doi].

81. **Gunn, JS.** 2000. Mechanisms of bacterial resistance and response to bile. Microbes Infect. **2:**907-913. doi: S1286-4579(00)00392-0 [pii].

82. **Hernandez, SB, Cota, I, Ducret, A, Aussel, L, Casadesus, J.** 2012. Adaptation and preadaptation of Salmonella enterica to Bile. PLoS Genet. **8:**e1002459. doi: 10.1371/journal.pgen.1002459 [doi].

83. **Prieto, AI, Ramos-Morales, F, Casadesus, J.** 2006. Repair of DNA damage induced by bile salts in Salmonella enterica. Genetics. **174:**575-584. doi: genetics.106.060889 [pii].

84. **Wood, JM.** 2006. Osmosensing by bacteria. Sci. STKE. **2006:**pe43. doi: stke.3572006pe43 [pii].

85. **Mizusaki, H, Takaya, A, Yamamoto, T, Aizawa, S.** 2008. Signal pathway in salt-activated expression of the Salmonella pathogenicity island 1 type III secretion system in Salmonella enterica serovar Typhimurium. J. Bacteriol. **190:**4624-4631. doi: 10.1128/JB.01957-07 [doi].

86. **Tartera, C, Metcalf, ES.** 1993. Osmolarity and growth phase overlap in regulation of Salmonella typhi adherence to and invasion of human intestinal cells. Infect. Immun. **61:**3084-3089.

87. **Jang, MH, Kweon, MN, Iwatani, K, Yamamoto, M, Terahara, K, Sasakawa, C, Suzuki, T, Nochi, T, Yokota, Y, Rennert, PD, Hiroi, T, Tamagawa, H, Iijima, H, Kunisawa, J, Yuki, Y, Kiyono, H.** 2004. Intestinal villous M cells: an antigen entry site in the mucosal epithelium. Proc. Natl. Acad. Sci. U. S. A. **101:**6110-6115. doi: 10.1073/pnas.0400969101 [doi].

88. **Jones, BD, Ghori, N, Falkow, S.** 1994. Salmonella typhimurium initiates murine infection by penetrating and destroying the specialized epithelial M cells of the Peyer's patches. J. Exp. Med. **180:**15-23.

89. **Lievin-Le Moal, V, Servin, AL.** 2013. Pathogenesis of human enterovirulent bacteria: lessons from cultured, fully differentiated human colon cancer cell lines. Microbiol. Mol. Biol. Rev. **77:**380-439. doi: 10.1128/MMBR.00064-12 [doi].

90. **Murray, RA, Lee, CA.** 2000. Invasion genes are not required for Salmonella enterica serovar typhimurium to breach the intestinal epithelium: evidence that salmonella pathogenicity island 1 has alternative functions during infection. Infect. Immun. **68:**5050-5055.

91. **Schwan, WR, Huang, XZ, Hu, L, Kopecko, DJ.** 2000. Differential bacterial survival, replication, and apoptosis-inducing ability of Salmonella serovars within human and murine macrophages. Infect. Immun. **68:**1005-1013.

92. **Cirillo, DM, Valdivia, RH, Monack, DM, Falkow, S.** 1998. Macrophage-dependent induction of the Salmonella pathogenicity island 2 type III secretion system and its role in intracellular survival. Mol. Microbiol. **30:**175-188.

93. **Hallstrom, K, McCormick, BA.** 2011. Salmonella Interaction with and Passage through the Intestinal Mucosa: Through the Lens of the Organism. Front. Microbiol. **2:**88. doi: 10.3389/fmicb.2011.00088 [doi].

94. **Takeuchi, A.** 1967. Electron microscope studies of experimental Salmonella infection. I. Penetration into the intestinal epithelium by Salmonella typhimurium. Am. J. Pathol. **50:**109-136.

95. **Vazquez-Torres, A, Jones-Carson, J, Bäumler, AJ, Falkow, S, Valdivia, R, Brown, W, Le, M, Berggren, R, Parks, WT, Fang, FC.** 1999. Extraintestinal dissemination of Salmonella by CD18-expressing phagocytes. Nature. **401:**804-808.

96. **Finlay, BB, Ruschkowski, S, Dedhar, S.** 1991. Cytoskeletal rearrangements accompanying salmonella entry into epithelial cells. J. Cell. Sci. **99 (Pt 2):**283-296.

97. **Francis, CL, Ryan, TA, Jones, BD, Smith, SJ, Falkow, S.** 1993. Ruffles induced by Salmonella and other stimuli direct macropinocytosis of bacteria. .

98. **Pace, J, Hayman, MJ, Galán, JE.** 1993. Signal transduction and invasion of epithelial cells by S. typhimurium. Cell. **72:**505-514.

99. **Garcia-del Portillo, F, Finlay, BB.** 1994. Salmonella invasion of nonphagocytic cells induces formation of macropinosomes in the host cell. Infect. Immun. **62:**4641-4645.

100. **Hardt, WD, Chen, LM, Schuebel, KE, Bustelo, XR, Galan, JE.** 1998. S. typhimurium encodes an activator of Rho GTPases that induces membrane ruffling and nuclear responses in host cells. Cell. **93:**815-826. doi: S0092-8674(00)81442-7 [pii].

101. **Bakowski, MA, Cirulis, JT, Brown, NF, Finlay, BB, Brumell, JH.** 2007. SopD acts cooperatively with SopB during Salmonella enterica serovar Typhimurium invasion. Cell. Microbiol. **9:**2839-2855. doi: CMI1000 [pii].

102. **Jones, MA, Wood, MW, Mullan, PB, Watson, PR, Wallis, TS, Galyov, EE.** 1998. Secreted effector proteins of Salmonella dublin act in concert to induce enteritis. Infect. Immun. **66:**5799-5804.

103. **Kaniga, K, Trollinger, D, Galan, JE.** 1995. Identification of two targets of the type III protein secretion system encoded by the inv and spa loci of Salmonella typhimurium that have homology to the Shigella IpaD and IpaA proteins. J. Bacteriol. **177:**7078-7085.

104. **Radtke, AL, Wilson, JW, Sarker, S, Nickerson, CA.** 2010. Analysis of interactions of Salmonella type three secretion mutants with 3-D intestinal epithelial cells. PLoS One. **5:**e15750. doi: 10.1371/journal.pone.0015750 [doi].

105. **Wood, MW, Jones, MA, Watson, PR, Siber, AM, McCormick, BA, Hedges, S, Rosqvist, R, Wallis, TS, Galyov, EE.** 2000. The secreted effector protein of Salmonella dublin, SopA, is translocated into eukaryotic cells and influences the induction of enteritis. Cell. Microbiol. **2:**293-303. doi: cmi54 [pii].

106. **Zhou, D, Mooseker, MS, Galan, JE.** 1999. Role of the S. typhimurium actin-binding protein SipA in bacterial internalization. Science. **283:**2092-2095.

107. **Gewirtz, AT, Simon, PO,Jr, Schmitt, CK, Taylor, LJ, Hagedorn, CH, O'Brien, AD, Neish, AS, Madara, JL.** 2001. Salmonella typhimurium translocates flagellin across intestinal epithelia, inducing a proinflammatory response. J. Clin. Invest. **107:**99-109. doi: 10.1172/JCI10501 [doi].

108. **McCormick, BA, Hofman, PM, Kim, J, Carnes, DK, Miller, SI, Madara, JL.** 1995. Surface attachment of Salmonella typhimurium to intestinal epithelia imprints the subepithelial matrix with gradients chemotactic for neutrophils. J. Cell Biol. **131:**1599-1608.

109. **McCormick, BA, Miller, SI, Carnes, D, Madara, JL.** 1995. Transepithelial signaling to neutrophils by salmonellae: a novel virulence mechanism for gastroenteritis. Infect. Immun. **63:**2302-2309.

110. **Ohl, ME, Miller, SI.** 2001. Salmonella: a model for bacterial pathogenesis. Annu. Rev. Med. **52:**259-274. doi: 52/1/259 [pii].

111. **Brawn, LC, Hayward, RD, Koronakis, V.** 2007. Salmonella SPI1 effector SipA persists after entry and cooperates with a SPI2 effector to regulate phagosome maturation and intracellular replication. Cell. Host Microbe. **1:**63-75. doi: S1931-3128(07)00005-4 [pii].

112. **Brumell, JH, Goosney, DL, Finlay, BB.** 2002. SifA, a type III secreted effector of Salmonella typhimurium, directs Salmonella-induced filament (Sif) formation along microtubules. Traffic. **3:**407-415. doi: tra030604 [pii].

113. **Kuhle, V, Hensel, M.** 2004. Cellular microbiology of intracellular Salmonella enterica: functions of the type III secretion system encoded by Salmonella pathogenicity island 2. Cell Mol. Life Sci. **61:**2812-2826. doi: 10.1007/s00018-004-4248-z [doi].

114. **Ochman, H, Soncini, FC, Solomon, F, Groisman, EA.** 1996. Identification of a pathogenicity island required for Salmonella survival in host cells. Proc. Natl. Acad. Sci. U. S. A. **93:**7800-7804.

115. **Coburn, B, Li, Y, Owen, D, Vallance, BA, Finlay, BB.** 2005. Salmonella enterica serovar Typhimurium pathogenicity island 2 is necessary for complete virulence in a mouse model of infectious enterocolitis. Infect. Immun. **73:**3219-3227. doi: 73/6/3219 [pii].

116. **Deiwick, J, Salcedo, SP, Boucrot, E, Gilliland, SM, Henry, T, Petermann, N, Waterman, SR, Gorvel, JP, Holden, DW, Meresse, S.** 2006. The translocated Salmonella effector proteins SseF and SseG interact and are required to establish an intracellular replication niche. Infect. Immun. **74:**6965-6972. doi: IAI.00648-06 [pii].

117. **Meresse, S, Unsworth, KE, Habermann, A, Griffiths, G, Fang, F, Martinez-Lorenzo, MJ, Waterman, SR, Gorvel, JP, Holden, DW.** 2001. Remodelling of the actin cytoskeleton is essential for replication of intravacuolar Salmonella. Cell. Microbiol. **3:**567-577. doi: cmi141 [pii].

118. **Salcedo, SP, Holden, DW.** 2003. SseG, a virulence protein that targets Salmonella to the Golgi network. EMBO J. **22:**5003-5014. doi: 10.1093/emboj/cdg517 [doi].

119. **Pfeifer, CG, Marcus, SL, Steele-Mortimer, O, Knodler, LA, Finlay, BB.** 1999. Salmonella typhimurium virulence genes are induced upon bacterial invasion into phagocytic and nonphagocytic cells. Infect. Immun. **67:**5690-5698.

120. **Valdivia, RH, Falkow, S.** 1997. Fluorescence-based isolation of bacterial genes expressed within host cells. Science. **277:**2007-2011.

121. **Valdivia, RH, Falkow, S.** 1997. Probing bacterial gene expression within host cells. Trends Microbiol. **5:**360-363. doi: S0966-842X(97)01111-6 [pii].

122. **Deiwick, J, Nikolaus, T, Erdogan, S, Hensel, M.** 1999. Environmental regulation of Salmonella pathogenicity island 2 gene expression. Mol. Microbiol. **31:**1759-1773.

123. **Miller, SI.** 1991. PhoP/PhoQ: macrophage-specific modulators of Salmonella virulence? Mol. Microbiol. **5:**2073-2078.

124. **Prost, LR, Miller, SI.** 2008. The Salmonellae PhoQ sensor: mechanisms of detection of phagosome signals. Cell. Microbiol. **10:**576-582. doi: 10.1111/j.1462-5822.2007.01111.x [doi].

125. **Groisman, EA.** 2001. The pleiotropic two-component regulatory system PhoP-PhoQ. J. Bacteriol. **183:**1835-1842. doi: 10.1128/JB.183.6.1835-1842.2001 [doi].

126. **Ibarra, JA, Steele-Mortimer, O.** 2009. Salmonella--the ultimate insider. Salmonella virulence factors that modulate intracellular survival. Cell. Microbiol. **11:**1579-1586. doi: 10.1111/j.1462-5822.2009.01368.x [doi].

127. **de Jong, HK, Parry, CM, van der Poll, T, Wiersinga, WJ.** 2012. Host-pathogen interaction in invasive Salmonellosis. PLoS Pathog. **8:**e1002933. doi: 10.1371/journal.ppat.1002933 [doi].

128. **Crawford, RW, Rosales-Reyes, R, Ramirez-Aguilar Mde, L, Chapa-Azuela, O, Alpuche-Aranda, C, Gunn, JS.** 2010. Gallstones play a significant role in Salmonella spp. gallbladder colonization and carriage. Proc. Natl. Acad. Sci. U. S. A. **107:**4353-4358. doi: 10.1073/pnas.1000862107 [doi].

129. **Bistrian, R, Dorn, A, Mobest, DC, Ruster, B, Ludwig, R, Scheele, J, Seifried, E, Martin, H, Henschler, R.** 2009. Shear stress-mediated adhesion of acute myeloid leukemia and KG-1 cells to endothelial cells involves functional P-selectin. Stem Cells Dev. **18:**1235-1242. doi: 10.1089/scd.2008.0380 [doi].

130. **Chai, Q, Wang, XL, Zeldin, DC, Lee, HC.** 2013. Role of caveolae in shear stress-mediated endothelium-dependent dilation in coronary arteries. Cardiovasc. Res. **100:**151-159. doi: 10.1093/cvr/cvt157 [doi].

131. **Du, Z, Duan, Y, Yan, Q, Weinstein, AM, Weinbaum, S, Wang, T.** 2004. Mechanosensory function of microvilli of the kidney proximal tubule. Proc. Natl. Acad. Sci. U. S. A. **101:**13068-13073. doi: 10.1073/pnas.0405179101 [doi].

132. **Guo, P, Weinstein, AM, Weinbaum, S.** 2000. A hydrodynamic mechanosensory hypothesis for brush border microvilli. Am. J. Physiol. Renal Physiol. **279:**F698-712.

133. **Kawai, Y, Kaidoh, M, Yokoyama, Y, Ohhashi, T.** 2012. Pivotal roles of shear stress in the microenvironmental changes that occur within sentinel lymph nodes. Cancer. Sci. **103:**1245-1252. doi: 10.1111/j.1349-7006.2012.02289.x [doi].

134. **Vessieres, E, Freidja, ML, Loufrani, L, Fassot, C, Henrion, D.** 2012. Flow (shear stress)-mediated remodeling of resistance arteries in diabetes. Vascul Pharmacol. **57:**173-178. doi: 10.1016/j.vph.2012.03.006 [doi].

135. **Nickerson, CA, Ott, CM, Wilson, JW, Ramamurthy, R, Pierson, DL.** 2004. Microbial responses to microgravity and other low-shear environments. Microbiol. Mol. Biol. Rev. **68:**345-361. doi: 10.1128/MMBR.68.2.345-361.2004 [doi].

136. **Cai, Z, Xin, J, Pollock, DM, Pollock, JS.** 2000. Shear stress-mediated NO production in inner medullary collecting duct cells. Am. J. Physiol. Renal Physiol. **279:**F270-4.

137. **Beeson, JG, Rogerson, SJ, Cooke, BM, Reeder, JC, Chai, W, Lawson, AM, Molyneux, ME, Brown, GV.** 2000. Adhesion of Plasmodium falciparum-infected erythrocytes to hyaluronic acid in placental malaria. Nat. Med. **6:**86-90. doi: 10.1038/71582 [doi].

138. **Basson, MD.** 2003. Paradigms for mechanical signal transduction in the intestinal epithelium. Category: molecular, cell, and developmental biology. Digestion. **68:**217-225. doi: 76385 [doi].

139. **Islam, N, Kim, Y, Ross, JM, Marten, MR.** 2014. Proteomic analysis of Staphylococcus aureus biofilm cells grown under physiologically relevant fluid shear stress conditions. Proteome Sci. **12:**21-5956-12-21. eCollection 2014. doi: 10.1186/1477-5956-12-21 [doi].

140. **Kostenko, V, Salek, MM, Sattari, P, Martinuzzi, RJ.** 2010. Staphylococcus aureus biofilm formation and tolerance to antibiotics in response to oscillatory shear stresses of physiological levels. FEMS Immunol. Med. Microbiol. **59:**421-431. doi: 10.1111/j.1574-695X.2010.00694.x [doi].

141. **Kolluru, GK, Sinha, S, Majumder, S, Muley, A, Siamwala, JH, Gupta, R, Chatterjee, S.** 2010. Shear stress promotes nitric oxide production in endothelial cells by sub-cellular delocalization of eNOS: A basis for shear stress mediated angiogenesis. Nitric Oxide. **22:**304-315. doi: 10.1016/j.niox.2010.02.004 [doi].

142. **Mashour, GA, Boock, RJ.** 1999. Effects of shear stress on nitric oxide levels of human cerebral endothelial cells cultured in an artificial capillary system. Brain Res. **842:**233-238. doi: S0006-8993(99)01872-7 [pii].

143. **Nickerson, CA, Ott, CM, Mister, SJ, Morrow, BJ, Burns-Keliher, L, Pierson, DL.** 2000. Microgravity as a novel environmental signal affecting Salmonella enterica serovar Typhimurium virulence. Infect. Immun. **68:**3147-3152.

144. **Nickerson, CA, Ott, CM, Wilson, JW, Ramamurthy, R, LeBlanc, CL, Honer zu Bentrup, K, Hammond, T, Pierson, DL.** 2003. Low-shear modeled microgravity: a global environmental regulatory signal affecting bacterial gene expression, physiology, and pathogenesis. J. Microbiol. Methods. **54:**1-11. doi: S0167701203000186 [pii].

145. **Rosado, H, Doyle, D, Hinds, J, Taylor D.** 2009. Low-shear modelled microgravity alters expression of virulence determinants of *Staphylococcusaureus*. Acta Astronaut. **66:**408-413.

146. **Wilson, JW, Ramamurthy, R, Porwollik, S, McClelland, M, Hammond, T, Allen, P, Ott, CM, Pierson, DL, Nickerson, CA.** 2002. Microarray analysis identifies Salmonella genes belonging to the low-shear modeled microgravity regulon. Proc. Natl. Acad. Sci. U. S. A. **99:**13807-13812. doi: 10.1073/pnas.212387899 [doi].

147. **Stepp, DW, Merkus, D, Nishikawa, Y, Chilian, WM.** 2001. Nitric oxide limits coronary vasoconstriction by a shear stress-dependent mechanism. Am. J. Physiol. Heart Circ. Physiol. **281:**H796-803.

148. **Tao, J, Yang, Z, Wang, JM, Tu, C, Pan, SR.** 2006. Effects of fluid shear stress on eNOS mRNA expression and NO production in human endothelial progenitor cells. Cardiology. **106:**82-88. doi: 92636 [pii].

149. **Wedgwood, S, Bekker, JM, Black, SM.** 2001. Shear stress regulation of endothelial NOS in fetal pulmonary arterial endothelial cells involves PKC. Am. J. Physiol. Lung Cell. Mol. Physiol. **281:**L490-8.

150. **Castro, SL, Nelman-Gonzalez, M, Nickerson, CA, Ott, CM.** 2011. Induction of attachment-independent biofilm formation and repression of Hfq expression by low-fluid-shear culture of Staphylococcus aureus. Appl. Environ. Microbiol. **77:**6368-6378. doi: 10.1128/AEM.00175-11 [doi].

151. **Crabbe, A, Pycke, B, Van Houdt, R, Monsieurs, P, Nickerson, C, Leys, N, Cornelis, P.** 2010. Response of Pseudomonas aeruginosa PAO1 to low shear modelled microgravity involves AlgU regulation. Environ. Microbiol. **12:**1545-1564. doi: 10.1111/j.1462-2920.2010.02184.x [doi].

152. **Gao, Q, Fang, A, Pierson, DL, Mishra, SK, Demain, AL.** 2001. Shear stress enhances microcin B17 production in a rotating wall bioreactor, but ethanol stress does not. Appl. Microbiol. Biotechnol. **56:**384-387.

153. **Soni, A, O'Sullivan, L, Quick, LN, Ott, CM, Nickerson, CA, Wilson, JW.** 2014. Conservation of the Low-shear Modeled Microgravity Response in Enterobacteriaceae and Analysis of the trp Genes in this Response. Open Microbiol. J. **8:**51-58. doi: 10.2174/1874285801408010051 [doi].

154. **Nauman, EA, Ott, CM, Sander, E, Tucker, DL, Pierson, D, Wilson, JW, Nickerson, CA.** 2007. Novel quantitative biosystem for modeling physiological fluid shear stress on cells. Appl. Environ. Microbiol. **73:**699-705. doi: AEM.02428-06 [pii].

155. **Crabbe, A, Schurr, MJ, Monsieurs, P, Morici, L, Schurr, J, Wilson, JW, Ott, CM, Tsaprailis, G, Pierson, DL, Stefanyshyn-Piper, H, Nickerson, CA.** 2011. Transcriptional and proteomic responses of Pseudomonas aeruginosa PAO1 to spaceflight conditions involve Hfq regulation and reveal a role for oxygen. Appl. Environ. Microbiol. **77:**1221-1230. doi: 10.1128/AEM.01582-10 [doi].

156. **Fang, A, Pierson, DL, Koenig, DW, Mishra, SK, Demain, AL.** 1997. Effect of simulated microgravity and shear stress on microcin B17 production by Escherichia coli and on its excretion into the medium. Appl. Environ. Microbiol. **63:**4090-4092.

157. **Jennings, ME, Quick, LN, Soni, A, Davis, RR, Crosby, K, Ott, CM, Nickerson, CA, Wilson, JW.** 2011. Characterization of the Salmonella enterica serovar Typhimurium ydcI gene, which encodes a conserved DNA binding protein required for full acid stress resistance. J. Bacteriol. **193:**2208-2217. doi: 10.1128/JB.01335-10 [doi].

158. **Pacello, F, Rotilio, G, Battistoni, A.** 2012. Low-Shear modeled microgravity enhances Salmonella Enterica Resistance to hydrogen peroxide through a mechanism involving KatG and KatN. The Open Microbiology Journal. **6:**53.

159. **Wilson, JW, Ott, CM, Ramamurthy, R, Porwollik, S, McClelland, M, Pierson, DL, Nickerson, CA.** 2002. Low-Shear modeled microgravity alters the Salmonella enterica serovar typhimurium stress response in an RpoS-independent manner. Appl. Environ. Microbiol. **68:**5408-5416.

160. **Nickerson, CA, Goodwin, TJ, Terlonge, J, Ott, CM, Buchanan, KL, Uicker, WC, Emami, K, LeBlanc, CL, Ramamurthy, R, Clarke, MS, Vanderburg, CR, Hammond, T, Pierson, DL.** 2001. Three-dimensional tissue assemblies: novel models for the study of Salmonella enterica serovar Typhimurium pathogenesis. Infect. Immun. **69:**7106-7120. doi: 10.1128/IAI.69.11.7106-7120.2001 [doi].

161. **Stock, UA, Vacanti, JP.** 2001. Cardiovascular physiology during fetal development and implications for tissue engineering. Tissue Eng. **7:**1-7. doi: 10.1089/107632701300003241 [doi].

162. **Greene, MF, Creasy, RK, Resnik, R, Iams, JD, Lockwood, CJ, Moore, T.** 2008. Creasy and Resnik's maternal-fetal medicine: principles and practice. Elsevier Health Sciences.

163. **Goodwin, T, Prewett, T, Wolf, D, Spaulding, G.** 1993. Reduced shear stress: a major component in the ability of mam- malian tissues to form three-dimensional assemblies in simulated microgravity. J Cell Biochem. **51:**301-311.

164. **Wilson, JW, Ott, CM, Honer zu Bentrup, K, Ramamurthy, R, Quick, L, Porwollik, S, Cheng, P, McClelland, M, Tsaprailis, G, Radabaugh, T, Hunt, A, Fernandez, D, Richter, E, Shah, M, Kilcoyne, M, Joshi, L, Nelman-Gonzalez, M, Hing, S, Parra, M, Dumars, P, Norwood, K, Bober, R, Devich, J, Ruggles, A, Goulart, C, Rupert, M, Stodieck, L, Stafford, P, Catella, L, Schurr, MJ, Buchanan, K, Morici, L, McCracken, J, Allen, P, Baker-Coleman, C, Hammond, T, Vogel, J, Nelson, R, Pierson, DL, Stefanyshyn-Piper, HM, Nickerson, CA.** 2007. Space flight alters bacterial gene expression and virulence and reveals a role for global regulator Hfq. Proc. Natl. Acad. Sci. U. S. A. **104:**16299-16304. doi: 0707155104 [pii].

165. **Wilson, JW, Ott, CM, Quick, L, Davis, R, Honer zu Bentrup, K, Crabbe, A, Richter, E, Sarker, S, Barrila, J, Porwollik, S, Cheng, P, McClelland, M, Tsaprailis, G, Radabaugh, T, Hunt, A, Shah, M, Nelman-Gonzalez, M, Hing, S, Parra, M, Dumars, P, Norwood, K, Bober, R, Devich, J, Ruggles, A, CdeBaca, A, Narayan, S, Benjamin, J, Goulart, C, Rupert, M, Catella, L, Schurr, MJ, Buchanan, K, Morici, L, McCracken, J, Porter, MD, Pierson, DL, Smith, SM, Mergeay, M, Leys, N, Stefanyshyn-Piper, HM, Gorie, D, Nickerson, CA.** 2008. Media ion composition

controls regulatory and virulence response of Salmonella in spaceflight. PLoS One. **3:**e3923. doi: 10.1371/journal.pone.0003923 [doi].

166. **Degenhardt, L, Whiteford, HA, Ferrari, AJ, Baxter, AJ, Charlson, FJ, Hall, WD, Freedman, G, Burstein, R, Johns, N, Engell, RE.** 2013. Global burden of disease attributable to illicit drug use and dependence: findings from the Global Burden of Disease Study 2010. The Lancet. **382:**1564-1574.

167. **Cohen, MS, Hellmann, N, Levy, JA, DeCock, K, Lange, J.** 2008. The spread, treatment, and prevention of HIV-1: evolution of a global pandemic. J. Clin. Invest. **118:**1244-1254. doi: 10.1172/JCI34706 [doi].

168. **Siegel, R, Ma, J, Zou, Z, Jemal, A.** 2014. Cancer statistics, 2014. CA: A Cancer Journal for Clinicians. **64:**9-29.

169. **World Health Organization.** November 2014. **HIV/AIDS**. .

170. **World Health Organization.** 2014. Global update on the health sector response to HIV, 2014. .

171. **Zitvogel, L, Apetoh, L, Ghiringhelli, F, Kroemer, G.** 2008. Immunological aspects of cancer chemotherapy. Nature Reviews Immunology. **8:**59-73.

172. **LaRocque, RC, Rao, SR, Lee, J, Ansdell, V, Yates, JA, Schwartz, BS, Knouse, M, Cahill, J, Hagmann, S, Vinetz, J, Connor, BA, Goad, JA, Oladele, A, Alvarez, S, Stauffer, W, Walker, P, Kozarsky, P, Franco-Paredes, C, Dismukes, R, Rosen, J, Hynes, NA, Jacquerioz, F, McLellan, S, Hale, D, Sofarelli, T, Schoenfeld, D, Marano, N, Brunette, G, Jentes, ES, Yanni, E, Sotir, MJ, Ryan, ET, Global TravEpiNet Consortium.** 2012. Global TravEpiNet: a national consortium of clinics providing care to international travelers--analysis of demographic characteristics, travel destinations, and pretravel healthcare of high-risk US international travelers, 2009-2011. Clin. Infect. Dis. **54:**455-462. doi: 10.1093/cid/cir839 [doi].

173. **Miller, JM, Tam, TW, Maloney, S, Fukuda, K, Cox, N, Hockin, J, Kertesz, D, Klimov, A, Cetron, M.** 2000. Cruise ships: high-risk passengers and the global spread of new influenza viruses. Clin. Infect. Dis. **31:**433-438. doi: CID994031 [pii].

174. **Molton, JS, Tambyah, PA, Ang, BS, Ling, ML, Fisher, DA.** 2013. The global spread of healthcare-associated multidrug-resistant bacteria: a perspective from Asia. Clin. Infect. Dis. **56:**1310-1318. doi: 10.1093/cid/cit020 [doi].

175. **Perrin, L, Kaiser, L, Yerly, S.** 2003. Travel and the spread of HIV-1 genetic variants. The Lancet Infectious Diseases. **3:**22-27.

176. **Kariuki, S, Revathi, G, Kariuki, N, Kiiru, J, Mwituria, J, Muyodi, J, Githinji, JW, Kagendo, D, Munyalo, A, Hart, CA.** 2006. Invasive multidrug-resistant non-typhoidal Salmonella infections in Africa: zoonotic or anthroponotic transmission? J. Med. Microbiol. **55:**585-591. doi: 55/5/585 [pii].

177. **Gordon, MA, Kankwatira, AM, Mwafulirwa, G, Walsh, AL, Hopkins, MJ, Parry, CM, Faragher, EB, Zijlstra, EE, Heyderman, RS, Molyneux, ME.** 2010. Invasive non-typhoid salmonellae establish systemic intracellular infection in HIV-infected adults: an emerging disease pathogenesis. Clin. Infect. Dis. **50:**953-962. doi: 10.1086/651080 [doi].

178. **MacLennan, CA.** 2014. Antibodies and Protection Against Invasive Salmonella Disease. Frontiers in Immunology. **5:**.

179. **Netea, MG, Joosten, LA, Keuter, M, Wagener, F, Stalenhoef, AF, van der Meer, JW, Kullberg, BJ.** 2009. Circulating lipoproteins are a crucial component of host defense against invasive Salmonella typhimurium infection. PLoS One. **4:**e4237. doi: 10.1371/journal.pone.0004237 [doi].

180. **Gondwe, EN, Molyneux, ME, Goodall, M, Graham, SM, Mastroeni, P, Drayson, MT, MacLennan, CA.** 2010. Importance of antibody and complement for oxidative burst and killing of invasive nontyphoidal Salmonella by blood cells in Africans. Proc. Natl. Acad. Sci. U. S. A. **107:**3070-3075. doi: 10.1073/pnas.0910497107 [doi].

181. **Nyirenda, TS, Seeley, AE, Mandala, WL, Drayson, MT, MacLennan, CA.** 2010. Early interferon-gamma production in human lymphocyte subsets in response to nontyphoidal Salmonella demonstrates inherent capacity in innate cells. PLoS One. **5:**e13667. doi: 10.1371/journal.pone.0013667 [doi].

182. **Leekitcharoenphon, P, Friis, C, Zankari, E, Svendsen, CA, Price, LB, Rahmani, M, Herrero-Fresno, A, Fashae, K, Vandenberg, O, Aarestrup, FM, Hendriksen, RS.** 2013. Genomics of an emerging clone of Salmonella serovar Typhimurium ST313 from Nigeria and the Democratic Republic of Congo. J. Infect. Dev. Ctries. **7:**696-706. doi: 10.3855/jidc.3328 [doi].

183. **Wain, J, Keddy, KH, Hendriksen, RS, Rubino, S.** 2013. Using next generation sequencing to tackle non-typhoidal Salmonella infections. J. Infect. Dev. Ctries. **7:**1-5. doi: 10.3855/jidc.3080 [doi].

184. **Keddy, KH, Dwarika, S, Crowther, P, Perovic, O, Wadula, J, Hoosen, A, Sooka, A, Crewe-Brown, HH, Smith, AM.** 2009. Genotypic and demographic characterization of invasive isolates of Salmonella Typhimurium in HIV co-infected patients in South Africa. J. Infect. Dev. Ctries. **3:**585-592.

185. **Bronowski, C, Fookes, MC, Gilderthorp, R, Ashelford, KE, Harris, SR, Phiri, A, Hall, N, Gordon, MA, Wain, J, Hart, CA, Wigley, P, Thomson, NR, Winstanley, C.** 2013. Genomic characterisation of invasive non-typhoidal Salmonella enterica Subspecies enterica Serovar Bovismorbificans isolates from Malawi. PLoS Negl Trop. Dis. **7:**e2557. doi: 10.1371/journal.pntd.0002557 [doi].

186. **Msefula, CL, Kingsley, RA, Gordon, MA, Molyneux, E, Molyneux, ME, MacLennan, CA, Dougan, G, Heyderman, RS.** 2012. Genotypic homogeneity of multidrug resistant S. Typhimurium infecting distinct adult and childhood susceptibility groups in Blantyre, Malawi. PLoS One. **7:**e42085. doi: 10.1371/journal.pone.0042085 [doi].

187. **Felix, A, Pitt, RM.** 1951. The pathogenic and immunogenic activities of Salmonella typhi in relation to its antigenic constituents. J. Hyg. (Lond). **49:**92-110.

188. **Hoiseth, SK, Stocker, BA.** 1981. Aromatic-dependent Salmonella typhimurium are non-virulent and effective as live vaccines. Nature. **291:**238-239.

189. **Nickerson, CA, Curtiss, R,3rd.** 1997. Role of sigma factor RpoS in initial stages of Salmonella typhimurium infection. Infect. Immun. **65:**1814-1823.

190. **Reed, LJ, Muench, H.** 1938. A simple method of estimating fifty percent endpoints. Am. J. Hyg. **27:**493-497.

191. **Lockman, HA, Curtiss, R,3rd.** 1990. Salmonella typhimurium mutants lacking flagella or motility remain virulent in BALB/c mice. Infect. Immun. **58:**137-143.

192. **Meyer, PN, Wilmes-Riesenberg, MR, Stathopoulos, C, Curtiss, R,3rd.** 1998. Virulence of a Salmonella typhimurium OmpD mutant. Infect. Immun. **66:**387-390.

193. **Riesenberg-Wilmes, MR, Bearson, B, Foster, JW, Curtis, R,3rd.** 1996. Role of the acid tolerance response in virulence of Salmonella typhimurium. Infect. Immun. **64:**1085-1092.

194. **Bearson, BL, Wilson, L, Foster, JW.** 1998. A low pH-inducible, PhoPQ-dependent acid tolerance response protects Salmonella typhimurium against inorganic acid stress. J. Bacteriol. **180:**2409-2417.

195. **Hall, H, Karem, K, Foster, J.** 1995. Molecular responses of microbes to environmental pH stress. Adv. Microb. Physiol. **37:**229-272.

196. **Le Bouguenec, C, Schouler, C.** 2011. Sugar metabolism, an additional virulence factor in enterobacteria. Int. J. Med. Microbiol. **301:**1-6. doi: 10.1016/j.ijmm.2010.04.021 [doi].

197. **Xue, C.** 2012. Cryptococcus and beyond--inositol utilization and its implications for the emergence of fungal virulence. PLoS Pathog. **8:**e1002869. doi: 10.1371/journal.ppat.1002869 [doi].

198. **Kroger, C, Stolz, J, Fuchs, TM.** 2010. myo-Inositol transport by Salmonella enterica serovar Typhimurium. Microbiology. **156:**128-138. doi: 10.1099/mic.0.032250-0 [doi].

199. **Ahmed, R, Soule, G, Demczuk, WH, Clark, C, Khakhria, R, Ratnam, S, Marshall, S, Ng, LK, Woodward, DL, Johnson, WM, Rodgers, FG.** 2000. Epidemiologic typing of Salmonella enterica serotype enteritidis in a Canada-wide outbreak of gastroenteritis due to contaminated cheese. J. Clin. Microbiol. **38:**2403-2406.

200. **Robbe-Saule, V, Coynault, C, Ibanez-Ruiz, M, Hermant, D, Norel, F.** 2001. Identification of a non-haem catalase in Salmonella and its regulation by RpoS (sigmaS). Mol. Microbiol. **39:**1533-1545. doi: mmi2340 [pii].

201. **Foster, JW, Hall, HK.** 1990. Adaptive acidification tolerance response of Salmonella typhimurium. J. Bacteriol. **172:**771-778.

202. **Lin, J, Smith, MP, Chapin, KC, Baik, HS, Bennett, GN, Foster, JW.** 1996. Mechanisms of acid resistance in enterohemorrhagic Escherichia coli. Appl. Environ. Microbiol. **62:**3094-3100.

203. **Waterman, SR, Small, PL.** 1998. Acid-sensitive enteric pathogens are protected from killing under extremely acidic conditions of pH 2.5 when they are inoculated onto certain solid food sources. Appl. Environ. Microbiol. **64:**3882-3886.

204. **Gorden, J, Small, PL.** 1993. Acid resistance in enteric bacteria. Infect. Immun. **61:**364-367.

205. **Carsiotis, M, Weinstein, DL, Karch, H, Holder, IA, O'Brien, AD.** 1984. Flagella of Salmonella typhimurium are a virulence factor in infected C57BL/6J mice. Infect. Immun. **46:**814-818.

206. **Haiko, J, Westerlund-Wikstrom, B.** 2013. The role of the bacterial flagellum in adhesion and virulence. Biology (Basel). **2:**1242-1267. doi: 10.3390/biology2041242 [doi].

207. **Olsen, JE, Hoegh-Andersen, KH, Casadesus, J, Rosenkranzt, J, Chadfield, MS, Thomsen, LE.** 2013. The role of flagella and chemotaxis genes in host pathogen interaction of the host adapted Salmonella enterica serovar Dublin compared to the broad host range serovar S. Typhimurium. BMC Microbiol. **13:**67-2180-13-67. doi: 10.1186/1471-2180-13-67 [doi].

208. **van Asten, FJ, Hendriks, HG, Koninkx, JF, van Dijk, JE.** 2004. Flagella-mediated bacterial motility accelerates but is not required for Salmonella serotype Enteritidis invasion of differentiated Caco-2 cells. Int. J. Med. Microbiol. **294:**395-399. doi: S1438-4221(04)00076-1 [pii].

209. **Schmitt, CK, Ikeda, JS, Darnell, SC, Watson, PR, Bispham, J, Wallis, TS, Weinstein, DL, Metcalf, ES, O'Brien, AD.** 2001. Absence of all components of the flagellar export and synthesis machinery differentially alters virulence of Salmonella enterica serovar Typhimurium in models of typhoid fever, survival in macrophages, tissue culture invasiveness, and calf enterocolitis. Infect. Immun. **69:**5619-5625.

210. **Stecher, B, Hapfelmeier, S, Muller, C, Kremer, M, Stallmach, T, Hardt, WD.** 2004. Flagella and chemotaxis are required for efficient induction of Salmonella enterica serovar Typhimurium colitis in streptomycin-pretreated mice. Infect. Immun. **72:**4138-4150. doi: 10.1128/IAI.72.7.4138-4150.2004 [doi].

211. **Lee, MD, Curtiss, R,3rd, Peay, T.** 1996. The effect of bacterial surface structures on the pathogenesis of Salmonella typhimurium infection in chickens. Avian Dis. **40:**28-36.

212. **Jones, BD, Lee, CA, Falkow, S.** 1992. Invasion by Salmonella typhimurium is affected by the direction of flagellar rotation. Infect. Immun. **60:**2475-2480.

213. **Liu, SL, Ezaki, T, Miura, H, Matsui, K, Yabuuchi, E.** 1988. Intact motility as a Salmonella typhi invasion-related factor. Infect. Immun. **56:**1967-1973.

214. **La Ragione, RM, Cooley, WA, Velge, P, Jepson, MA, Woodward, MJ.** 2003. Membrane ruffling and invasion of human and avian cell lines is reduced for aflagellate mutants of Salmonella enterica serotype Enteritidis. Int. J. Med. Microbiol. **293:**261-272. doi: S1438-4221(04)70160-5 [pii].

215. **Dibb-Fuller, MP, Allen-Vercoe, E, Thorns, CJ, Woodward, MJ.** 1999. Fimbriae-and flagella-mediated association with and invasion of cultured epithelial cells by Salmonella enteritidis. Microbiology. **145 (Pt 5):**1023-1031.

216. **Kalai Chelvam, K, Chai, LC, Thong, KL.** 2014. Variations in motility and biofilm formation of Salmonella enterica serovar Typhi. Gut Pathog. **6:**2-4749-6-2. doi: 10.1186/1757-4749-6-2 [doi].

217. **Ernst, T, Chang, L, Arnold, S.** 2003. Increased glial metabolites predict increased working memory network activation in HIV brain injury. Neuroimage. **19:**1686-1693. doi: S1053811903002325 [pii].

218. **Furuyama, W, Enomoto, M, Mossaad, E, Kawai, S, Mikoshiba, K, Kawazu, S.** 2014. An interplay between 2 signaling pathways: melatonin-cAMP and IP3-Ca2+

signaling pathways control intraerythrocytic development of the malaria parasite Plasmodium falciparum. Biochem. Biophys. Res. Commun. **446:**125-131. doi: 10.1016/j.bbrc.2014.02.070 [doi].

219. **van Santen, S, de Mast, Q, Swinkels, DW, van der Ven, AJ.** 2013. The iron link between malaria and invasive non-typhoid Salmonella infections. Trends Parasitol. **29:**220-227. doi: 10.1016/j.pt.2013.03.006 [doi].

220. **EDSALL, G, GAINES, S, LANDY, M, TIGERTT, WD, SPRINZ, H, TRAPANI, RJ, MANDEL, AD, BENENSON, AS.** 1960. Studies on infection and immunity in experimental typhoid fever. I. Typhoid fever in chimpanzees orally infected with Salmonella typhosa. J. Exp. Med. **112:**143-166.

221. **Barrila, J, Radtke, AL, Crabbe, A, Sarker, SF, Herbst-Kralovetz, MM, Ott, CM, Nickerson, CA.** 2010. Organotypic 3D cell culture models: using the rotating wall vessel to study host-pathogen interactions. Nat. Rev. Microbiol. **8:**791-801. doi: 10.1038/nrmicro2423 [doi].

222. **Carterson, AJ, Honer zu Bentrup, K, Ott, CM, Clarke, MS, Pierson, DL, Vanderburg, CR, Buchanan, KL, Nickerson, CA, Schurr, MJ.** 2005. A549 lung epithelial cells grown as three-dimensional aggregates: alternative tissue culture model for Pseudomonas aeruginosa pathogenesis. Infect. Immun. **73:**1129-1140. doi: 73/2/1129 [pii].

223. **Gao, H, Ayyaswamy, PS, Ducheyne, P.** 1997. Dynamics of a microcarrier particle in the simulated microgravity environment of a rotating-wall vessel. Microgravity Sci Technol. **10:**154-165.

224. **Skardal, A, Sarker, SF, Crabbe, A, Nickerson, CA, Prestwich, GD.** 2010. The generation of 3-D tissue models based on hyaluronan hydrogel-coated microcarriers within a rotating wall vessel bioreactor. Biomaterials. **31:**8426-8435. doi: 10.1016/j.biomaterials.2010.07.047 [doi].

225. **De Weirdt, R, Crabbe, A, Roos, S, Vollenweider, S, Lacroix, C, van Pijkeren, JP, Britton, RA, Sarker, S, Van de Wiele, T, Nickerson, CA.** 2012. Glycerol supplementation enhances L. reuteri's protective effect against S. Typhimurium colonization in a 3-D model of colonic epithelium. PLoS One. **7:**e37116. doi: 10.1371/journal.pone.0037116 [doi].

226. **Straub, TM, Bartholomew, RA, Valdez, CO, Valentine, NB, Dohnalkova, A, Ozanich, RM, Bruckner-Lea, CJ, Call, DR.** 2011. Human norovirus infection of caco-2 cells grown as a three-dimensional tissue structure. J. Water. Health. **9:**225-240.

227. **Zwezdaryk, KJ, Warner, JA, Machado, HL, Morris, CA, Honer zu Bentrup, K.** 2012. Rotating cell culture systems for human cell culture: human trophoblast cells as a model. J. Vis. Exp. **(59). pii: 3367. doi:**10.3791/3367. doi: 10.3791/3367 [doi].

228. **Flora, AD, Teel, LD, Smith, MA, Sinclair, JF, Melton-Celsa, AR, O'Brien, AD.** 2013. Ricin Crosses Polarized Human Intestinal Cells and Intestines of Ricin-Gavaged Mice without Evident Damage and Then Disseminates to Mouse Kidneys. PloS One. **8:**e69706.

229. **Honer zu Bentrup, K, Ramamurthy, R, Ott, CM, Emami, K, Nelman-Gonzalez, M, Wilson, JW, Richter, EG, Goodwin, TJ, Alexander, JS, Pierson, DL, Pellis, N, Buchanan, KL, Nickerson, CA.** 2006. Three-dimensional organotypic models of human colonic epithelium to study the early stages of enteric salmonellosis. Microbes Infect. **8:**1813-1825. doi: S1286-4579(06)00143-2 [pii].

230. **Navran, S.** 2008. The application of low shear modeled microgravity to 3-D cell biology and tissue engineering. Biotechnol. Annu. Rev. **14:**275-296. doi: 10.1016/S1387-2656(08)00011-2 [doi].

231. **Sainz, B,Jr, TenCate, V, Uprichard, SL.** 2009. Three-dimensional Huh7 cell culture system for the study of Hepatitis C virus infection. Virol. J. **6:**103-422X-6-103. doi: 10.1186/1743-422X-6-103 [doi].

232. **Nickerson, CA, Ott, CM.** 2004. A new dimension in modeling infectious disease. ASM News. **70:**169-175.

233. **Unsworth, BR, Lelkes, PI.** 1998. Growing tissues in microgravity. Nat. Med. **4:**901-907.

234. **Beacham, DA, Cukierman, E.** 2005. Stromagenesis: the changing face of fibroblastic microenvironments during tumor progression, p. 329-341. *In* Anonymous Seminars in cancer biology. Elsevier.

235. **Debnath, J, Brugge, JS.** 2005. Modelling glandular epithelial cancers in three-dimensional cultures. Nature Reviews Cancer. **5:**675-688.

236. **Ingber, DE.** 2008. Tensegrity-based mechanosensing from macro to micro. Prog. Biophys. Mol. Biol. **97:**163-179.

237. **Ingram, M, Techy, G, Saroufeem, R, Yazan, O, Narayan, K, Goodwin, T, Spaulding, G.** 1997. Three-dimensional growth patterns of various human tumor cell lines in simulated microgravity of a NASA bioreactor. In Vitro Cellular & Developmental Biology-Animal. **33:**459-466.

238. **Kim, JB.** 2005. Three-dimensional tissue culture models in cancer biology, p. 365-377. *In* Anonymous Seminars in cancer biology. Elsevier.

239. **Weigelt, B, Bissell, MJ.** 2008. Unraveling the microenvironmental influences on the normal mammary gland and breast cancer, p. 311-321. *In* Anonymous Seminars in cancer biology. Elsevier.

240. **Schmeichel, KL, Bissell, MJ.** 2003. Modeling tissue-specific signaling and organ function in three dimensions. J. Cell. Sci. **116:**2377-2388. doi: 10.1242/jcs.00503 [doi].

241. **Chan, K, Kim, CC, Falkow, S.** 2005. Microarray-based detection of Salmonella enterica serovar Typhimurium transposon mutants that cannot survive in macrophages and mice. Infect. Immun. **73:**5438-5449. doi: 73/9/5438 [pii].

242. **Ramsden, AE, Holden, DW, Mota, LJ.** 2007. Membrane dynamics and spatial distribution of Salmonella-containing vacuoles. Trends Microbiol. **15:**516-524.

243. **Duell, BL, Cripps, AW, Schembri, MA, Ulett, GC.** 2011. Epithelial cell coculture models for studying infectious diseases: benefits and limitations. J. Biomed. Biotechnol. **2011:**852419. doi: 10.1155/2011/852419 [doi].

244. **Spottl, T, Hausmann, M, Gunckel, M, Herfarth, H, Herlyn, M, Schoelmerich, J, Rogler, G.** 2006. A new organotypic model to study cell interactions in the intestinal mucosa. Eur. J. Gastroenterol. Hepatol. **18:**901-909. doi: 00042737-200608000-00017 [pii].

245. **Hedbrant, A, Erlandsson, A, Delbro, D, Wijkander, J.** 2015. Conditioned media from human macrophages of M1 phenotype attenuate the cytotoxic effect of 5fluorouracil on the HT29 colon cancer cell line. Int. J. Oncol. **46:**37-46. doi: 10.3892/ijo.2014.2696 [doi].

246. **Wu, TH, Li, YY, Wu, TL, Chang, JW, Chou, WC, Hsieh, LL, Chen, JR, Yeh, KY.** 2014. Culture supernatants of different colon cancer cell lines induce specific phenotype switching and functional alteration of THP-1 cells. Cell. Immunol. **290:**107-115. doi: 10.1016/j.cellimm.2014.05.015 [doi].

247. **Crabbe, A, Sarker, SF, Van Houdt, R, Ott, CM, Leys, N, Cornelis, P, Nickerson, CA.** 2011. Alveolar epithelium protects macrophages from quorum sensing-induced cytotoxicity in a three-dimensional co-culture model. Cell. Microbiol. **13:**469-481. doi: 10.1111/j.1462-5822.2010.01548.x [doi].

248. **Lee, BH, Kushwah, R, Wu, J, Ng, P, Palaniyar, N, Grinstein, S, Philpott, DJ, Hu, J.** 2010. Adenoviral vectors stimulate innate immune responses in macrophages through cross-talk with epithelial cells. Immunol. Lett. **134:**93-102. doi: 10.1016/j.imlet.2010.09.003 [doi].

249. **Muller, L, Riediker, M, Wick, P, Mohr, M, Gehr, P, Rothen-Rutishauser, B.** 2010. Oxidative stress and inflammation response after nanoparticle exposure: differences between human lung cell monocultures and an advanced three-dimensional model of the human epithelial airways. J. R. Soc. Interface. **7 Suppl 1:**S27-40. doi: 10.1098/rsif.2009.0161.focus [doi].

250. **Wiegand, C, Abel, M, Ruth, P, Hipler, UC.** 2009. HaCaT keratinocytes in co-culture with Staphylococcus aureus can be protected from bacterial damage by polihexanide. Wound Repair Regen. **17:**730-738. doi: 10.1111/j.1524-475X.2009.00536.x [doi].

251. **van Hoffen, E, Korthagen, NM, de Kivit, S, Schouten, B, Bardoel, B, Duivelshof, A, Knol, J, Garssen, J, Willemsen, LE.** 2010. Exposure of intestinal epithelial cells to UV-killed Lactobacillus GG but not Bifidobacterium breve enhances the effector immune response in vitro. Int. Arch. Allergy Immunol. **152:**159-168. doi: 10.1159/000265537 [doi].

252. **Xu, T, Maloy, S, McGuire, KL.** 2009. Macrophages influence Salmonella host-specificity in vivo. Microb. Pathog. **47:**212-222. doi: 10.1016/j.micpath.2009.07.004 [doi].

253. **Sundstrom, C, Nilsson, K.** 1976. Establishment and characterization of a human histiocytic lymphoma cell line (U-937). Int. J. Cancer. **17:**565-577.

254. **Rovera, G, O'Brien, TG, Diamond, L.** 1979. Induction of differentiation in human promyelocytic leukemia cells by tumor promoters. Science. **204:**868-870.

255. **Smith, PD, Smythies, LE, Shen, R, Greenwell-Wild, T, Gliozzi, M, Wahl, SM.** 2011. Intestinal macrophages and response to microbial encroachment. Mucosal Immunol. **4:**31-42. doi: 10.1038/mi.2010.66 [doi].

256. **Murray, PJ, Wynn, TA.** 2011. Protective and pathogenic functions of macrophage subsets. Nature Reviews Immunology. **11:**723-737.

257. **Kim, YG, Kamada, N, Shaw, MH, Warner, N, Chen, GY, Franchi, L, Nunez, G.** 2011. The Nod2 sensor promotes intestinal pathogen eradication via the chemokine CCL2-dependent recruitment of inflammatory monocytes. Immunity. **34:**769-780. doi: 10.1016/j.immuni.2011.04.013 [doi].

258. **Bain, CC, Mowat, AM.** 2011. Intestinal macrophages - specialised adaptation to a unique environment. Eur. J. Immunol. **41:**2494-2498. doi: 10.1002/eji.201141714 [doi].

259. **Charles, RC, Harris, JB, Chase, MR, Lebrun, LM, Sheikh, A, LaRocque, RC, Logvinenko, T, Rollins, SM, Tarique, A, Hohmann, EL, Rosenberg, I, Krastins, B, Sarracino, DA, Qadri, F, Calderwood, SB, Ryan, ET.** 2009. Comparative proteomic

analysis of the PhoP regulon in Salmonella enterica serovar Typhi versus Typhimurium. PLoS One. **4:**e6994. doi: 10.1371/journal.pone.0006994 [doi].

260. **Deng, W, Liou, SR, Plunkett, G,3rd, Mayhew, GF, Rose, DJ, Burland, V, Kodoyianni, V, Schwartz, DC, Blattner, FR.** 2003. Comparative genomics of Salmonella enterica serovar Typhi strains Ty2 and CT18. J. Bacteriol. **185:**2330-2337.

261. **Liu, SL, Sanderson, KE.** 1995. Rearrangements in the genome of the bacterium Salmonella typhi. Proc. Natl. Acad. Sci. U. S. A. **92:**1018-1022.

262. **Pickard, D, Wain, J, Baker, S, Line, A, Chohan, S, Fookes, M, Barron, A, Gaora, PO, Chabalgoity, JA, Thanky, N, Scholes, C, Thomson, N, Quail, M, Parkhill, J, Dougan, G.** 2003. Composition, acquisition, and distribution of the Vi exopolysaccharide-encoding Salmonella enterica pathogenicity island SPI-7. J. Bacteriol. **185:**5055-5065.

263. **Townsend, SM, Kramer, NE, Edwards, R, Baker, S, Hamlin, N, Simmonds, M, Stevens, K, Maloy, S, Parkhill, J, Dougan, G, Baumler, AJ.** 2001. Salmonella enterica serovar Typhi possesses a unique repertoire of fimbrial gene sequences. Infect. Immun. **69:**2894-2901. doi: 10.1128/IAI.69.5.2894-2901.2001 [doi].

264. **Zhang, XL, Tsui, IS, Yip, CM, Fung, AW, Wong, DK, Dai, X, Yang, Y, Hackett, J, Morris, C.** 2000. Salmonella enterica serovar typhi uses type IVB pili to enter human intestinal epithelial cells. Infect. Immun. **68:**3067-3073.

265. **Miyake, M, Zhao, L, Ezaki, T, Hirose, K, Khan, AQ, Kawamura, Y, Shima, R, Kamijo, M, Masuzawa, T, Yanagihara, Y.** 1998. Vi-deficient and nonfimbriated mutants of Salmonella typhi agglutinate human blood type antigens and are hyperinvasive. FEMS Microbiol. Lett. **161:**75-82. doi: S0378-1097(98)00052-4 [pii].

266. **Bishop, A, House, D, Perkins, T, Baker, S, Kingsley, RA, Dougan, G.** 2008. Interaction of Salmonella enterica serovar Typhi with cultured epithelial cells: roles of surface structures in adhesion and invasion. Microbiology. **154:**1914-1926. doi: 10.1099/mic.0.2008/016998-0 [doi].

267. **Mills, SD, Finlay, BB.** 1994. Comparison of Salmonella typhi and Salmonella typhimurium invasion, intracellular growth and localization in cultured human epithelial cells. Microb. Pathog. **17:**409-423. doi: S0882-4010(84)71086-2 [pii].

268. **Kintz, E, Davies, MR, Hammerlof, DL, Canals, R, Hinton, JC, van der Woude, MW.** 2015. A BTP1 prophage gene present in invasive non-typhoidal Salmonella determines composition and length of the O-antigen of the lipopolysaccharide. Mol. Microbiol. . doi: 10.1111/mmi.12933 [doi].

269. **Strandberg, KL, Richards, SM, Gunn, JS.** 2012. Cathelicidin antimicrobial peptide expression is not induced or required for bacterial clearance during salmonella enterica infection of human monocyte-derived macrophages. Infect. Immun. **80:**3930-3938. doi: 10.1128/IAI.00672-12 [doi].

270. **Grant, AJ, Morgan, FJ, McKinley, TJ, Foster, GL, Maskell, DJ, Mastroeni, P.** 2012. Attenuated Salmonella Typhimurium lacking the pathogenicity island-2 type 3 secretion system grow to high bacterial numbers inside phagocytes in mice. PLoS Pathog. **8:**e1003070. doi: 10.1371/journal.ppat.1003070 [doi].

271. **Yue, M, Schifferli, DM.** 2014. Allelic variation in Salmonella: an underappreciated driver of adaptation and virulence. Front. Microbiol. **4:**419. doi: 10.3389/fmicb.2013.00419 [doi].

272. **McLaughlin, LM, Govoni, GR, Gerke, C, Gopinath, S, Peng, K, Laidlaw, G, Chien, YH, Jeong, HW, Li, Z, Brown, MD, Sacks, DB, Monack, D.** 2009. The Salmonella SPI2 effector SseI mediates long-term systemic infection by modulating host cell migration. PLoS Pathog. **5:**e1000671. doi: 10.1371/journal.ppat.1000671 [doi].

273. **Thornbrough, JM, Worley, MJ.** 2012. A naturally occurring single nucleotide polymorphism in the Salmonella SPI-2 type III effector srfH/sseI controls early extraintestinal dissemination. PLoS One. **7:**e45245. doi: 10.1371/journal.pone.0045245 [doi].

274. **Worley, MJ, Nieman, GS, Geddes, K, Heffron, F.** 2006. Salmonella typhimurium disseminates within its host by manipulating the motility of infected cells. Proc. Natl. Acad. Sci. U. S. A. **103:**17915-17920. doi: 0604054103 [pii].

275. **Wolf, D, Schwartz, R.** 1992. Experimental Measurement of the Orbital Paths of Particles Sedimenting Within a Rotating Viscous Fluid as Influenced by Gravity. . NASA Tech. **Paper 3200:**.

276. **Wolf, D, Schwartz, R.** 1991. Analysis of Gravity-Induced Particle Motion and Fluid Perfusion Flow in the NASA-Designed Rotating Zero-Head-Space Tissue Culture Vessel. NASA Tech. **Paper 3143:**.

277. **Hammond, TG, Hammond, JM.** 2001. Optimized suspension culture: the rotating-wall vessel. Am. J. Physiol. Renal Physiol. **281:**F12-25.

278. **Chopra, V, Fadl, A, Sha, J, Chopra, S, Galindo, C, Chopra, A.** 2006. Alterations in the virulence potential of enteric pathogens and bacterial–host cell interactions under simulated microgravity conditions. Journal of Toxicology and Environmental Health, Part A. **69:**1345-1370.

279. **Crabbé, A, De Boever, P, Van Houdt, R, Moors, H, Mergeay, M, Cornelis, P.** 2008. Use of the rotating wall vessel technology to study the effect of shear stress on growth behaviour of Pseudomonas aeruginosa PA01. Environ. Microbiol. **10:**2098-2110.

280. **Lynch, SV, Mukundakrishnan, K, Benoit, MR, Ayyaswamy, PS, Matin, A.** 2006. Escherichia coli biofilms formed under low-shear modeled microgravity in a ground-based system. Appl. Environ. Microbiol. **72:**7701-7710. doi: AEM.01294-06 [pii].

281. **Allen, CA, Niesel, DW, Torres, AG.** 2008. The effects of low□shear stress on Adherent□invasive Escherichia coli. Environ. Microbiol. **10:**1512-1525.

282. **Tucker, DL, Ott, CM, Huff, S, Fofanov, Y, Pierson, DL, Willson, RC, Fox, GE.** 2007. Characterization of Escherichia coli MG1655 grown in a low-shear modeled microgravity environment. BMC Microbiol. **7:**15. doi: 1471-2180-7-15 [pii].

283. **Baker, PW, Meyer, ML, Leff, LG.** 2004. Escherichia coli growth under modeled reduced gravity. Microgravity Sci Technol. **15:**39-44.

284. **Lynch, SV, Brodie, EL, Matin, A.** 2004. Role and regulation of sigma S in general resistance conferred by low-shear simulated microgravity in Escherichia coli. J. Bacteriol. **186:**8207-8212. doi: 186/24/8207 [pii].

285. **Demain, AL, Fang, A.** 2001. Secondary metabolism in simulated microgravity. The Chemical Record. **1:**333-346.

286. **Vukanti, R, Mintz, E, Leff, L.** 2008. Changes in gene expression of E. coli under conditions of modeled reduced gravity. Microgravity-Science and Technology. **20:**41-57.

287. **Beuls, E, Houdt, RV, Leys, N, Dijkstra, C, Larkin, O, Mahillon, J.** 2009. Bacillus thuringiensis conjugation in simulated microgravity. Astrobiology. **9:**797-805.

288. **Mastroleo, F, Van Houdt, R, Atkinson, S, Mergeay, M, Hendrickx, L, Wattiez, R, Leys, N.** 2013. Modelled microgravity cultivation modulates N-acylhomoserine lactone production in Rhodospirillum rubrum S1H independently of cell density. Microbiology. **159:**2456-2466. doi: 10.1099/mic.0.066415-0 [doi].

289. **Searles, SC, Woolley, CM, Petersen, RA, Hyman, LE, Nielsen-Preiss, SM.** 2011. Modeled microgravity increases filamentation, biofilm formation, phenotypic switching, and antimicrobial resistance in Candida albicans. Astrobiology. **11:**825-836.

290. **Gulig, GA, Curtiss, R3.** 1987. Plasmid-associated virulence of Salmonella typhimurium. Infect Immun. **55:**2891-2901.

291. **Tsao YD, Boyd E, Wolf DA, and Spaulding GF.** 1994. Fluid dynamics within a rotating bioreactor in space and earth environments. J Spacecraft Rockets. **31:**937-943.

292. **Wangdi, T, Winter, SE, Baumler, AJ.** 2012. Typhoid fever: "you can't hit what you can't see". Gut Microbes. **3:**88-92. doi: 10.4161/gmic.18602 [doi].

293. **Mattatall, NR, Sanderson, KE.** 1996. Salmonella typhimurium LT2 possesses three distinct 23S rRNA intervening sequences. J. Bacteriol. **178:**2272-2278.

294. **Kadam, SK, Rehemtulla, A, Sanderson, KE.** 1985. Cloning of rfaG, B, I, and J genes for glycosyltransferase enzymes for synthesis of the lipopolysaccharide core of Salmonella typhimurium. J. Bacteriol. **161:**277-284.